



# QUICKREEF® TESTING REPORT

---

ACES 24-003

**University of South Alabama**  
**Center for Applied Coastal Engineering & Science**

150 Student Services Drive

Phone: (251) 460-6174

Mobile, Alabama 36688-0002

Email: [bwebb@southalabama.edu](mailto:bwebb@southalabama.edu)



**Center for Applied  
Coastal Engineering  
and Science**

# Testing Summary

This report describes the results of reduced scale physical experiments to evaluate the performance and hydrodynamic stability of QuickReef® products manufactured by Native Shorelines, a Davey Company. Experiments were carried out in the University of South Alabama's Large Wave Flume (LWF) facility within the Center for Applied Coastal Engineering and Science. These tests were carried out under a testing services agreement (ACES 24-003) between the University of South Alabama and Native Shorelines dated February 6, 2024.

Three unique QuickReef® product setups were tested between the dates of February 6-16, 2024. Testing focused on the 24x80, Defender™, and 21x60 (with cap) products. Limited testing of a fourth setup, the 21x60 (without cap), took place on February 19, 2024. During each experiment, water level measurements were obtained at eight locations—four locations before and after the model testing area—to evaluate wave reflection and wave transmission. An acoustic Doppler velocimeter (ADV) was located on the up-wave (stoss) side of the model to measure the three-dimensional velocity field near the structure. Six-axis accelerometers were adhered to the back side of selected model components to monitor movement under the various wave conditions.

This report provides a description of the testing facility, an overview of the testing/experimental plan, a summary of the testing results, and a brief discussion that synthesizes the results. All raw and processed data, as well as MATLAB scripts, synthesis spreadsheets, experiment records, and lab notes have already been shared electronically through a Google Drive folder. A physical duplicate of all pertinent testing files will be transmitted on a USB drive upon project closeout.

The wave attenuating characteristics of the 24x80 and Defender™ structure types are strongly dependent upon the relative freeboard, which is the ratio of freeboard to wave height. Wave transmission coefficients are easily predicted using simple exponential functions and yield errors around 15 percent of observed values. The 21x60 structure exhibited slightly different behavior, where wave transmission was better correlated to freeboard, but experienced an increase in wave transmission with increasing amounts of freeboard. This may have been due to wave leakage around the end of the structures, or due to overtopping through runup enhanced by the model's cap.

Wave reflection coefficients across all QuickReef® products were typically equivalent to or much less than values often attributed to rubble mound structures. Wave reflection coefficients were larger when water levels were below the structure crest, and smaller when water levels increased above the crest. Wave reflections were sensitive to both water level (freeboard) and wave steepness.

Though a number of QuickReef® panels were instrumented with accelerometers to track motion, few of the panels moved during these experiments. Accelerations and rotations measured during the experiments were very small and perhaps attributed only to an unstable configuration in the model setup owing to protruding aggregates creating a pivot around which the panel could wobble or rock back and forth.

# Table of Contents

<b>TESTING SUMMARY</b>	<b>2</b>
<b>TABLE OF CONTENTS</b>	<b>3</b>
<b>LIST OF TABLES</b>	<b>4</b>
<b>LIST OF FIGURES</b>	<b>5</b>
<b>INTRODUCTION</b>	<b>8</b>
<b>FACILITY DESCRIPTION</b>	<b>8</b>
<b>MODELS AND SCALING</b>	<b>11</b>
<b>TESTING PLAN</b>	<b>14</b>
<b>MEASUREMENT PLAN</b>	<b>19</b>
<b>METHODS</b>	<b>22</b>
<b>RESULTS</b>	<b>26</b>
24x80 MODEL RESULTS	27
DEFENDER™ MODEL RESULTS	35
21x60 (WITH CAP) MODEL RESULTS	43
<b>DISCUSSION</b>	<b>52</b>
<b>REFERENCES</b>	<b>57</b>
<b>APPENDIX</b>	<b>58</b>
24x80 MODEL - WAVE HEIGHT PROFILES	58
DEFENDER™ MODEL - WAVE HEIGHT PROFILES	60
21x60 (WITH CAP) MODEL - WAVE HEIGHT PROFILES	62

# List of Tables

TABLE 1. TESTING CONDITIONS FOR THE 24x80 MODEL.....	15
TABLE 2. TESTING CONDITIONS FOR THE DEFENDER™ MODEL.....	16
TABLE 3. TESTING CONDITIONS FOR THE 21x60 (WITH CAP) MODEL.....	17
TABLE 4. TESTING CONDITIONS FOR THE 21x60 (NO CAP) MODEL.....	18
TABLE 5. WAVE GAUGE LOCATIONS.....	19
TABLE 6. LOCATION INFORMATION FOR THE NORTEK ADV.....	20
TABLE 7. SAMPLE WAVE SUMMARY OUTPUT FOR A SINGLE TEST OF THE 24x80 MODEL.....	26
TABLE 8. SAMPLE ADV SUMMARY OUTPUT FOR A SINGLE TEST OF THE 24x80 MODEL.....	27
TABLE 9. SUMMARY WAVE RESULTS FOR THE 24x80 MODEL.....	30
TABLE 10. SUMMARY WAVE RESULTS CORRELATION MATRIX FOR THE 24x80 MODEL.....	31
TABLE 11. SUMMARY WAVE RESULTS FOR THE DEFENDER™ MODEL.....	38
TABLE 12. SUMMARY WAVE RESULTS CORRELATION MATRIX FOR THE DEFENDER™ MODEL.....	39
TABLE 13. SUMMARY WAVE RESULTS FOR THE 21x60 MODEL (WITH CAP).....	46
TABLE 14. SUMMARY WAVE RESULTS CORRELATION MATRIX FOR THE 21x60 MODEL (WITH CAP).....	47
TABLE 15. WAVE TRANSMISSION MODEL ERROR ANALYSIS.....	54

# List of Figures

FIGURE 1. PLANFORM, PROFILE, AND CROSS-SECTION DIAGRAMS OF THE LWF.....	9
FIGURE 2. BED ELEVATION PROFILE AND WAVE PROBE LOCATIONS FOR THE 24x80 AND DEFENDER™ TESTING CONFIGURATIONS. ....	10
FIGURE 3. BED ELEVATION PROFILE AND WAVE PROBE LOCATIONS FOR THE 21x60 TESTING CONFIGURATION. ....	10
FIGURE 4. OVERVIEW AND DIMENSIONING OF THE 24x80 SCALED TESTING MODEL. ....	11
FIGURE 5. OVERVIEW AND DIMENSIONING OF THE DEFENDER™ SCALED TESTING MODEL. ....	12
FIGURE 6. OVERVIEW AND DIMENSIONING OF THE 21x60 (WITH CAP) SCALED TESTING MODEL. ....	12
FIGURE 7. OVERVIEW AND DIMENSIONING OF THE 21x60 (WITHOUT CAP) SCALED TESTING MODEL. ....	13
FIGURE 8. GENERAL LAYOUT OF MODEL COMPONENTS AND THEIR LABELS, ADV LOCATION, AND ACCELEROMETER LOCATIONS (NUMBERS) FOR THE 24x80 MODEL. ....	21
FIGURE 9. GENERAL LAYOUT OF MODEL COMPONENTS AND THEIR LABELS, ADV LOCATION, AND ACCELEROMETER LOCATIONS (NUMBERS) FOR THE DEFENDER™ MODEL. ....	21
FIGURE 10. GENERAL LAYOUT OF MODEL COMPONENTS AND THEIR LABELS, ADV LOCATION, AND ACCELEROMETER LOCATIONS (NUMBERS) FOR THE 21x60 (WITH AND WITHOUT CAP) MODELS. ....	21
FIGURE 11. EXPLANATORY GRAPHICS FOR WAVE TRANSMISSION ANALYSES.....	23
FIGURE 12. DEFINITION SKETCH FOR THE RELATIVE FREEBOARD VARIABLE. ....	25
FIGURE 13. INCIDENT WAVE HEIGHTS ALONG FLUME FOR 24x80 A SERIES TESTS (LOWEST WATER LEVEL).....	28
FIGURE 14. INCIDENT WAVE HEIGHTS ALONG FLUME FOR 24x80 D SERIES TESTS (WATER LEVEL AT CREST). ....	28
FIGURE 15. INCIDENT WAVE HEIGHTS ALONG FLUME FOR 24x80 F SERIES TESTS (HIGHEST WATER LEVEL). ....	29
FIGURE 16. WAVE TRANSMISSION AND WAVE REFLECTION COEFFICIENT VALUES AS A FUNCTION OF RELATIVE FREEBOARD FOR THE 24x80 MODEL. ....	31
FIGURE 17. SAMPLE VELOCITY MEASUREMENTS FROM EACH REPLICATE OF TEST B5 FOR THE 24x80 MODEL. ....	32
FIGURE 18. ACCELERATION MEASUREMENTS DURING ALL E SERIES TESTS FOR THE 24x80 MODEL. ....	33
FIGURE 19. ROTATIONAL MEASUREMENTS DURING ALL E SERIES TESTS FOR THE 24x80 MODEL. ....	34
FIGURE 20. INCIDENT WAVE HEIGHTS ALONG FLUME FOR DEFENDER™ A SERIES TESTS (LOWEST WATER LEVEL).....	36
FIGURE 21. INCIDENT WAVE HEIGHTS ALONG FLUME FOR DEFENDER™ D SERIES TESTS (WATER LEVEL AT CREST). ....	36
FIGURE 22. INCIDENT WAVE HEIGHTS ALONG FLUME FOR DEFENDER™ F SERIES TESTS (HIGHEST WATER LEVEL). ....	37
FIGURE 23. WAVE TRANSMISSION AND WAVE REFLECTION COEFFICIENT VALUES AS A FUNCTION OF RELATIVE FREEBOARD FOR THE DEFENDER™ MODEL. ....	39
FIGURE 24. SAMPLE VELOCITY MEASUREMENTS FROM EACH REPLICATE OF TEST B5 FOR THE DEFENDER™ MODEL. ....	40
FIGURE 25. ACCELERATION MEASUREMENTS DURING ALL B SERIES TESTS FOR THE DEFENDER™ MODEL. ....	41
FIGURE 26. ROTATIONAL MEASUREMENTS DURING ALL B SERIES TESTS FOR THE DEFENDER™ MODEL. ....	42
FIGURE 27. INCIDENT WAVE HEIGHTS ALONG FLUME FOR 21x60 (WITH CAP) A SERIES TESTS (LOWEST WATER LEVEL). .	44

FIGURE 28. INCIDENT WAVE HEIGHTS ALONG FLUME FOR 21x60 (WITH CAP) E SERIES TESTS (WATER LEVEL AT CREST).	44
FIGURE 29. INCIDENT WAVE HEIGHTS ALONG FLUME FOR 21x60 (WITH CAP) F SERIES TESTS (HIGHEST WATER LEVEL).	45
FIGURE 30. WAVE TRANSMISSION AND WAVE REFLECTION COEFFICIENT VALUES AS A FUNCTION OF RELATIVE FREEBOARD FOR THE 21x60 (WITH CAP) MODEL.	47
FIGURE 31. WAVE TRANSMISSION AND WAVE REFLECTION COEFFICIENT VALUES AS A FUNCTION OF PERCENT EMERGENCE FOR THE 21x60 (WITH CAP) MODEL.	48
FIGURE 32. SAMPLE VELOCITY MEASUREMENTS FROM EACH REPLICATE OF TEST B5 FOR THE 21x60 (WITH CAP) MODEL.	49
FIGURE 33. ACCELERATION MEASUREMENTS DURING ALL D SERIES TESTS FOR THE 21x60 (WITH CAP) MODEL.	50
FIGURE 34. ROTATIONAL MEASUREMENTS DURING ALL D SERIES TESTS FOR THE 21x60 (WITH CAP) MODEL.	51
FIGURE 35. PREDICTIVE MODEL OF WAVE TRANSMISSION FOR THE 24x80 MODEL (EQUATION 9).	52
FIGURE 36. PREDICTIVE MODEL OF WAVE TRANSMISSION FOR THE DEFENDER™ MODEL (EQUATION 10).	53
FIGURE 37. PREDICTIVE MODEL OF WAVE TRANSMISSION FOR THE 21x60 (WITH CAP) MODEL (EQUATION 11).	53
FIGURE 38. TRENDS IN WAVE REFLECTION AS FUNCTIONS OF WAVE STEEPNESS AND RELATIVE FREEBOARD FOR THE 24x80 MODEL.	55
FIGURE 39. TRENDS IN WAVE REFLECTION AS FUNCTIONS OF WAVE STEEPNESS AND RELATIVE FREEBOARD FOR THE DEFENDER™ MODEL.	56
FIGURE 40. TRENDS IN WAVE REFLECTION AS FUNCTIONS OF WAVE STEEPNESS AND RELATIVE FREEBOARD FOR THE 21x60 (WITH CAP) MODEL.	56
FIGURE 41. MEASURED WAVE HEIGHT VARIATION ALONG THE FLUME FOR A TESTS OF THE 24x80 MODEL.	58
FIGURE 42. MEASURED WAVE HEIGHT VARIATION ALONG THE FLUME FOR B TESTS OF THE 24x80 MODEL.	58
FIGURE 43. MEASURED WAVE HEIGHT VARIATION ALONG THE FLUME FOR D TESTS OF THE 24x80 MODEL.	58
FIGURE 44. MEASURED WAVE HEIGHT VARIATION ALONG THE FLUME FOR E TESTS OF THE 24x80 MODEL.	58
FIGURE 45. MEASURED WAVE HEIGHT VARIATION ALONG THE FLUME FOR F TESTS OF THE 24x80 MODEL.	58
FIGURE 46. INCIDENT WAVE HEIGHT VARIATION ALONG THE FLUME FOR A TESTS OF THE 24x80 MODEL.	59
FIGURE 47. INCIDENT WAVE HEIGHT VARIATION ALONG THE FLUME FOR B TESTS OF THE 24x80 MODEL.	59
FIGURE 48. INCIDENT WAVE HEIGHT VARIATION ALONG THE FLUME FOR D TESTS OF THE 24x80 MODEL.	59
FIGURE 49. INCIDENT WAVE HEIGHT VARIATION ALONG THE FLUME FOR E TESTS OF THE 24x80 MODEL.	59
FIGURE 50. INCIDENT WAVE HEIGHT VARIATION ALONG THE FLUME FOR F TESTS OF THE 24x80 MODEL.	59
FIGURE 51. MEASURED WAVE HEIGHT VARIATION ALONG THE FLUME FOR A TESTS OF THE DEFENDER™ MODEL.	60
FIGURE 52. MEASURED WAVE HEIGHT VARIATION ALONG THE FLUME FOR B TESTS OF THE DEFENDER™ MODEL.	60
FIGURE 53. MEASURED WAVE HEIGHT VARIATION ALONG THE FLUME FOR D TESTS OF THE DEFENDER™ MODEL.	60
FIGURE 54. MEASURED WAVE HEIGHT VARIATION ALONG THE FLUME FOR E TESTS OF THE DEFENDER™ MODEL.	60
FIGURE 55. MEASURED WAVE HEIGHT VARIATION ALONG THE FLUME FOR F TESTS OF THE DEFENDER™ MODEL.	60
FIGURE 56. INCIDENT WAVE HEIGHT VARIATION ALONG THE FLUME FOR A TESTS OF THE DEFENDER™ MODEL.	61

FIGURE 57. INCIDENT WAVE HEIGHT VARIATION ALONG THE FLUME FOR B TESTS OF THE DEFENDER™ MODEL. ....	61
FIGURE 58 .INCIDENT WAVE HEIGHT VARIATION ALONG THE FLUME FOR D TESTS OF THE DEFENDER™ MODEL. ....	61
FIGURE 59. INCIDENT WAVE HEIGHT VARIATION ALONG THE FLUME FOR E TESTS OF THE DEFENDER™ MODEL. ....	61
FIGURE 60. INCIDENT WAVE HEIGHT VARIATION ALONG THE FLUME FOR F TESTS OF THE DEFENDER™ MODEL. ....	61
FIGURE 61. MEASURED WAVE HEIGHT VARIATION ALONG THE FLUME FOR A TESTS OF THE 21x60(WITH CAP) MODEL. ....	62
FIGURE 62. MEASURED WAVE HEIGHT VARIATION ALONG THE FLUME FOR B TESTS OF THE 21x60 (WITH CAP) MODEL....	62
FIGURE 63. MEASURED WAVE HEIGHT VARIATION ALONG THE FLUME FOR D TESTS OF THE 21x60 (WITH CAP) MODEL. ...	62
FIGURE 64. MEASURED WAVE HEIGHT VARIATION ALONG THE FLUME FOR E TESTS OF THE 21x60 (WITH CAP) MODEL....	62
FIGURE 65. MEASURED WAVE HEIGHT VARIATION ALONG THE FLUME FOR F TESTS OF THE 21x60 (WITH CAP) MODEL....	62
FIGURE 66. INCIDENT WAVE HEIGHT VARIATION ALONG THE FLUME FOR A TESTS OF THE 21x60 (WITH CAP) MODEL.....	63
FIGURE 67. INCIDENT WAVE HEIGHT VARIATION ALONG THE FLUME FOR B TESTS OF THE 21x60 (WITH CAP) MODEL.....	63
FIGURE 68. INCIDENT WAVE HEIGHT VARIATION ALONG THE FLUME FOR D TESTS OF THE 21x60 (WITH CAP) MODEL.....	63
FIGURE 69. INCIDENT WAVE HEIGHT VARIATION ALONG THE FLUME FOR E TESTS OF THE 21x60 (WITH CAP) MODEL.....	63
FIGURE 70. INCIDENT WAVE HEIGHT VARIATION ALONG THE FLUME FOR F TESTS OF THE 21x60 (WITH CAP) MODEL. ....	63

# Introduction

This report describes the results of reduced scale physical experiments to evaluate the performance and hydrodynamic stability of QuickReef® products manufactured by Native Shorelines, a Davey Company. Experiments were carried out in the University of South Alabama's Large Wave Flume (LWF) facility within the Center for Applied Coastal Engineering and Science. These tests were carried out under a testing services agreement (ACES 24-003) between the University of South Alabama and Native Shorelines dated February 6, 2024.

Three unique QuickReef® product setups were tested between the dates of February 6-16, 2024. Testing focused on the 24x80, Defender™, and 21x60 (with cap) products. Limited testing of a fourth setup, the 21x60 (without cap), took place on February 19, 2024. During each experiment, water level measurements were obtained at eight locations—four locations before and after the model testing area—to evaluate wave reflection and wave transmission. An acoustic Doppler velocimeter (ADV) was located on the up-wave (stoss) side of the model to measure the three-dimensional velocity field near the structure. Six-axis accelerometers were adhered to the back side of selected model components to monitor movement under the various wave conditions.

This report provides a description of the testing facility, an overview of the testing/experimental plan, a summary of the testing results, and a brief discussion that synthesizes the results. All raw and processed data, as well as MATLAB scripts, synthesis spreadsheets, experiment records, and lab notes have already been shared electronically through a Google Drive folder. A physical duplicate of all pertinent testing files will be transmitted on a USB drive upon project closeout.

## Facility Description

The LWF consists of a 17.5-m long by 1.5-m wide by 1.0-m deep channel, computer-controlled piston style wavemaker, and two recirculating pumps for generating currents (not used as part of this testing). The channel rests in a steel frame and consists of stainless-steel bed panels and glass wall panels (Figure 1). A sand ( $d_{50} = 0.31$  mm) beach aids in wave energy dissipation at the far end of the tank. The sand elevation profiles for the various testing setups are described below.

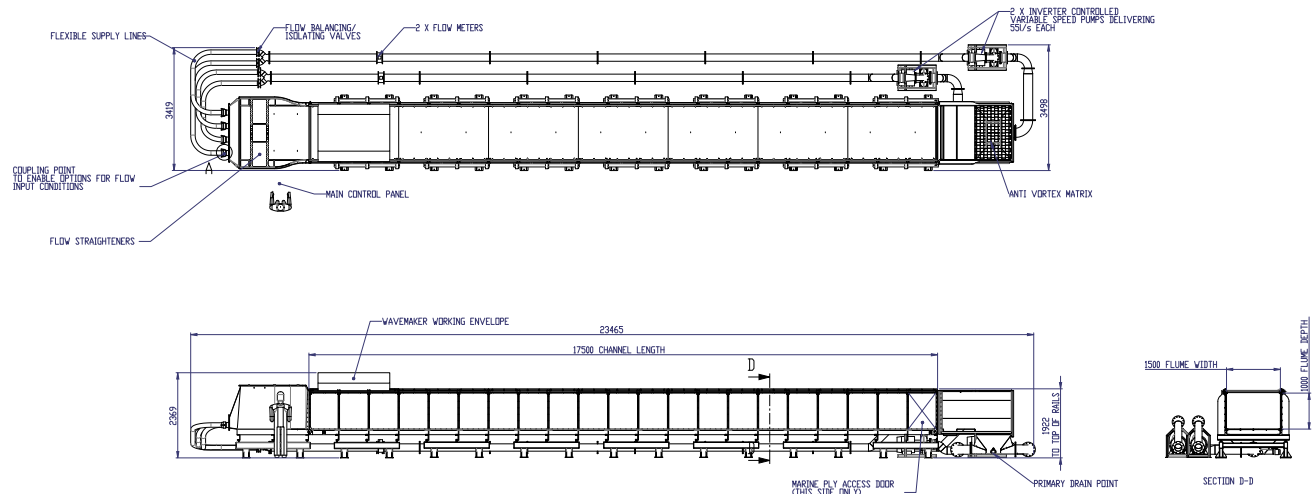


Figure 1. Planform, profile, and cross-section diagrams of the LWF.

The piston style wavemaker is controlled by computer software provided by the manufacturer, HR Wallingford. The HR Merlin Wave Generation Programme (Version 2.24-1) accepts user definitions of water depth, wave amplitude, wave frequency, wave type, test duration, and model/prototype scale. For the purpose of these experiments, the software scaling option was not used and all experiments were performed using a software scale value of 1.0. Model and prototype ratios, Froude scaling, and experimental parameters are described in a subsequent section of this report.

Prior to testing, the sand beach was reconfigured to accommodate the unique testing configurations of the various models. The bed elevation profile shown in Figure 2 corresponds to the conditions used in both the 24x80 and Defender™ testing configurations. The sand depth throughout most of the flume was 5 cm and the beach slope was approximately 1:3. Because the 21x60 product scaling rendered a much shorter structure height, the bed profile was manipulated in the testing area. As shown in Figure 3, the bed elevation was built up to an elevation of approximately 30 cm (above the tank floor). The beach slope leading up to the model testing area was approximately 1:6. The bed elevation profile data are available in the “QuickReef Flume Bed Profiles.xlsx” file.

Though a complete description of measurements is provided in the subsequent section of this report, they are briefly summarized here as part of the facility description. Measurements for these experiments focused on water levels (from which wave characteristics were derived), velocities, and movement/rotation of model components. Water levels were sampled at the eight locations shown in Figure 2 and Figure 3. Their exact locations are provided later in the report. HR Wallingford manufactures these twin wire resistive wave probes. The wave probes were calibrated, prepared, and sampled using the software program provided by the manufacturer: HR DAQ Data Acquisition and Analysis Software Programme (Version 1.24.130). A Nortek Vectrino ADV was used to sample the velocity field at a point on the exposed (up-wave or stoss) side of the model. Though the ADV was configured using Nortek’s software Vectrino Plus (Version 1.09), data acquisition took place using the HR DAQ program to synchronize the time-series measurements from the wave probes and the ADV. The six-axis accelerometers were sampled using a custom code sketch created in the Arduino IDE (Version 1.8.13) programming environment and synchronized with the computer clock time. This allowed for overall time

synchronization with the wave probe and ADV measurements by utilizing the computer clock timestamp provided on each data acquisition file.

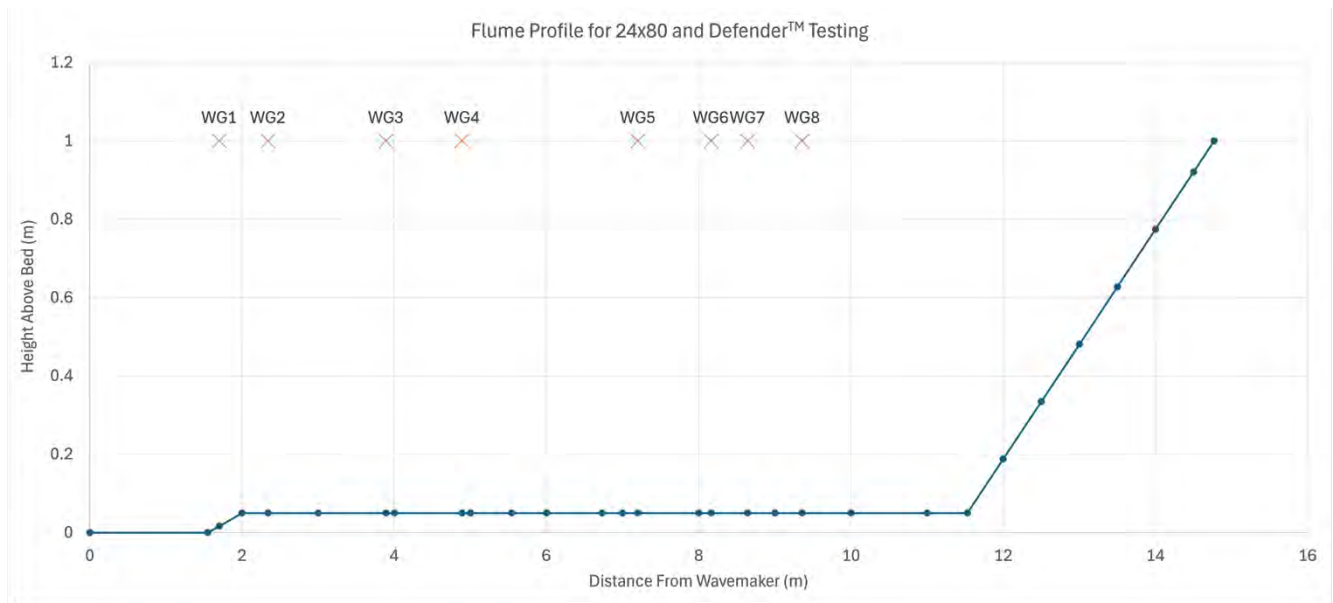


Figure 2. Bed elevation profile and wave probe locations for the 24x80 and Defender™ testing configurations.

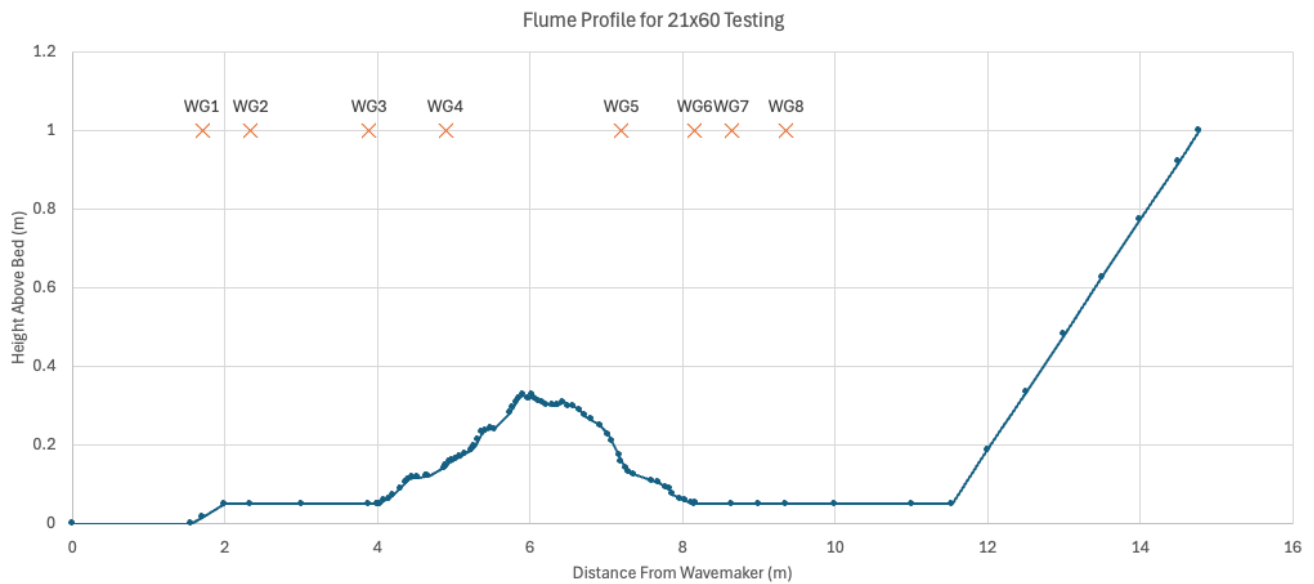


Figure 3. Bed elevation profile and wave probe locations for the 21x60 testing configuration.

# Models and Scaling

The QuickReef® models tested during this series of experiments include the 24x80 (Figure 4), Defender™ (Figure 5), 21x60 with cap (Figure 6), and 21x60 without cap (Figure 7). The figures below show the testing models in the reduced scale used during the experiments. A combination of model geometry, tank dimensions, and Froude scaling relationships were used to determine the final scale ratios for each model. The 24x80 model was scaled by 60%, resulting in a model:prototype scale ratio of 1:1.67. The Defender™ product was scaled by 33% for a scale ratio of 1:3.03. The 21x60 model was scaled by 50% yielding a scale ratio of 1:2. Note that the 1:2 scale was used for both configurations of the 21x60 model (i.e., with and without cap).

Froude scaling was used to relate desired prototype conditions, including tidal datums, wave heights, and wave periods, to their model equivalents in the LWF. The water levels and wave characteristics simulated in the LWF are therefore representative of typical and very minor storm event conditions that tend to dominate typical deployments. These conditions were determined through consultation with the client and their representatives at Southern Shores Engineering, LLC. The model and prototype conditions for each experiment are provided in the subsequent section of this report.

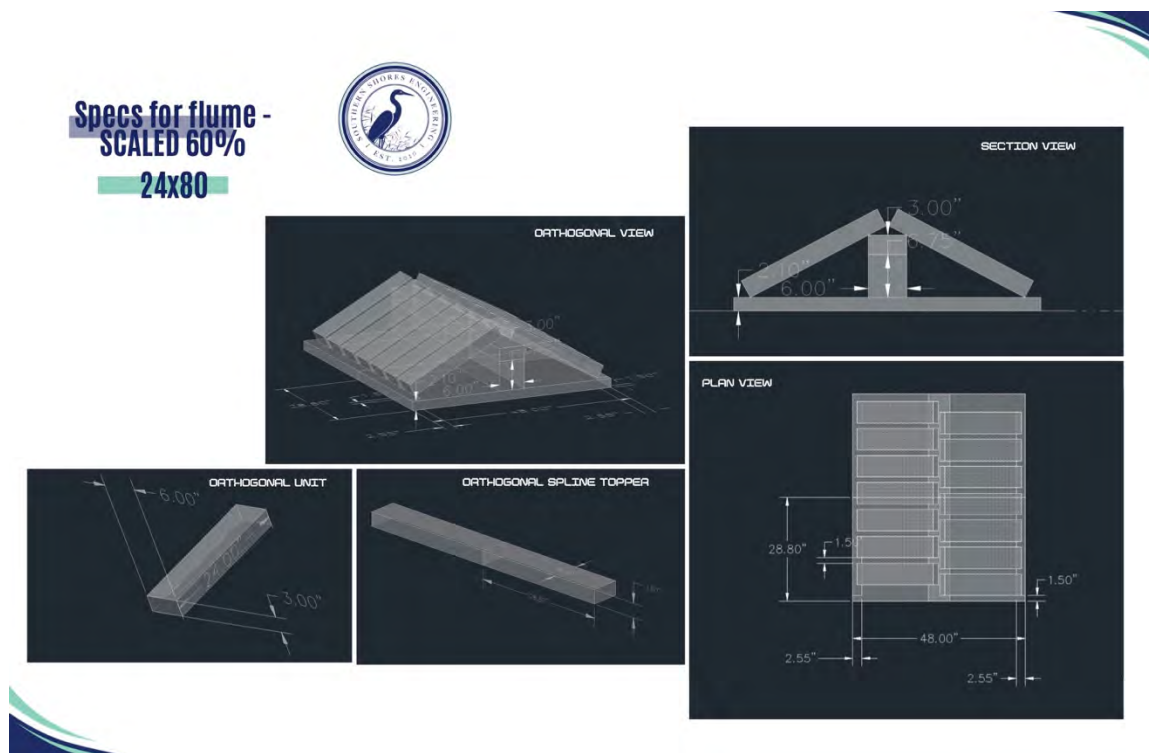


Figure 4. Overview and dimensioning of the 24x80 scaled testing model.

**Specs for flume -  
SCALED 1/3  
DEFENDER 48"x48"x16.5"**

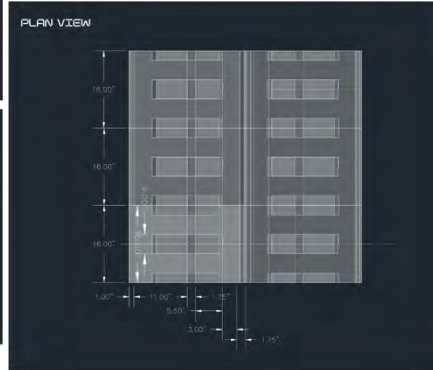
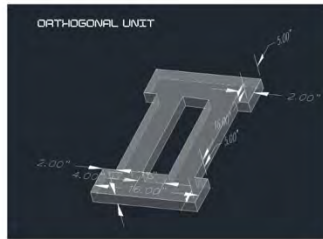


Figure 5. Overview and dimensioning of the Defender™ scaled testing model.

**Specs for flume -  
SCALED 50%  
21x60 w/ Cap**

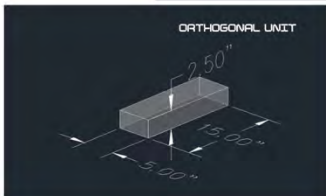
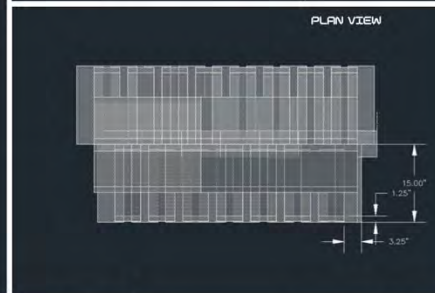
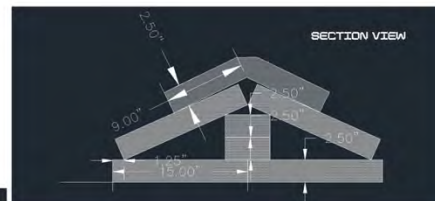
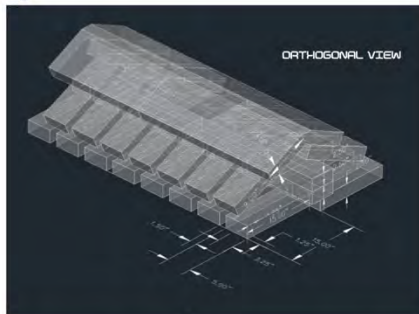


Figure 6. Overview and dimensioning of the 21x60 (with cap) scaled testing model.

Specs for flume -  
SCALED 50%  
21x60

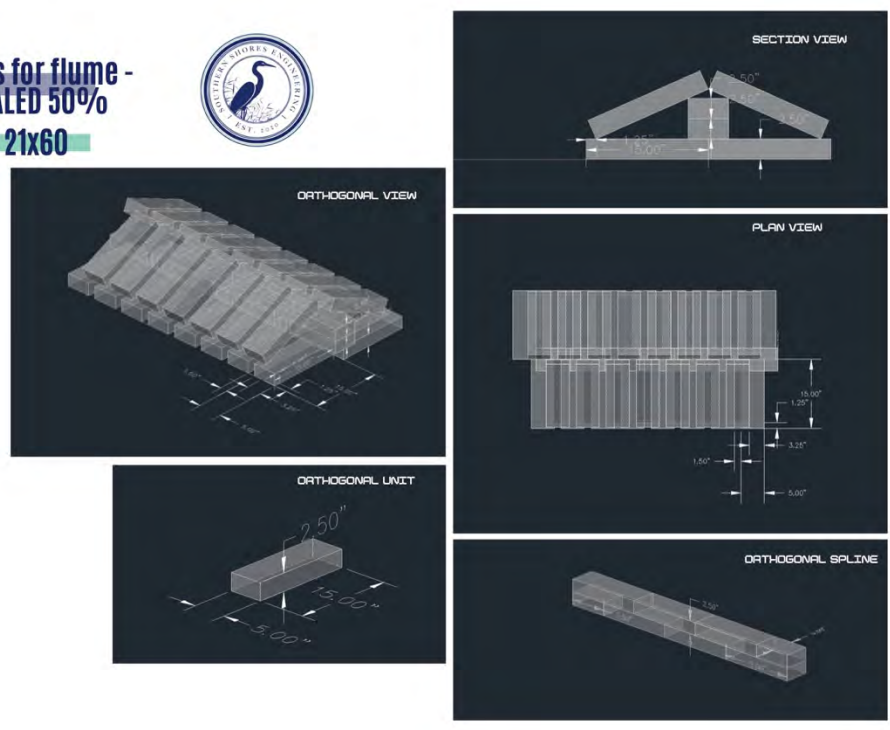


Figure 7. Overview and dimensioning of the 21x60 (without cap) scaled testing model.

# Testing Plan

Most of the testing setups consisted of experiments using five unique water levels (depths) and as many as seven unique wave conditions. With one exception, wave conditions were monochromatic. Replicates of three (designated a, b, and c) were used for each experiment. A total of 309 tests were performed across all setups, with the 24x80 and Defender™ products each having 96 tests, the 21x60 (with cap) having 105 tests, and the 21x60 (without cap) having just 12 tests. Most test durations were 60 seconds in length, except for irregular wave cases which used durations exceeding 180 seconds.

The water level and wave conditions were chosen in consultation with the client and their representatives from Southern Shores Engineering, LLC to span a range of typical tidal/synoptic tide, meteorological, and vessel wake conditions. Testing conditions did not intentionally focus on extreme event inundation or wave conditions, though some specific combinations of higher water levels and wave conditions could indeed reflect a mild storm condition at some deployment locations. The distribution of water levels relative to the crest of each structure was intentionally chosen to reflect typical tidal datums in North Carolina. For the 24x80 and Defender™ models, experiments were performed for two unique water levels below the structure crest (i.e., lower tides), one water level at the crest, and two water levels above the crest (i.e., higher tides and mild storms). Due to the small vertical dimensions of the 21x60 model, only one water level above the crest was used, while one water level coincident with the crest and three water levels below the crest served as the remaining tests.

The defining characteristics for each model test include the water depth in the LWF, the forced wave height, and the forced wave period. These values are provided for both model and prototype scales in the tables that follow. Note that the naming convention for all test case names shown in these tables includes a capital letter (A-F) designating the water level condition, where A is the lowest water level and F is the highest water level, followed by a number (1-7) designating the wave characteristics. Generally speaking, lower case numbers correspond to shorter wave periods and, therefore, higher wave steepness values. Higher case numbers typically signify longer wave periods and lower wave steepness values.

Not shown in the tables below are the replicate test cases and their designations. The conditions for each combination of water level, wave height, and wave period remain constant across all three replicates so there is no need to include them in the table. However, the replicate results do appear in some of the synthesized data spreadsheets, raw data, and processed data outputs. Replicate designations used lowercase letters a, b, and c appended to the case names shown in the table below. For example, case A1 would consist of replicate experiments labeled A1a, A1b, and A1c in the lab notes, raw data, and processed data files.

Note that in the tables below, H<sub>0</sub> and T<sub>0</sub> are used to specifically denote the wave conditions forced at the wavemaker. This is important because additional numeric values will be used to denote wave characteristics at the eight wave probe locations where water levels were measured during the tests. Also note that for all cases except A1, the H<sub>0</sub> and T<sub>0</sub> represent monochromatic conditions. For all model tests, the H<sub>0</sub> and T<sub>0</sub> associated with Case Name A1 should be interpreted as H<sub>m0</sub> and T<sub>p</sub>: the spectrally significant wave height and peak wave period.

Table 1. Testing Conditions for the 24x80 Model

24x80 Case Name	MODEL SCALE			PROTOTYPE SCALE		
	Tank Depth (mm)	T0 (s)	H0 (mm)	Tank Depth (mm)	T0 (s)	H0 (mm)
A1	190	2.00	160.00	317	2.58	266.67
A2	190	1.21	50.00	317	1.56	83.33
A3	190	1.50	60.00	317	1.94	100.00
A7	190	2.70	70.00	317	3.49	116.67
B1	330	1.20	90.00	550	1.55	150.00
B2	330	2.70	90.00	550	3.49	150.00
B3	330	1.21	120.00	550	1.56	200.00
B4	330	1.49	120.00	550	1.93	200.00
B5	330	1.89	160.00	550	2.44	266.67
B6	330	2.33	160.00	550	3.00	266.67
B7	330	2.70	200.00	550	3.49	333.33
D1	470	1.20	200.00	783	1.55	333.33
D2	470	1.90	200.00	783	2.45	333.33
D3	470	1.50	220.00	783	1.94	366.67
D4	470	1.90	220.00	783	2.45	366.67
D5	470	1.50	240.00	783	1.94	400.00
D6	470	1.90	240.00	783	2.45	400.00
D7	470	2.70	240.00	783	3.49	400.00
E1	550	1.50	250.00	916	1.94	416.67
E2	550	1.90	250.00	916	2.45	416.67
E3	550	1.50	240.00	916	1.94	400.00
E4	550	1.90	240.00	916	2.45	400.00
E5	550	1.50	220.00	916	1.94	366.67
E6	550	1.90	200.00	916	2.45	333.33
E7	550	2.70	200.00	916	3.49	333.33
F1	650	1.50	250.00	1083	1.94	416.67
F2	650	1.90	250.00	1083	2.45	416.67
F3	650	1.50	240.00	1083	1.94	400.00
F4	650	1.90	240.00	1083	2.45	400.00
F5	650	1.50	220.00	1083	1.94	366.67
F6	650	1.90	200.00	1083	2.45	333.33
F7	650	2.70	200.00	1083	3.49	333.33

Table 2. Testing Conditions for the Defender™ Model

Defender™ Case Name	MODEL SCALE			PROTOTYPE SCALE		
	Tank Depth (mm)	T0 (s)	H0 (mm)	Tank Depth (mm)	T0 (s)	H0 (mm)
A1	280	1.49	88.00	848	2.59	266.67
A2	280	0.90	28.00	848	1.57	84.85
A3	280	1.12	34.00	848	1.95	103.03
A7	280	2.01	38.00	848	3.50	115.15
B1	375	0.89	50.00	1136	1.55	151.52
B2	375	2.01	50.00	1136	3.50	151.52
B3	375	0.90	66.00	1136	1.57	200.00
B4	375	1.11	66.00	1136	1.93	200.00
B5	375	1.41	88.00	1136	2.45	266.67
B6	375	1.73	88.00	1136	3.01	266.67
B7	375	2.01	112.00	1136	3.50	339.39
D1	480	0.89	112.00	1455	1.55	339.39
D2	480	1.42	112.00	1455	2.47	339.39
D3	480	1.12	122.00	1455	1.95	369.70
D4	480	1.42	122.00	1455	2.47	369.70
D5	480	1.12	134.00	1455	1.95	406.06
D6	480	1.42	134.00	1455	2.47	406.06
D7	480	2.01	134.00	1455	3.50	406.06
E1	585	1.12	138.00	1773	1.95	418.18
E2	585	1.42	138.00	1773	2.47	418.18
E3	585	1.12	134.00	1773	1.95	406.06
E4	585	1.42	134.00	1773	2.47	406.06
E5	585	1.12	122.00	1773	1.95	369.70
E6	585	1.42	112.00	1773	2.47	339.39
E7	585	2.01	112.00	1773	3.50	339.39
F1	682	1.12	138.00	2067	1.95	418.18
F2	682	1.42	138.00	2067	2.47	418.18
F3	682	1.12	134.00	2067	1.95	406.06
F4	682	1.42	134.00	2067	2.47	406.06
F5	682	1.12	122.00	2067	1.95	369.70
F6	682	1.42	112.00	2067	2.47	339.39
F7	682	2.01	112.00	2067	3.50	339.39

Table 3. Testing Conditions for the 21x60 (with cap) Model

21x60 cap Case Name	MODEL SCALE			PROTOTYPE SCALE		
	Tank Depth (mm)	T0 (s)	H0 (mm)	Tank Depth (mm)	T0 (s)	H0 (mm)
A1	436	1.83	134.00	872	2.59	268.00
A2	436	1.10	42.00	872	1.56	84.00
A3	436	1.37	50.00	872	1.94	100.00
A4	436	1.73	50.00	872	2.45	100.00
A5	436	1.37	58.00	872	1.94	116.00
A6	436	1.73	58.00	872	2.45	116.00
A7	436	2.47	58.00	872	3.49	116.00
B1	504	1.10	76.00	1008	1.55	152.00
B2	504	2.47	76.00	1008	3.49	152.00
B3	504	1.10	100.00	1008	1.56	200.00
B4	504	1.36	100.00	1008	1.93	200.00
B5	504	1.72	134.00	1008	2.44	268.00
B6	504	2.12	134.00	1008	3.00	268.00
B7	504	2.47	166.00	1008	3.49	332.00
D1	572	1.10	166.00	1144	1.55	332.00
D2	572	1.73	166.00	1144	2.45	332.00
D3	572	1.37	184.00	1144	1.94	368.00
D4	572	1.73	184.00	1144	2.45	368.00
D5	572	1.37	200.00	1144	1.94	400.00
D6	572	1.73	200.00	1144	2.45	400.00
D7	572	2.47	166.00	1144	3.49	332.00
E1	640	1.37	208.00	1280	1.94	416.00
E2	640	1.73	208.00	1280	2.45	416.00
E3	640	1.37	200.00	1280	1.94	400.00
E4	640	1.73	200.00	1280	2.45	400.00
E5	640	1.37	184.00	1280	1.94	368.00
E6	640	1.73	166.00	1280	2.45	332.00
E7	640	2.47	166.00	1280	3.49	332.00
F1	708	1.37	208.00	1416	1.94	416.00
F2	708	1.73	208.00	1416	2.45	416.00
F3	708	1.37	200.00	1416	1.94	400.00
F4	708	1.73	200.00	1416	2.45	400.00
F5	708	1.37	184.00	1416	1.94	368.00
F6	708	1.73	166.00	1416	2.45	332.00
F7	708	2.47	166.00	1416	3.49	332.00

Table 4. Testing Conditions for the 21x60 (no cap) Model

21x60 no cap Case Name	MODEL SCALE			PROTOTYPE SCALE		
	Tank Depth (mm)	T0 (s)	H0 (mm)	Tank Depth (mm)	T0 (s)	H0 (mm)
B3	504	1.10	100.00	1008	1.56	200.00
B4	504	1.36	100.00	1008	1.93	200.00
B5	504	1.72	134.00	1008	2.44	268.00
B6	504	2.12	134.00	1008	3.00	268.00

Please refer to the spreadsheet labeled “QuickReef Master Experiment Spreadsheet Final.xlsx” for more information about the testing data and setups. Also, note that a digital copy of the lab notebook is provided in the file labeled “Lab Notebook QR Testing.xlsx.”

# Measurement Plan

The objectives of this project were to evaluate wave reflection, wave transmission, and hydrodynamic stability of structure components. To that end, the measurement plan was designed to capture time histories of water levels (at multiple locations on both sides of the structure), the three-dimensional velocity field (at a single point near the structure), and movement/displacement of components (on both sides of the structure). Time histories of water levels are used to subsequently determine wave height and period at multiple locations along the LWF. The velocity data were collected to complement the hydrodynamic stability investigation and to inform proposed numerical model calibration and validation by Southern Shores Engineering, LLC.

Water level time histories were obtained using eight, twin wire resistive wave probes manufactured by HR Wallingford. Water levels were calibrated using the procedures outlined in the HR DAQ software, resulting in a three-point regression between voltage change and water level change. Water levels were sampled at a frequency of 10 Hz and were collected continuously throughout each experiment (i.e., 60 seconds for monochromatic waves and 180+ seconds for irregular waves). Wave gauge locations (Table 5) were established prior to all model testing and remained in the same locations throughout the duration of testing. In this report, all location/position data along the flume in the “x-coordinate” are defined relative to the wavemaker ( $x=0$  m). Four wave probes were situated on either side of the model testing area, which generally spanned the range  $4.9 \text{ m} < \text{testing area} < 7.2 \text{ m}$ .

Table 5. Wave Gauge Locations

Wave Gauge Name	Location (x) (m)
WG1	1.70
WG2	2.34
WG3	3.89
WG4	4.89
WG5	7.20
WG6	8.16
WG7	8.64
WG8	9.36

The use of four wave probes on either side of the model testing area was intentional. The HR DAQ software includes a reflection analysis procedure that uses data from four wave probes to estimate the distribution of wave reflection coefficients across the range of wave frequencies detected. The reflection analysis procedure is based on a least squares method for separating incident and reflected waves using surface elevation time series from an arbitrary number of wave gauges (in this case, four gauges). This method is based on a frequency-domain manipulation of one-sided water surface elevation spectra derived from the measured time series data. Here, linear wave theory is used in both the calculation of the wavenumber and in the superposition of monochromatic signals to represent the measured surface time series. The

least squares method used in this “N-gauge” method is based on the work of Mansard and Funke (1980) with improvements by Isaacson (1991) and Zelt and Skjelbreia (1992).

Using four wave probes on either side of the model testing area allows for the separation of the incident and reflected waves on the up-wave side of the structure, as well as separation of the transmitted and reflected waves (from the beach) on the down-wave, or lee, side of the structure. This measurement plan for water levels allows for the determination of accurate reflection and transmission coefficients for each structure and experiment.

A Nortek Vectrino ADV was used to sample the three-dimensional velocity field continuously during each experiment. The Vectrino sampled at a rate of 100 Hz using a nominal range of +/- 1 m/s; a transmit length of 1.8 mm; and a sampling volume of 7.0 mm in height and 6.0 mm in diameter. The Vectrino was always located on the up-wave side of the structure (in the x-direction), but the cross-tank or spanwise location (y-direction) and height above the bed (z-direction) varied from model to model to accommodate their different geometries. See Table 6 for more information about ADV locations for each model geometry. In terms of coordinate axes, the x-direction is defined as positive in the direction of wave travel and then a right-handed coordinate system defines the positive y-direction as across the flume (towards the back wall of the lab opposite the entrance and staging areas), and the positive z-direction as being oriented vertically upward towards the ceiling. A similar coordinate axis system is used for all aspects of this testing.

Table 6. Location Information for the Nortek ADV

Model Type	Height Above Bottom (m)	X Location (m)	Y Location
24x80 Defender™	0.126	5.904	Between Panels A and B
21x60 cap	0.055	5.968	Middle of Panel B
21x60 no cap	0.067	5.986	Between Panels D and E
	0.075	5.986	Between Panels D and E

Component stability under wave loading was evaluated using custom-made, six-axis accelerometers (Adafruit LSM6DSOX 6 DoF Accelerometer and Gyroscope). The accelerometers were potted in epoxy and then affixed to the rear of specific component panels on both sides (up- and down-wave) of the structure using epoxy, plastic mounts, and nylon cable ties. Wires were bundled and hidden within the structure cavities to avoid interference with the ADV measurements, then taped to the flume wall and led to the data logger. The data logger consisted of an Adafruit Feather 32u4 microcontroller and Adafruit DS321 real time clock synchronized to computer clock time (see “Experiment Data Record Times.xlsx” for more information about the start time of each experiment). All accelerometer data were sampled at a rate of 10 Hz. General schematics showing component labeling (letters) and sensor layout (numbers) are shown below (Figure 8-Figure 10) for each model. Note that these are stylized and not representative of scale in any dimension.

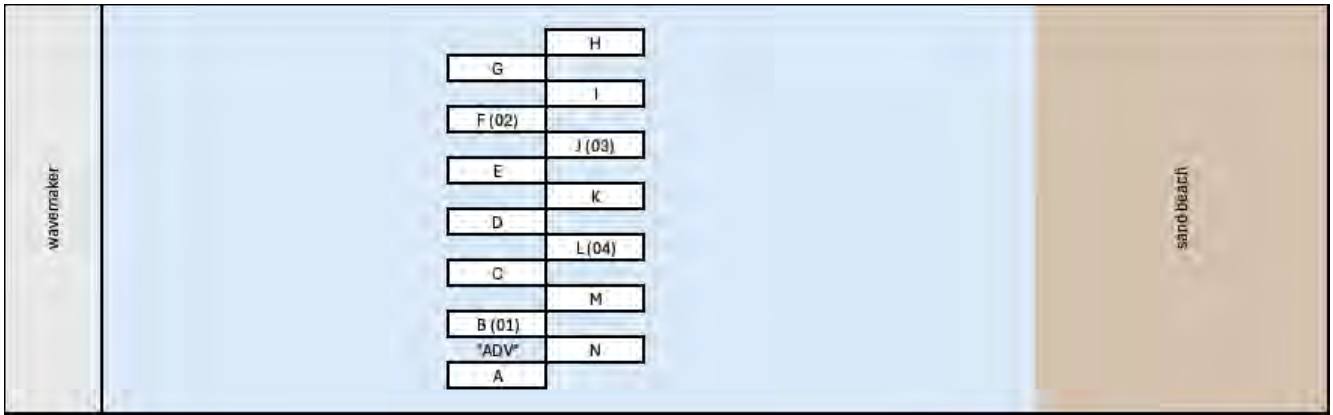


Figure 8. General layout of model components and their labels, ADV location, and accelerometer locations (numbers) for the 24x80 model.

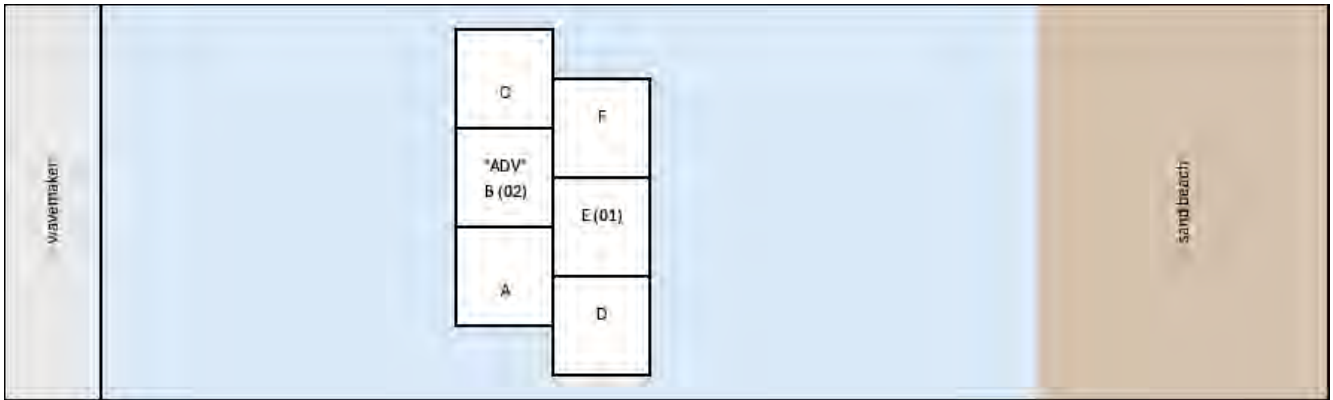


Figure 9. General layout of model components and their labels, ADV location, and accelerometer locations (numbers) for the Defender™ model.

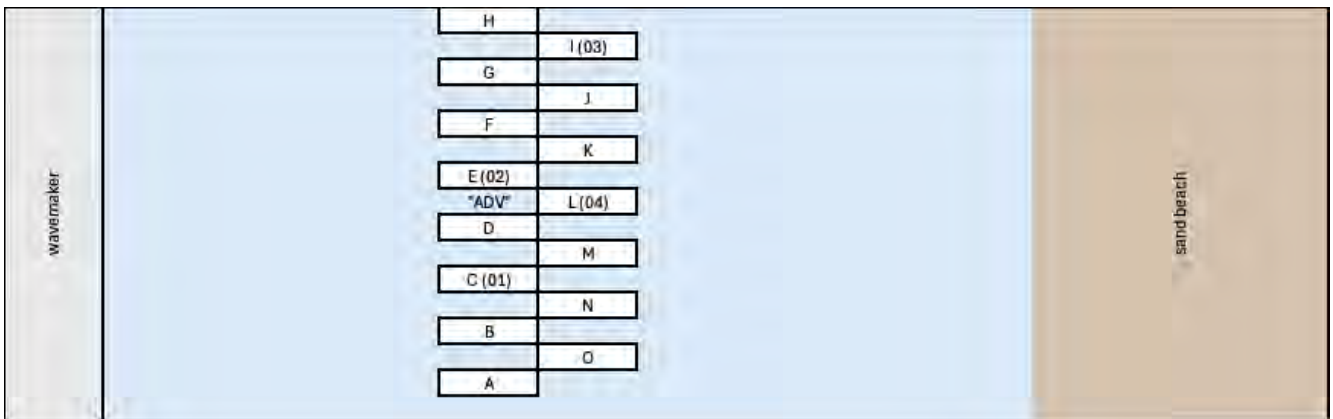


Figure 10. General layout of model components and their labels, ADV location, and accelerometer locations (numbers) for the 21x60 (with and without cap) models.

## Methods

This section briefly describes some of the pertinent methods used to post-process and analyze water level data from the eight wave probes, velocity data from the Nortek ADV, and component movement data from the six-axis accelerometers. Most of the post-processing and analysis efforts were allocated to reducing the water level data to separate the incident and reflected wave signals for the purpose of describing wave transmission and wave reflection. Some simple processing of the ADV data is described, as is the preparation and interpretation of the accelerometer data. Results are presented in a subsequent section.

Water level time histories were analyzed in MATLAB (Release 2023b) using a zero-crossing method for detecting individual wave events. Once detected, local maxima and minima in between the zero-crossings were used to estimate the wave height. The time difference between the values of the zero-crossings themselves served as estimates of the individual wave periods. The wave events were then sorted by rank order and the top 50 percent of wave events were analyzed to determine a representative wave height and period at each wave probe location. The summary spreadsheets were then used to ingest the results of these statistical analyses for each replicate and each test case. These summary spreadsheets report the averages and standard deviations of wave heights and wave periods for each replicate, along with a representative value taken as the average across all individual replicates. The number of wave events detected are also listed for each replicate, across all test cases, at every wave probe. The results, which can be seen in the Master Synthesis Spreadsheet described in the Results section, show the estimated average wave height and period across all replicates and cases for each gauge/probe location.

One can estimate a “bulk transmission coefficient” by taking the ratio of the transmitted wave height ( $H_5$ ) to the incident wave height ( $H_4$ ) as in Equation 1, but this value does not accurately portray the wave transmission alone. Instead, this bulk coefficient accounts for transmitted, reflected, and dissipated wave energy and, therefore, is less helpful from a design standpoint. A true transmission coefficient requires separation of incident and reflected wave signals on both sides of the structure. To that end, the HR DAQ software was used to estimate average reflection coefficients ( $K_r$ ) on both sides of the structure. Wave gauges 1-4 were used to estimate the structure reflection coefficient. Wave gauges 5-8 were used to estimate the beach reflection coefficient. These reflection coefficients are individually referred to as  $K_{r1|4}$  and  $K_{r5|8}$ , respectively. Generally speaking, the reflection coefficient is taken as the ratio of reflected wave height to incident wave height (Equation 2). An explanatory graphic is provided in Figure 11 to demonstrate the methodology applied to separation of incident, reflected, and transmitted wave signals.

$$K_t = \frac{H_t}{H_i} = \frac{H_5}{H_4} \quad (1)$$

$$K_r = \frac{H_r}{H_i} \quad (2)$$

## WAVE TRANSMISSION & REFLECTION CALCULATIONS

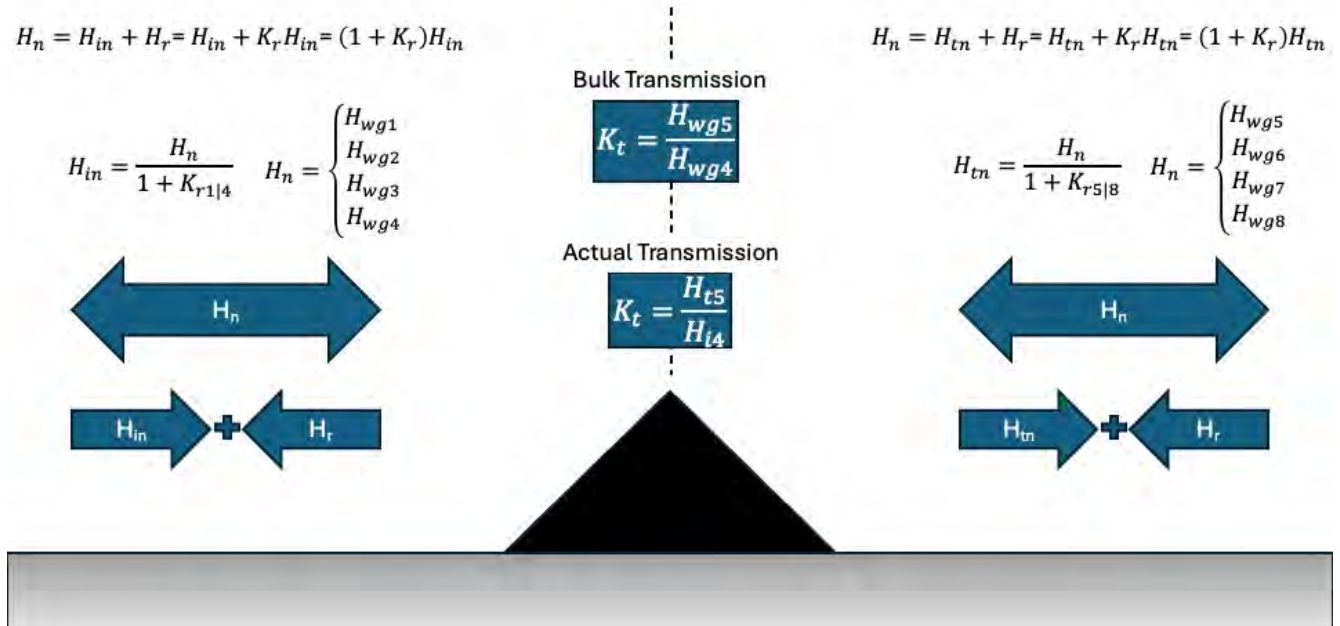


Figure 11. Explanatory graphics for wave transmission analyses.

As shown in Figure 11, the measured wave signal on either side of the structure represents the sum of incident and reflected wave signals. Once the reflection coefficients from either grouping of four wave probes is known, those signals can be decomposed as illustrated in the graphic. The resulting wave transmission coefficient can then be taken as the ratio of the transmitted wave height at wave probe 5 to the incident wave height detected at wave probe 4 (Equation 3).

$$K_t = \frac{H_{t5}}{H_{i4}} \quad (3)$$

When a wave encounters a structure, the wave energy often undergoes three main transformations: transmission, reflection, and dissipation. Consider this example: assuming a transmission coefficient of 0.4 and a reflection coefficient of 0.2, that would suggest that 40 percent of the wave height is transmitted past the structure while 20 percent of the wave height is reflected from the structure. The remaining 40 percent ( $100 - 40 - 20 = 60$ ) of the wave height must have been dissipated by or on the structure in some way. Similarly, we can estimate a dissipation coefficient as shown in Equation 4. Estimated values of  $K_d$  are provided in the Master Synthesis Spreadsheet, but no substantial analysis of their behavior is provided since we cannot say, definitely, what that dissipation coefficient actually accounts for or what is driving that dissipation.

$$K_d = 1 - K_t - K_r \quad (4)$$

Before describing a few other important parameters provided in the Master Synthesis Spreadsheet, some of which will be used below in the Results section, we should note two variations of the transmission and dissipation coefficients. In addition to the  $K_t$  and  $K_d$  values for actual (corrected) wave transmission and the corresponding value of wave dissipation, we also provide complementary values noted as  $K_{tavg}$  and  $K_{davg}$ . The average (corrected) wave transmission value is computed as shown in Equation 5, while the subsequent value of the average wave dissipation coefficient is provided in Equation 6. These might serve as the “best” estimates of those processes as they tend to smooth out a lot of complicated wave transformation processes that are occurring on either side of the structure.

$$K_{tavg} = \frac{\overline{H_{t5} + H_{t6}}}{\overline{H_{t3} + H_{t4}}} \quad (5)$$

$$K_{davg} = 1 - K_{tavg} - K_r \quad (6)$$

Interestingly, as will be shown in the Results section, plotting the values derived from Equations 1, 3, and 5 together on the same figure do not show a large amount of scatter. There is generally very good agreement in the values, and trends, of all three estimates of wave transmission. This is encouraging, as it suggests that predicting values of wave transmission in the field using either analytical methods or numerical modeling outputs may be somewhat insensitive to the methodology used. In other words, the variation of  $K_t$  with water levels is much stronger than any influence of wave reflection.

Other parameter values shown in the synthesis spreadsheets and referred to below in the Results section include emergence, freeboard, relative freeboard, wave steepness, and the Ursell number. Emergence, freeboard, and relative freeboard are related concepts and refer to the position of the water level relative to the structure crest. In this study, emergence is simply expressed as the percentage of the structure height above or below the water. Percent emergence is taken as positive when the water level is below the crest (i.e., emergent) and negative when the water level is above the crest (i.e., submerged). Freeboard is the distance between the water level and the structure crest, again taken as positive when emergent and negative when submerged. The relative freeboard is taken as the ratio of the freeboard to the incident wave height as shown in Figure 12. Relative freeboard is a very helpful concept as it incorporates the wave height and, therefore, captures some potential for wave transmission through overtopping. In other words, even for a large amount of emergent freeboard a very large incident wave height would result in a smaller value of relative freeboard and a corresponding increase in potential wave transmission (as shown in the results below).

Two other parameters that are more associated with the wave characteristics themselves are the wave steepness and Ursell number. The equation used to approximate wave steepness is:

$$\frac{H}{L} = \frac{H}{T\sqrt{gd}} \quad (7)$$

where  $H$  is wave height,  $L$  is wavelength,  $T$  is wave period,  $d$  is water depth, and  $g$  is gravitational acceleration. Here we have substituted the shallow water approximation for wavelength to simplify the analysis. Many wave transformations are sensitive to wave steepness. Similar to wave steepness, the Ursell number or Ursell parameter provides a measure of wave nonlinearity where higher numbers correspond to higher degrees of nonlinearity. The equation for Ursell number is given as:

$$U_r = \frac{HL^2}{d^3} = \frac{H(T\sqrt{gd})^2}{d^3} = \frac{HgT^2}{d^2} \quad (8)$$

where again the shallow water approximation for wavelength is used for simplicity.

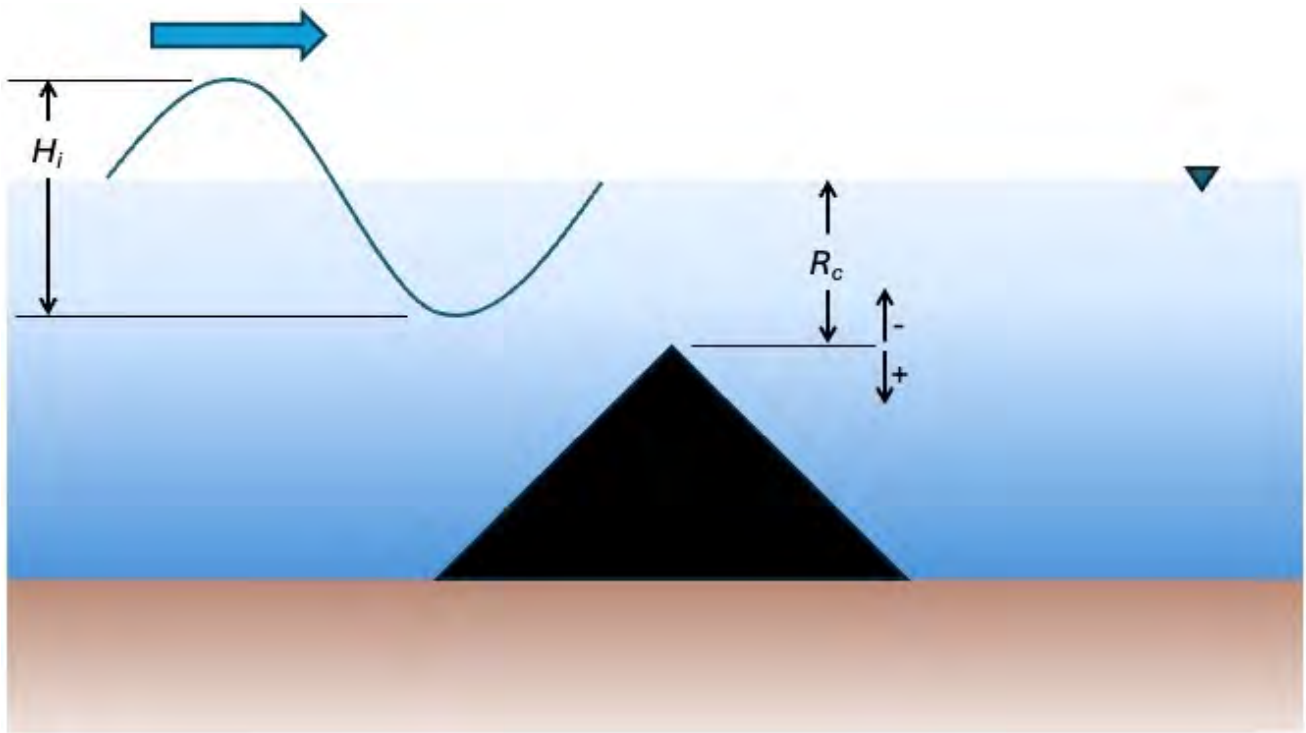


Figure 12. Definition sketch for the relative freeboard variable.

# Results

This section of the report provides a brief summary and description of results obtained after analyzing water level data from the eight wave probes, velocity data from the Nortek ADV, and component movement data from the six-axis accelerometers. Representative samples of velocity and accelerometer data are provided here but will not serve as the focus of the results. Rather, this section will primarily focus on wave reflection and transmission behavior as a function of water level and wave conditions. The complete analyses for all data are available in the processed data folder in the shared Google Drive. Analysis of the water level and velocity data are summarized by model type in separate spreadsheets (see for example Table 7 and Table 8, respectively). For the water level data, a spreadsheet labeled “Master Synthesis Spreadsheet.xlsx” contains a synthesis of all experimental testing. There are no summary spreadsheets or synthesis for the accelerometer data as component movement was not substantial.

Table 7. Sample Wave Summary Output for a Single Test of the 24x80 Model

Variable	Units	wg1	wg2	wg3	wg4	wg5	wg6	wg7	wg8
<b>All H avg</b>	mm	140.46	151.86	162.66	107.78	114.29	98.79	96.02	127.30
<b>All H std dev</b>	mm	2.55	14.86	3.41	9.09	36.81	16.49	8.64	30.21
<b>All H sorted avg</b>	mm	162.84	177.34	191.29	179.44	145.55	155.07	156.26	191.62
<b>All H sorted std dev</b>	mm	4.30	11.20	6.41	12.42	33.31	15.90	15.82	30.00
<b>All T avg</b>	s	2.68	2.63	2.68	1.67	2.40	1.73	1.73	2.26
<b>All T std dev</b>	s	0.00	0.06	0.01	0.19	0.40	0.26	0.35	0.53
<b>a: Avg H</b>	mm	143.37	167.86	164.73	118.28	81.16	95.08	104.65	145.43
<b>a: Std Dev H</b>	mm	33.32	38.98	44.04	81.08	41.61	70.97	77.57	82.81
<b>a: Sorted H</b>	mm	167.50	190.21	196.46	193.39	116.88	157.83	172.79	212.54
<b>a: Avg T</b>	s	2.68	2.69	2.67	1.88	1.95	2.01	2.13	2.55
<b>a: Std Dev T</b>	s	0.08	0.10	0.13	0.93	0.99	0.79	0.75	0.76
<b>a: Number of Waves</b>	-	19.00	19.00	19.00	31.00	30.00	28.00	27.00	22.00
<b>b: Avg H</b>	mm	139.38	149.23	164.52	102.55	107.80	116.81	96.03	144.06
<b>b: Std Dev H</b>	mm	32.77	37.35	42.53	76.48	42.33	57.19	61.78	76.93
<b>b: Sorted H</b>	mm	162.01	172.00	193.29	175.32	137.68	169.42	154.73	205.07
<b>b: Avg T</b>	s	2.68	2.62	2.68	1.56	2.59	1.64	1.56	2.59
<b>b: Std Dev T</b>	s	0.06	0.37	0.11	0.78	1.03	0.62	0.83	0.81
<b>b: Number of Waves</b>	-	20.00	20.00	19.00	33.00	22.00	31.00	31.00	22.00
<b>c: Avg H</b>	mm	138.64	138.49	158.72	102.51	153.92	84.47	87.38	92.43
<b>c: Std Dev H</b>	mm	30.75	45.57	39.87	70.64	42.24	60.67	55.11	70.88
<b>c: Sorted H</b>	mm	159.01	169.80	184.12	169.60	182.09	137.97	141.27	157.25
<b>c: Avg T</b>	s	2.68	2.57	2.69	1.56	2.67	1.52	1.48	1.65
<b>c: Std Dev T</b>	s	0.06	0.52	0.15	0.74	0.08	0.82	0.66	0.82
<b>c: Number of Waves</b>	-	19.00	20.00	19.00	33.00	19.00	36.00	33.00	35.00

Table 8. Sample ADV Summary Output for a Single Test of the 24x80 Model

Variable	Units	Replicate a	Replicate b	Replicate c	Average	Std Deviation
<b>U max</b>	m/s	0.64	0.72	1.66	1.00	0.57
<b>U 75th Percentile</b>	m/s	0.14	0.16	0.17	0.16	0.02
<b>U 50th Percentile</b>	m/s	0.06	0.08	0.08	0.07	0.01
<b>U 25th Percentile</b>	m/s	0.02	0.03	0.03	0.03	0.00
<b>U min</b>	m/s	-0.34	-1.69	-0.59	-0.87	0.72
<b>V max</b>	m/s	0.39	0.73	0.44	0.52	0.18
<b>V 75th Percentile</b>	m/s	0.07	0.09	0.09	0.08	0.01
<b>V 50th Percentile</b>	m/s	0.03	0.05	0.05	0.04	0.01
<b>V 25th Percentile</b>	m/s	0.01	0.01	0.01	0.01	0.00
<b>V min</b>	m/s	-0.48	-1.55	-1.56	-1.20	0.62
<b>W max</b>	m/s	0.15	0.18	0.18	0.17	0.02
<b>W 75th Percentile</b>	m/s	0.17	0.21	0.21	0.20	0.02
<b>W 50th Percentile</b>	m/s	0.11	0.13	0.13	0.12	0.01
<b>W 25th Percentile</b>	m/s	0.03	0.04	0.03	0.04	0.01
<b>W min</b>	m/s	-0.42	-0.47	-0.48	-0.46	0.03

The following subsections present representative results of wave transmission, wave reflection, velocity time histories, and acceleration/rotation time histories for the 24x80, Defender™, and 21x60 (with cap) models. Results for the 21x60 model without the cap are available only in the spreadsheets. There was not enough testing performed to draw meaningful conclusions from the data. All figures and tables shown below are available in the spreadsheets and/or processed data folders.

## 24x80 Model Results

Representative profiles of incident wave height as a function of distance along the flume are shown for the lowest water level (most emergence), the water level at the structure crest, and the highest level (most submergence) are provided in Figure 13, Figure 14, and Figure 15, respectively. All profiles of measured and incident wave height variation with flume length are shown in the appendices and are available in the Master Synthesis Spreadsheet file. These figures clearly show two behaviors: the reduction in wave height on the protected, or lee, side of the structure ( $x > 7000$  mm); and the increase in transmitted wave heights with increasing water levels. For reference, the model testing area generally corresponds to the area  $5000 \text{ mm} < x < 7000 \text{ mm}$ . As would be expected, wave attenuation (i.e., lower transmission) is strongest when water levels are low relative to the structure crest, and it is weakest when water levels are above the structure crest. This pattern is consistent with our understanding of wave transmission as a function of water level for many types of coastal engineering structures (e.g., breakwaters, reefs, sills, etc.).

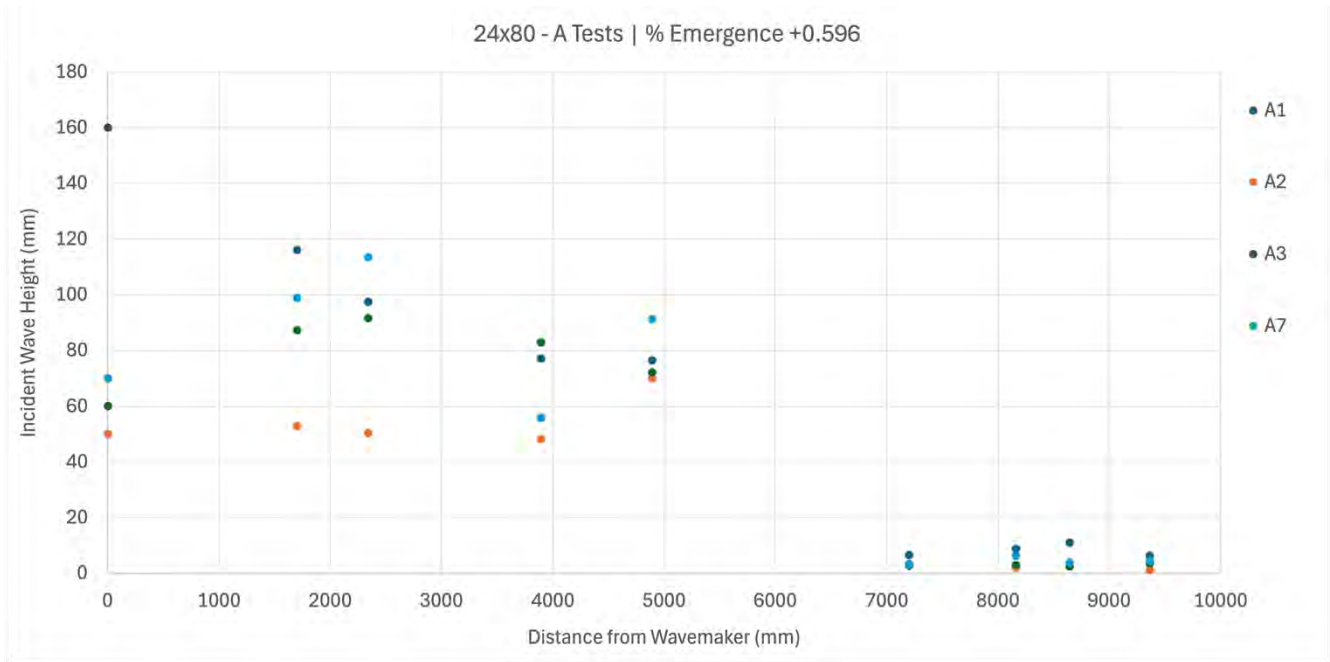


Figure 13. Incident wave heights along flume for 24x80 A series tests (lowest water level).

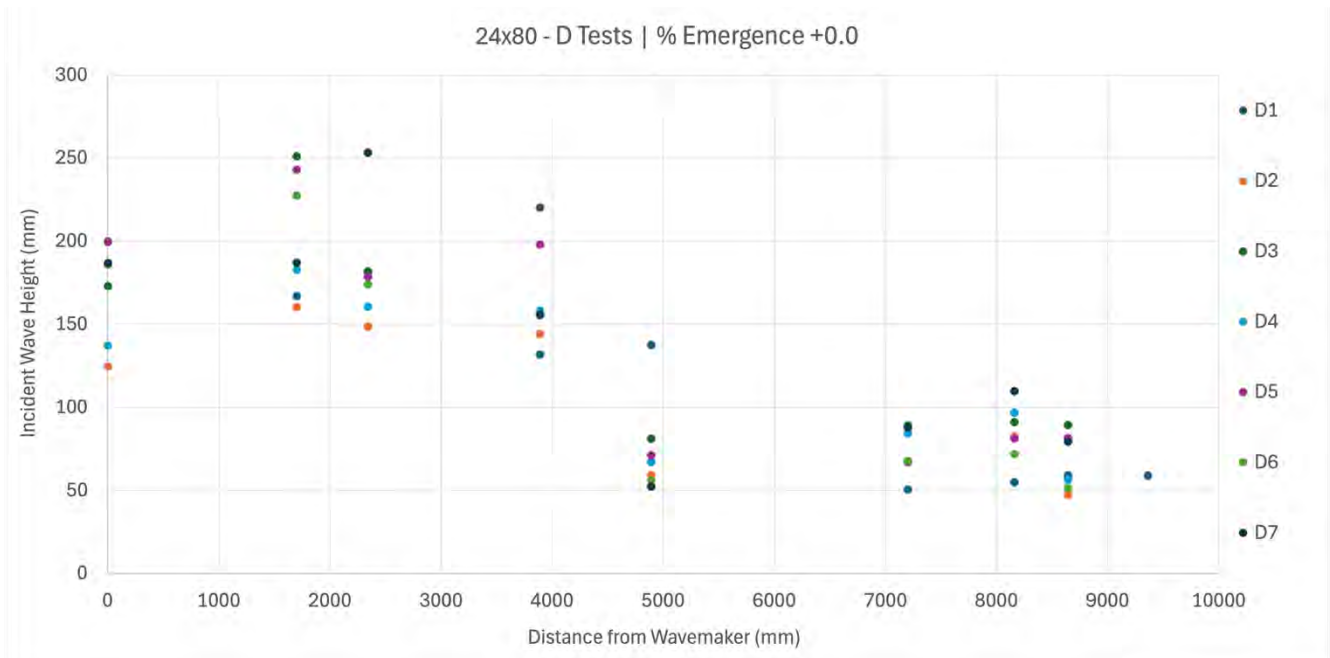


Figure 14. Incident wave heights along flume for 24x80 D series tests (water level at crest).

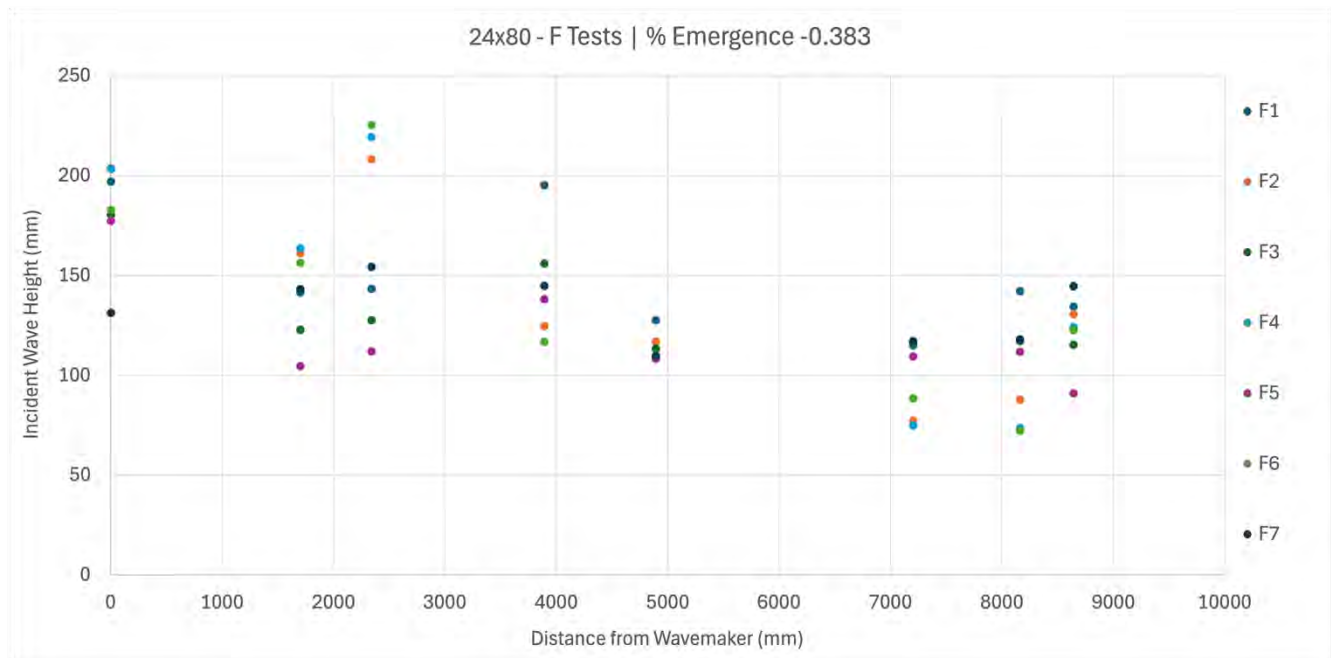


Figure 15. Incident wave heights along flume for 24x80 F series tests (highest water level).

Using the methodologies described previously, the transmission and reflection coefficients for each test case are summarized for the 24x80 model experiments in Table 9. Note that some values for dissipation ( $K_d$ ,  $K_{davg}$ ) appear in italics and gray text. These values should be considered irrelevant due to their sign. It does not make sense to have a negative value of dissipation, unless the structure is causing some sort of local amplification of the wave signal that is appearing as an artifact in this analysis. After taking an average of the replicates and performing the reflection analysis, it is not uncommon to obtain coefficient values that do not necessarily add up to a value of 1.0. Since we are not necessarily focusing on dissipation in this analysis, the questionable values are not a concern. However, it is important to note that some experiments and subsequent analysis return anomalous results, but they are few relative to the total number of experiments performed.

A correlation analysis was performed on most of the parameter values listed in Table 9 to determine the most salient relationships between wave transmission, wave reflection and other independent variables. The resulting correlation matrix is shown in Table 10. The independent variables for percent emergence, freeboard, and relative freeboard are essentially expressing the same thing, though the latter incorporates information about the wave height, which can be important for addressing transmission through wave overtopping. Though wave reflection and wave transmission appear to be better correlated to emergence and freeboard than to relative freeboard, the differences are so small that there is no statistical significance between the correlation values (0.43 vs 0.37 for reflection; -0.94 vs -0.88 for transmission). Therefore, subsequent behavior of wave transmission and reflection will consider the relative freeboard parameter only. Wave reflection appears to have a similar dependence on wave steepness (-0.45), though opposite in sign. Wave transmission appears to be dominated by relative freeboard, and has a relatively weak dependence on wave steepness by comparison (0.44).

Table 9. Summary Wave Results for the 24x80 Model

Case Name	Tank Depth (mm)	% Emerge	Freeboard (mm)	R <sub>c</sub> /H <sub>i</sub>	Ursell #	Wave Steepness	Bulk K <sub>t</sub>	K <sub>r</sub>	K <sub>d</sub>	K <sub>t</sub>	K <sub>davg</sub>	K <sub>tavg</sub>
A1	190	0.596	280	3.666	174	0.0586	0.12	0.45	0.47	0.09	0.45	0.10
A2	190	0.596	280	4.003	20	0.0304	0.06	0.32	0.63	0.05	0.63	0.05
A3	190	0.596	280	3.883	37	0.0293	0.05	0.32	0.65	0.04	0.65	0.04
A7	190	0.596	280	3.067	139	0.0190	0.06	0.27	0.69	0.04	0.66	0.07
B1	330	0.298	140	1.487	12	0.0417	0.13	0.45	0.41	0.14	0.37	0.19
B2	330	0.298	140	1.085	59	0.0185	0.26	0.36	0.41	0.23	0.46	0.18
B3	330	0.298	140	1.393	16	0.0553	0.15	0.52	0.33	0.14	0.31	0.16
B4	330	0.298	140	1.028	24	0.0447	0.14	0.46	0.39	0.15	0.39	0.15
B5	330	0.298	140	1.004	51	0.0471	0.15	0.57	0.26	0.17	0.21	0.22
B6	330	0.298	140	1.558	78	0.0382	0.23	0.36	0.40	0.25	0.41	0.24
B7	330	0.298	140	1.239	132	0.0411	0.29	0.39	0.31	0.30	0.38	0.23
D1	470	0	0	0.000	13	0.0776	0.41	0.10	0.53	0.37	0.50	0.39
D2	470	0	0	0.000	32	0.0490	0.47	0.28	0.31	0.41	0.29	0.43
D3	470	0	0	0.000	22	0.0683	0.38	0.15	0.48	0.37	0.42	0.42
D4	470	0	0	0.000	35	0.0539	0.48	0.27	0.30	0.43	0.25	0.48
D5	470	0	0	0.000	24	0.0745	0.37	0.12	0.52	0.36	0.51	0.37
D6	470	0	0	0.000	38	0.0588	0.45	0.19	0.45	0.36	0.43	0.38
D7	470	0	0	0.000	78	0.0414	0.42	0.34	0.33	0.34	0.32	0.34
E1	550	-0.17	-80	-0.362	18	0.0718	0.52	0.26	0.22	0.52	0.16	0.58
E2	550	-0.17	-80	-0.414	29	0.0566	0.64	0.16	0.25	0.58	0.38	0.46
E3	550	-0.17	-80	-0.351	18	0.0689	0.48	0.22	0.35	0.43	0.34	0.45
E4	550	-0.17	-80	-0.451	28	0.0544	0.66	0.20	0.16	0.64	0.32	0.48
E5	550	-0.17	-80	-0.379	16	0.0631	0.46	0.18	0.41	0.41	0.37	0.45
E6	550	-0.17	-80	-0.434	23	0.0453	0.70	0.24	0.06	0.70	0.24	0.52
E7	550	-0.17	-80	-0.388	47	0.0319	0.44	0.33	0.33	0.34	0.33	0.34
F1	650	-0.383	-180	-0.922	13	0.0660	0.64	0.26	0.09	0.65	0.02	0.72
F2	650	-0.383	-180	-1.444	21	0.0521	0.97	0.33	-0.26	0.94	0.09	0.58
F3	650	-0.383	-180	-1.154	13	0.0634	0.67	0.20	0.07	0.73	-0.01	0.81
F4	650	-0.383	-180	-1.540	20	0.0500	0.96	0.38	-0.31	0.93	0.08	0.55
F5	650	-0.383	-180	-1.303	11	0.0581	0.72	0.26	-0.04	0.78	-0.13	0.87
F6	650	-0.383	-180	-1.541	17	0.0417	0.91	0.40	-0.34	0.94	0.02	0.58
F7	650	-0.383	-180	-1.243	34	0.0293	0.81	0.24	0.00	0.76	0.00	0.76

Table 10. Summary Wave Results Correlation Matrix for the 24x80 Model

Correlation Matrix	Freeboard		Wave							
	% Emerge	(mm)	$R_c/H_i$	Ursell #	Steepness	$K_r$	$K_d$	$K_t$	$K_{davg}$	$K_{tavg}$
% Emergence	1.00									
Freeboard (mm)	1.00	1.00								
$R_c/H_i$	0.97	0.97	1.00							
Ursell #	0.57	0.57	0.55	1.00						
Wave Steepness	-0.43	-0.43	-0.43	-0.37	1.00					
$K_r$	0.43	0.43	0.37	0.30	-0.45	1.00				
$K_d$	0.77	0.77	0.75	0.31	-0.20	0.05	1.00			
$K_t$	-0.92	-0.92	-0.88	-0.45	0.29	-0.32	-0.85	1.00		
$K_{davg}$	0.81	0.81	0.79	0.39	-0.23	-0.07	0.94	-0.82	1.00	
$K_{tavg}$	-0.94	-0.94	-0.88	-0.50	0.44	-0.46	-0.82	0.89	-0.85	1.00

The relationships between wave transmission, wave reflection, and relative freeboard for the 24x80 model testing data are shown in Figure 16. Generally speaking, wave transmission decreases as relative freeboard increases (negatively correlated, -0.88), but wave reflection tends to increase with increasing values of relative freeboard (positively correlated, 0.37). These dependencies are further analyzed and described in the Discussion section.

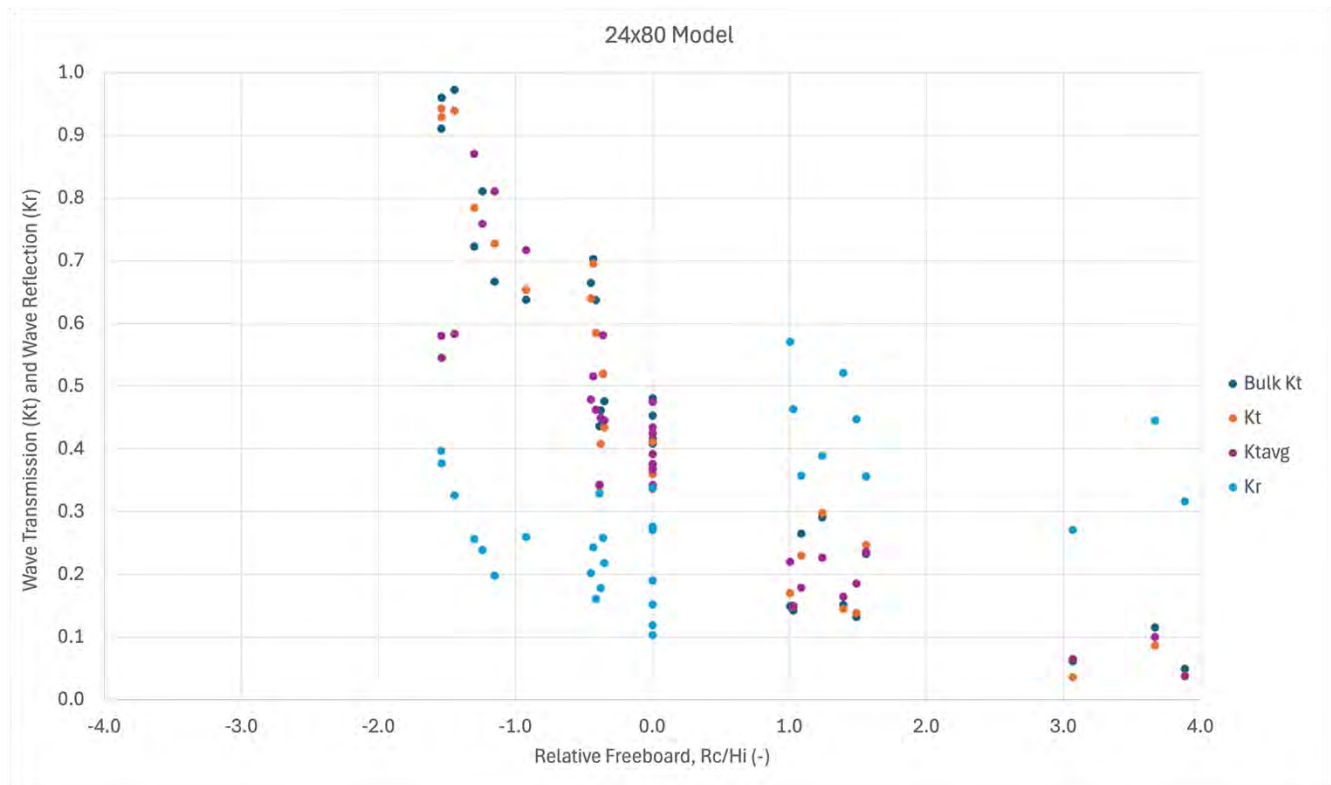


Figure 16. Wave transmission and wave reflection coefficient values as a function of relative freeboard for the 24x80 model.

Though not a focus of the overall experimental plan, velocity data were collected to aid in the calibration and/or validation of numerical modeling of the QuickReef® products. Representative velocity time histories for the 24x80 model test case B5 are provided in Figure 17. The “u” and “v” velocity components show a clear correspondence with the monochromatic wave forcing while the “w” velocity component remains small with little consistent phasing to the other components. Note the small magnitude of all velocity components, generally speaking.

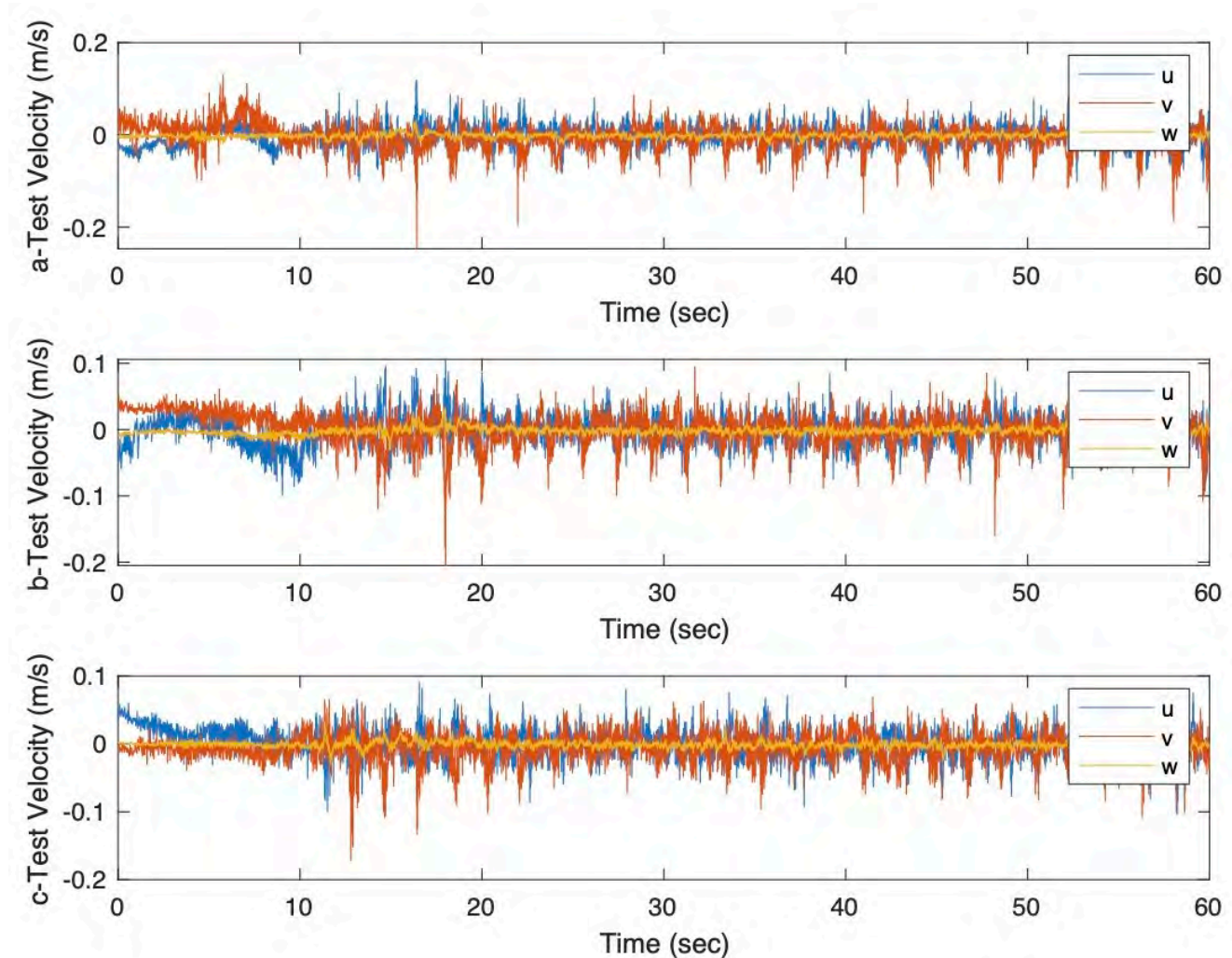


Figure 17. Sample velocity measurements from each replicate of test B5 for the 24x80 model.

The other potential use of the velocity measurements are to aid in the interpretation of the acceleration and rotation measurements collected to evaluate hydrodynamic stability. The testing configurations were mostly unable to motivate significant movement of the QuickReef® panels. Some minor movement was noted visually during experiments and appear in the accelerometer and gyroscope measurements shown in Figure 18 and Figure 19, respectively. For the 24x80 model testing, the only motion detected occurred for water levels D and E. Therefore, wave interactions with the structure crest appear to create conditions that may lead to component movement, particularly when the components have uneven surfaces and may easily rock or rotate in place. As shown in these representative results from water level case E (just above the structure crest), only Panel B experienced measurable movement, and those rotations were very small at  $< 1$  degree per second. This particular panel could have been placed

in an unstable configuration during testing due to the protrusion of aggregates in the concrete mix, leading to wobbling or a rocking motion during wave attack.

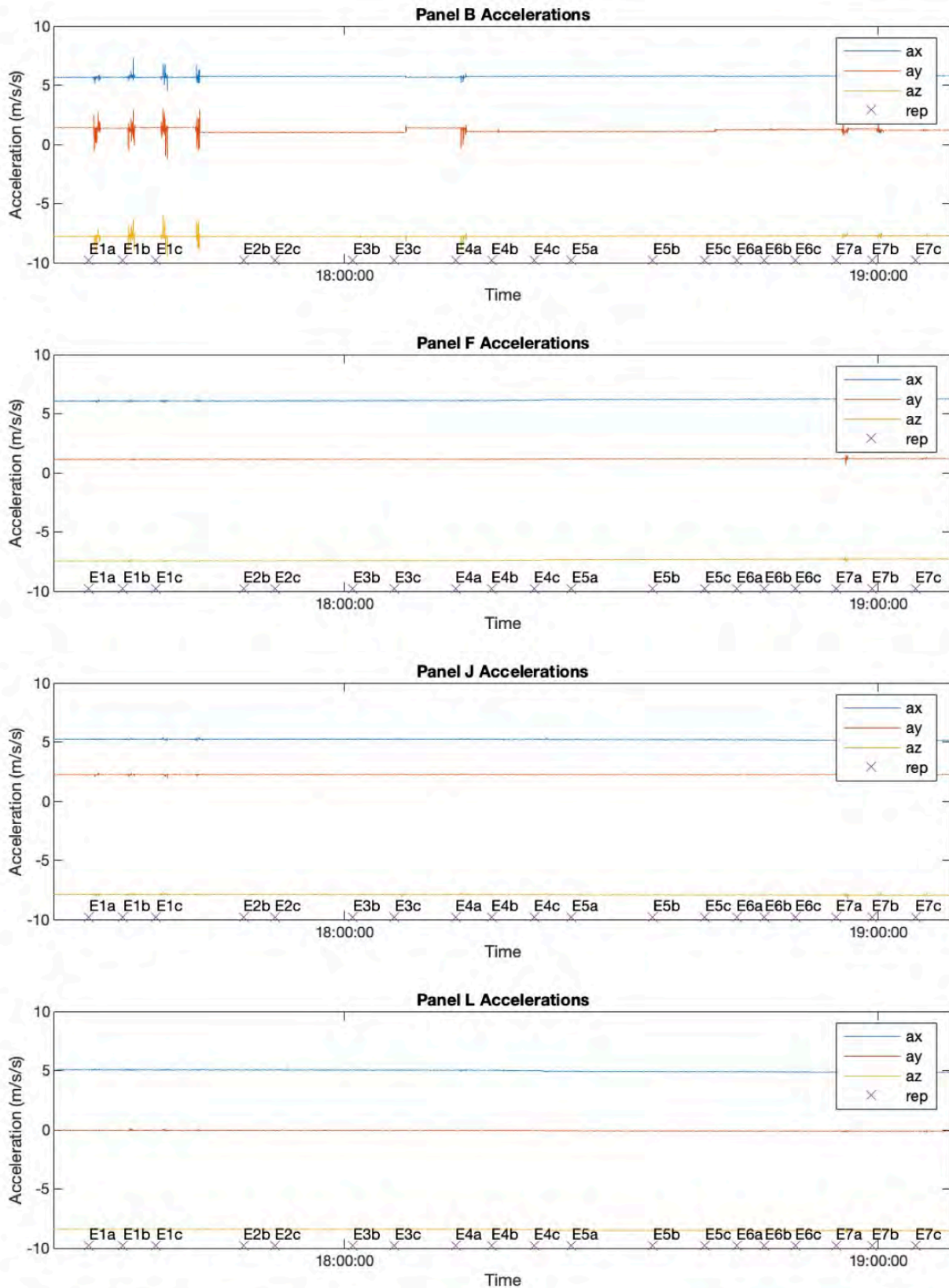


Figure 18. Acceleration measurements during all E series tests for the 24x80 model.

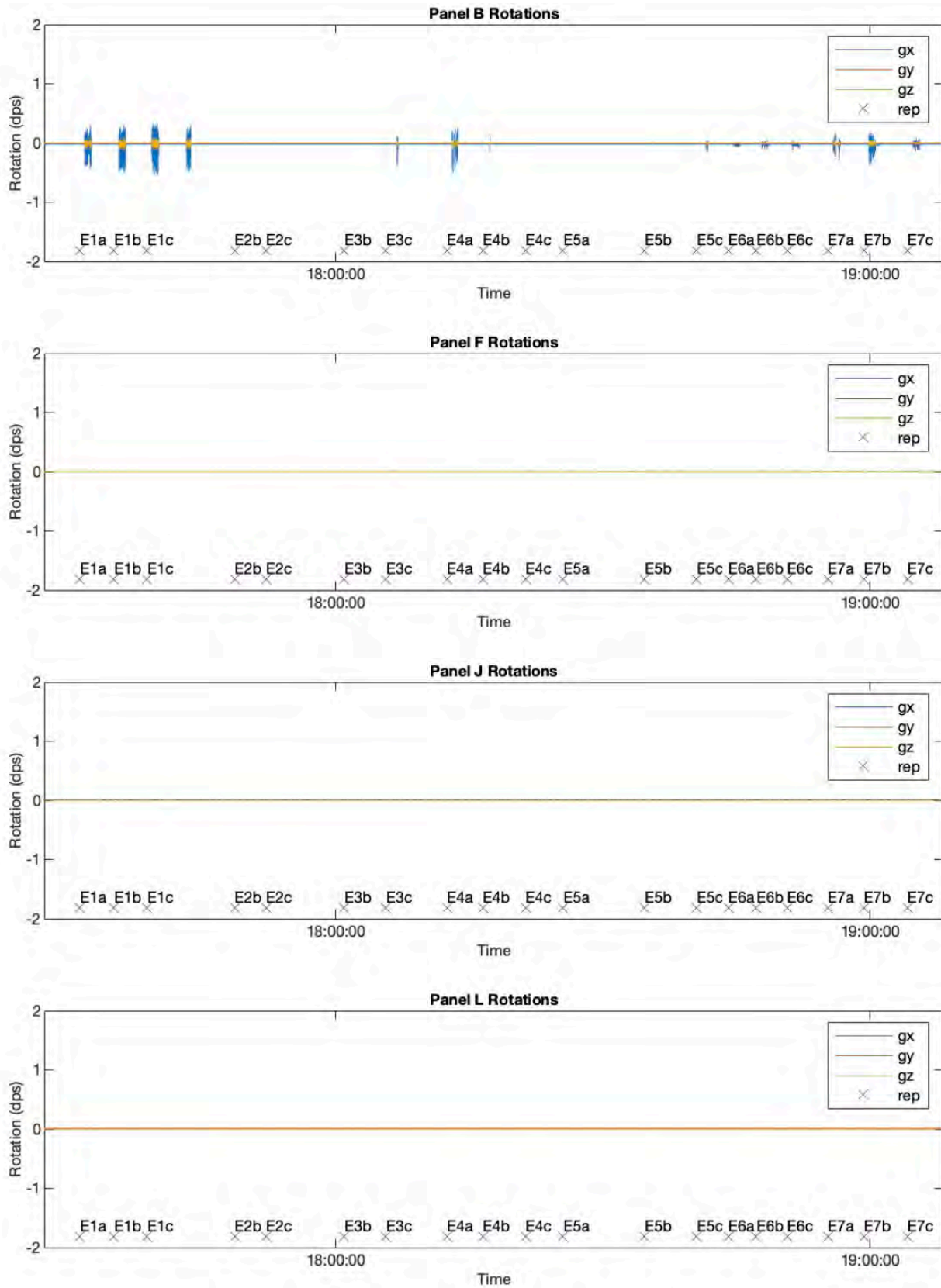


Figure 19. Rotational measurements during all E series tests for the 24x80 model.

## Defender™ Model Results

Representative profiles of incident wave height as a function of distance along the flume are shown for the lowest water level (most emergence), the water level at the structure crest, and the highest level (most submergence) are provided in Figure 20, Figure 21, and Figure 22, respectively. All profiles of measured and incident wave height variation with flume length are shown in the appendices and are available in the Master Synthesis Spreadsheet file. These figures clearly show two behaviors: the reduction in wave height on the protected, or lee, side of the structure ( $x > 7000$  mm); and the increase in transmitted wave heights with increasing water levels. For reference, the model testing area generally corresponds to the area  $5000 \text{ mm} < x < 7000 \text{ mm}$ . As would be expected, wave attenuation (i.e., lower transmission) is strongest when water levels are low relative to the structure crest, and it is weakest when water levels are above the structure crest. This pattern is consistent with our understanding of wave transmission as a function of water level for many types of coastal engineering structures (e.g., breakwaters, reefs, sills, etc.).

Using the methodologies described previously, the transmission and reflection coefficients for each test case are summarized for the Defender™ model experiments in Table 11. Note that some values for transmission ( $K_t$ ) and/or dissipation ( $K_d$ ,  $K_{davg}$ ) appear in italics and gray text. These values should be considered irrelevant due to their magnitude or their sign as described previously for the 24x80 model results.

A correlation analysis was performed on most of the parameter values listed in Table 11 to determine the most salient relationships between wave transmission, wave reflection and other independent variables. The resulting correlation matrix is shown in Table 12. The independent variables for percent emergence, freeboard, and relative freeboard are essentially expressing the same thing, though the latter incorporates information about the wave height, which can be important for addressing transmission through wave overtopping. Though wave reflection and wave transmission appear to be better correlated to emergence and freeboard than to relative freeboard, we recommend focusing on the relative freeboard parameter since it does incorporate incident wave height. Wave reflection appears to have a similar dependence on wave steepness (-0.58), though opposite in sign. Wave transmission appears to be dominated by relative freeboard and has a relatively weak dependence on wave steepness by comparison (0.61).

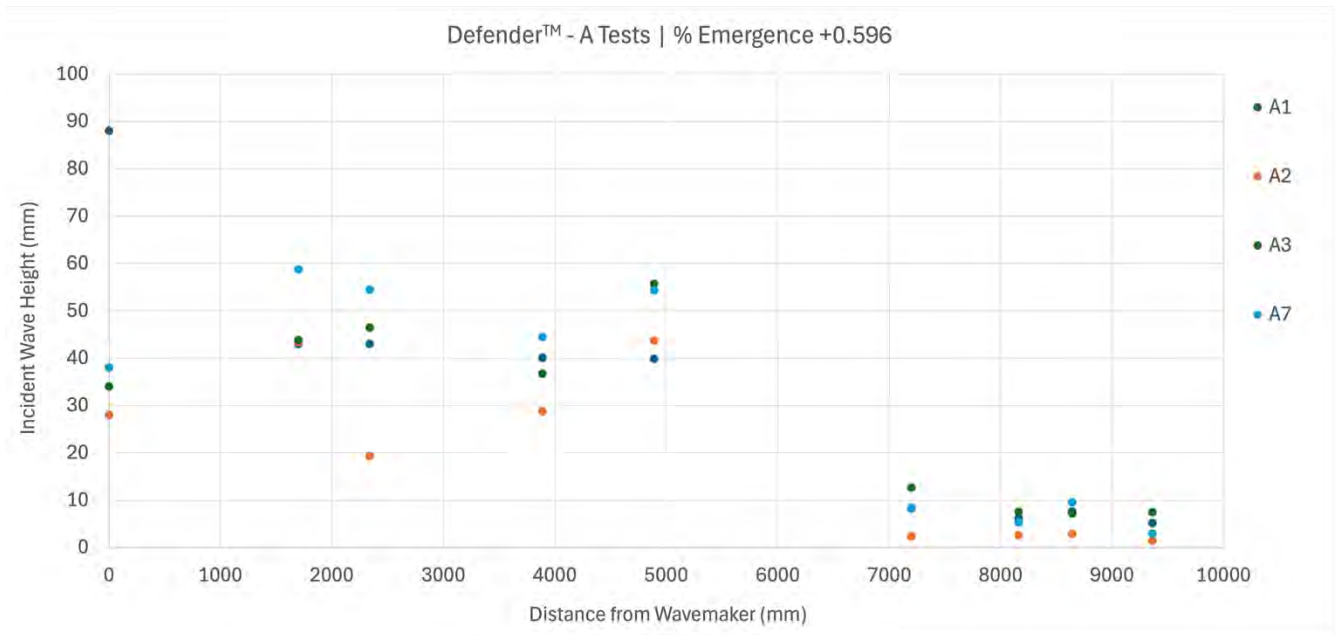


Figure 20. Incident wave heights along flume for Defender™ A series tests (lowest water level).

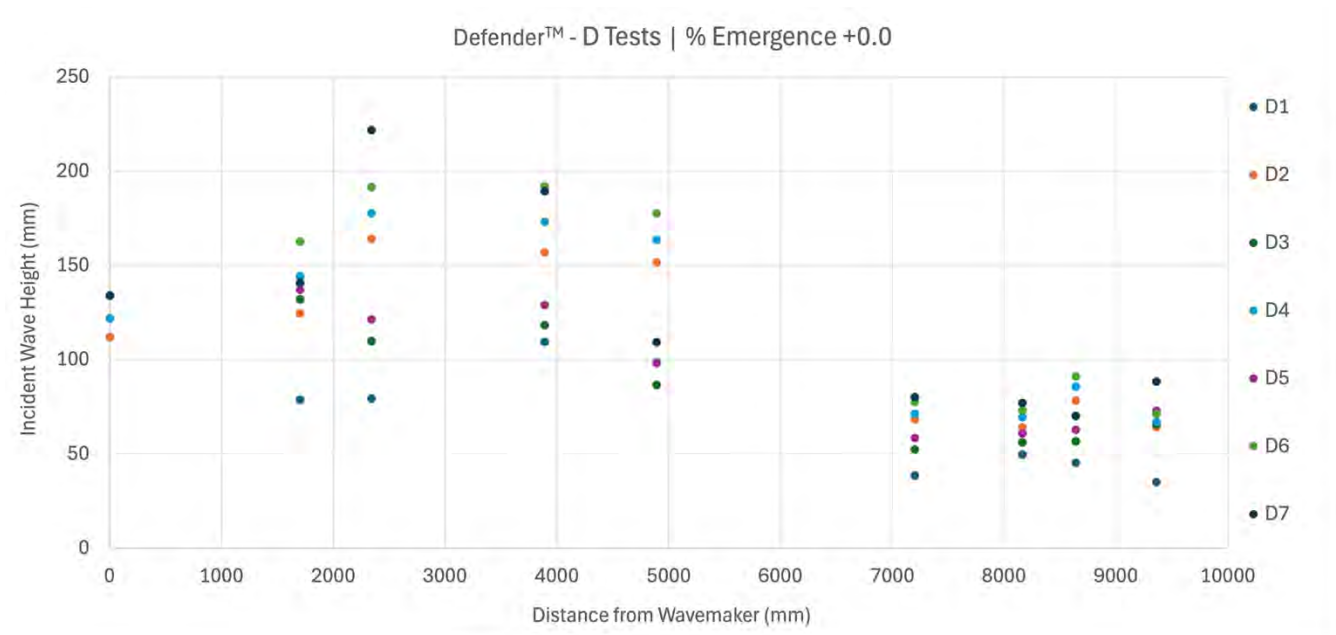


Figure 21. Incident wave heights along flume for Defender™ D series tests (water level at crest).

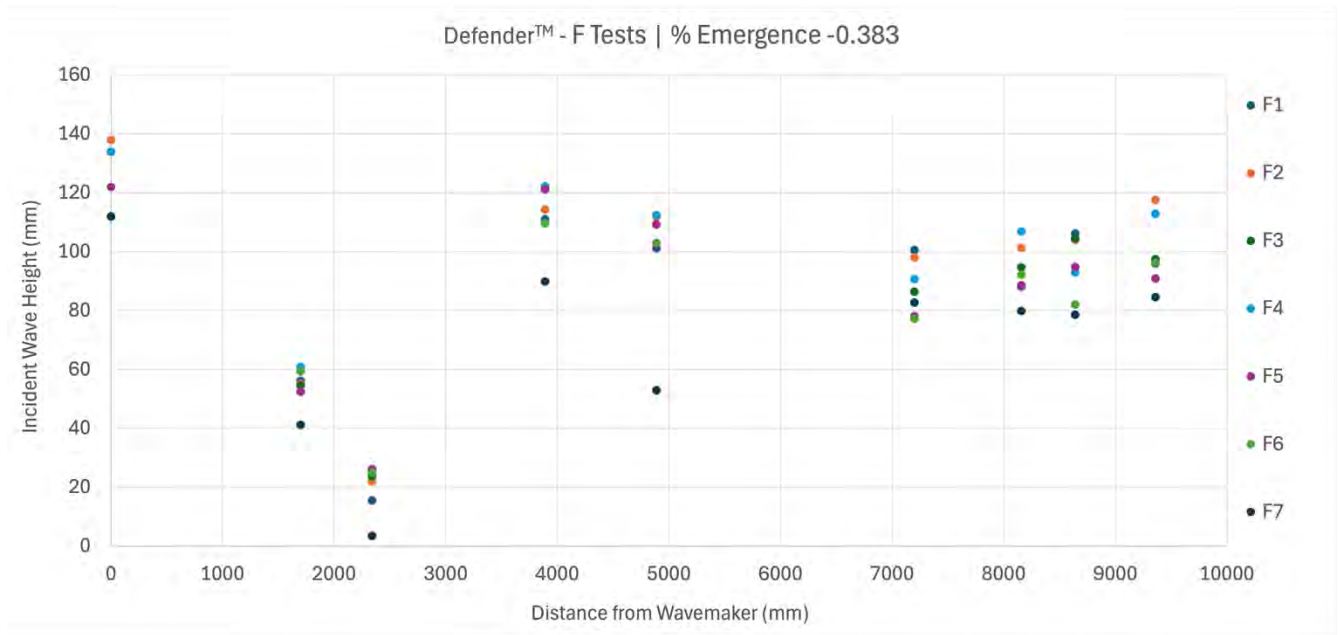


Figure 22. Incident wave heights along flume for Defender™ F series tests (highest water level).

Table 11. Summary Wave Results for the Defender™ Model

Case Name	Tank Depth (mm)	% Emerge	Freeboard (mm)	R <sub>c</sub> /H <sub>i</sub>	Ursell #	Wave Steepness	Bulk K <sub>t</sub>	K <sub>r</sub>	K <sub>d</sub>	K <sub>t</sub>	K <sub>davg</sub>	K <sub>tavg</sub>
A1	280	0.404	190	4.763	24	0.0356	0.29	0.35	0.45	0.21	0.47	0.18
A2	280	0.404	190	4.351	3	0.0188	0.08	0.33	0.62	0.05	0.60	0.07
A3	280	0.404	190	3.415	5	0.0183	0.32	0.33	0.45	0.23	0.45	0.22
A7	280	0.404	190	3.498	19	0.0114	0.21	0.32	0.53	0.15	0.54	0.14
B1	375	0.202	95	2.469	3	0.0293	0.26	0.44	0.29	0.26	0.32	0.24
B2	375	0.202	95	2.816	14	0.0130	0.43	0.66	-0.11	0.44	-0.09	0.43
B3	375	0.202	95	1.778	4	0.0382	0.26	0.33	0.41	0.26	0.44	0.23
B4	375	0.202	95	2.202	6	0.0310	0.35	0.42	0.23	0.35	0.35	0.23
B5	375	0.202	95	1.302	12	0.0325	0.22	0.40	0.36	0.23	0.37	0.23
B6	375	0.202	95	0.810	18	0.0265	0.18	0.41	0.43	0.16	0.33	0.26
B7	375	0.202	95	1.176	32	0.0291	0.42	0.50	0.05	0.45	0.13	0.37
D1	480	-0.021	-10	-0.102	4	0.0580	0.31	0.35	0.26	0.39	0.23	0.42
D2	480	-0.021	-10	-0.066	10	0.0363	0.38	0.43	0.12	0.45	0.14	0.43
D3	480	-0.021	-10	-0.115	7	0.0502	0.48	0.38	0.02	0.60	0.09	0.53
D4	480	-0.021	-10	-0.061	10	0.0396	0.35	0.42	0.15	0.44	0.17	0.42
D5	480	-0.021	-10	-0.102	7	0.0551	0.47	0.36	0.05	0.60	0.11	0.53
D6	480	-0.021	-10	-0.056	12	0.0435	0.35	0.40	0.16	0.44	0.19	0.41
D7	480	-0.021	-10	-0.091	23	0.0307	0.61	0.45	-0.19	0.73	0.02	0.53
E1	585	-0.245	-115	-0.821	5	0.0514	0.63	0.09	0.30	0.61	0.27	0.65
E2	585	-0.245	-115	-0.768	8	0.0406	0.55	0.14	0.30	0.56	0.27	0.59
E3	585	-0.245	-115	-0.830	5	0.0499	0.59	0.09	0.33	0.58	0.30	0.61
E4	585	-0.245	-115	-0.797	8	0.0394	0.54	0.16	0.26	0.57	0.26	0.58
E5	585	-0.245	-115	-0.962	4	0.0455	0.62	0.11	0.26	0.63	0.22	0.66
E6	585	-0.245	-115	-0.955	6	0.0329	0.55	0.17	0.24	0.59	0.22	0.61
E7	585	-0.245	-115	-1.069	13	0.0233	0.76	0.33	-0.25	0.92	0.00	0.67
F1	682	-0.451	-212	-2.096	4	0.0476	1.12	0.05	-0.05	0.99	0.06	0.89
F2	682	-0.451	-212	-1.895	6	0.0376	0.88	0.15	-0.02	0.88	-0.03	0.88
F3	682	-0.451	-212	-1.941	4	0.0463	0.89	0.06	0.15	0.79	0.16	0.78
F4	682	-0.451	-212	-1.885	6	0.0365	0.83	0.14	0.05	0.81	0.02	0.84
F5	682	-0.451	-212	-1.939	3	0.0421	0.78	0.09	0.20	0.71	0.19	0.72
F6	682	-0.451	-212	-2.057	5	0.0305	0.78	0.15	0.10	0.75	0.05	0.80
F7	682	-0.451	-212	-4.006	10	0.0215	1.15	0.54	-1.11	1.56	-0.68	1.14

Table 12. Summary Wave Results Correlation Matrix for the Defender™ Model

Correlation Matrix	% Emergence	Freeboard (mm)	$R_c/H_i$	Ursell #	Wave Steepness	$K_r$	$K_d$	$K_t$	$K_{davg}$	$K_{tavg}$
% Emergence	1.00									
Freeboard (mm)	1.00	1.00								
$R_c/H_i$	0.95	0.95	1.00							
Ursell #	0.42	0.42	0.33	1.00						
Wave Steepness	-0.45	-0.45	-0.46	-0.39	1.00					
$K_r$	0.63	0.63	0.46	0.52	-0.50	1.00				
$K_d$	0.51	0.51	0.61	-0.09	0.07	-0.27	1.00			
$K_t$	-0.84	-0.84	-0.86	-0.18	0.19	-0.25	-0.86	1.00		
$K_{davg}$	0.62	0.62	0.71	-0.02	-0.01	-0.18	0.97	-0.88	1.00	
$K_{tavg}$	-0.95	-0.95	-0.93	-0.30	0.32	-0.46	-0.71	0.95	-0.79	1.00

The relationships between wave transmission, wave reflection, and relative freeboard for the Defender™ model testing data are shown in Figure 23. Generally speaking, wave transmission decreases as relative freeboard increases (negatively correlated, -0.92), but wave reflection tends to increase with increasing values of relative freeboard (positively correlated, 0.42). These dependencies are further analyzed and described in the Discussion section.

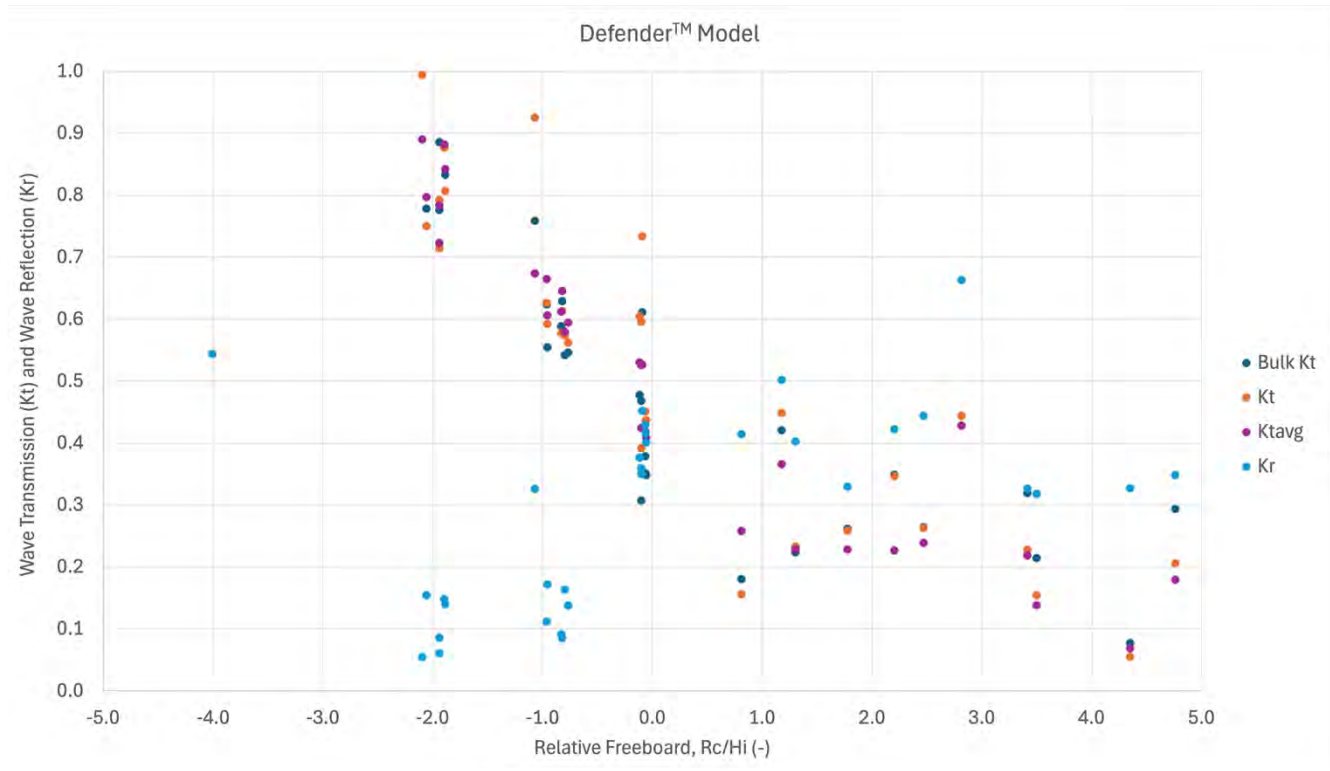


Figure 23. Wave transmission and wave reflection coefficient values as a function of relative freeboard for the Defender™ model.

Representative velocity time histories for the Defender™ model test case B5 are provided in Figure 24. The “u” and “v” velocity components show a clear correspondence with the monochromatic wave forcing while the “w” velocity component remains small with little consistent phasing to the other components. Note the small magnitude of all velocity components, generally speaking.

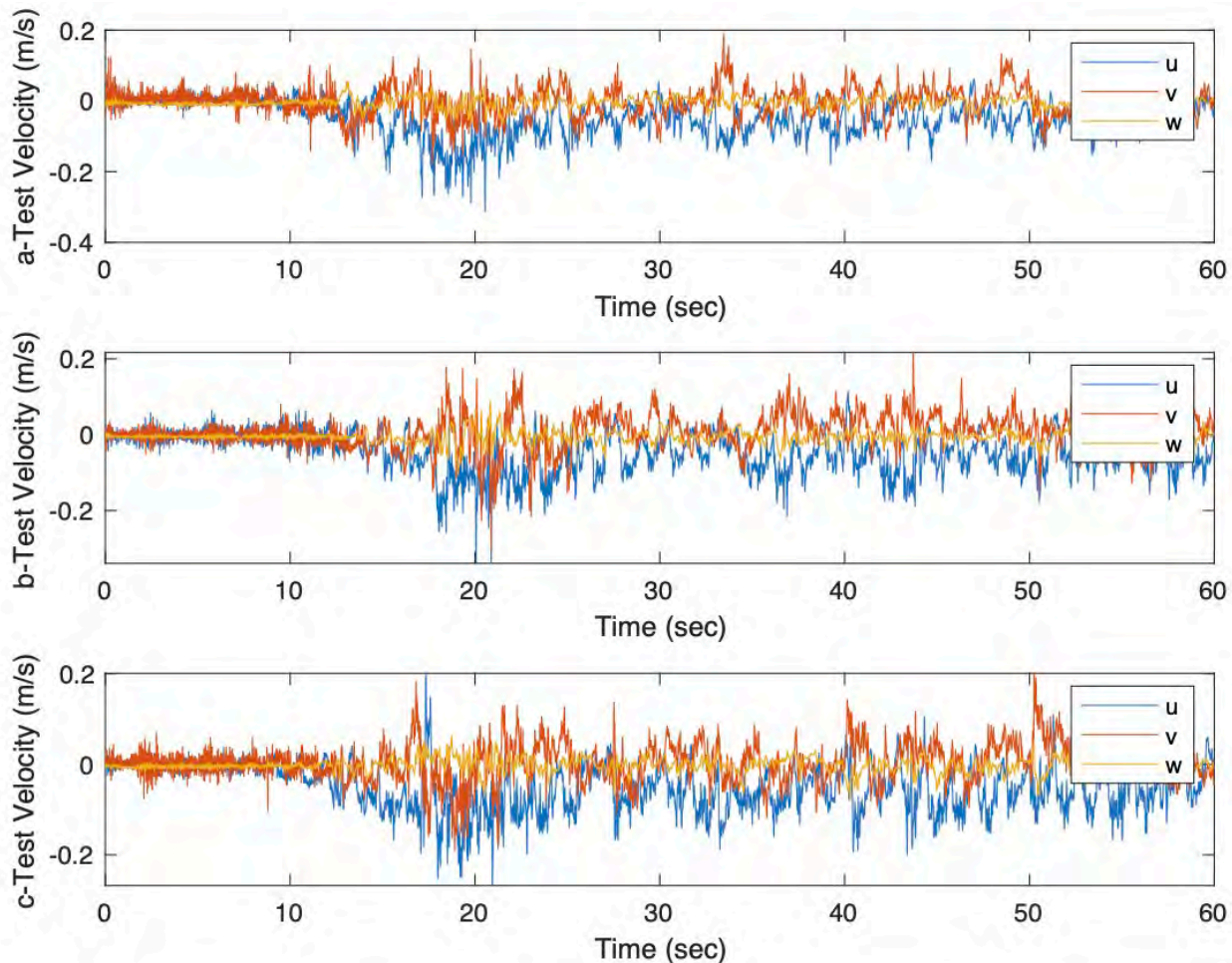


Figure 24. Sample velocity measurements from each replicate of test B5 for the Defender™ model.

The testing configurations were mostly unable to motivate significant movement of the Defender™ panels (they were quite heavy). Some minor movement was noted visually during experiments and appear in the accelerometer and gyroscope measurements shown in Figure 24 and Figure 25, respectively. For the Defender™ model testing, the only motion detected occurred for water levels B and D. Therefore, wave interactions with the structure crest appear to create conditions that may lead to component movement, particularly when the components have uneven surfaces and may easily rock or rotate in place. As shown in these representative results from water level case B (just below the structure crest), only Panel B experienced measurable movement, and those rotations were very small at  $< 0.1$  degree per second. This particular panel could have been placed in an unstable configuration during testing due to the protrusion of aggregates in the concrete mix, leading to wobbling or a rocking motion during wave attack.

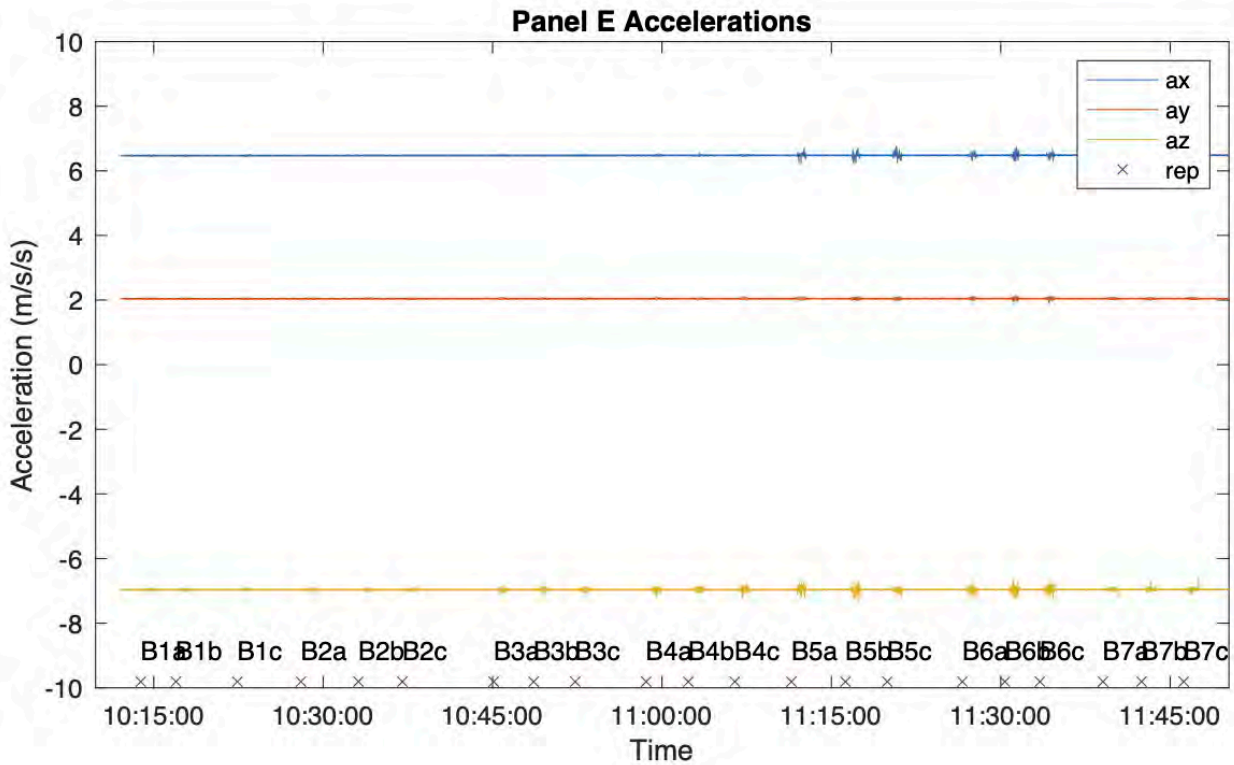
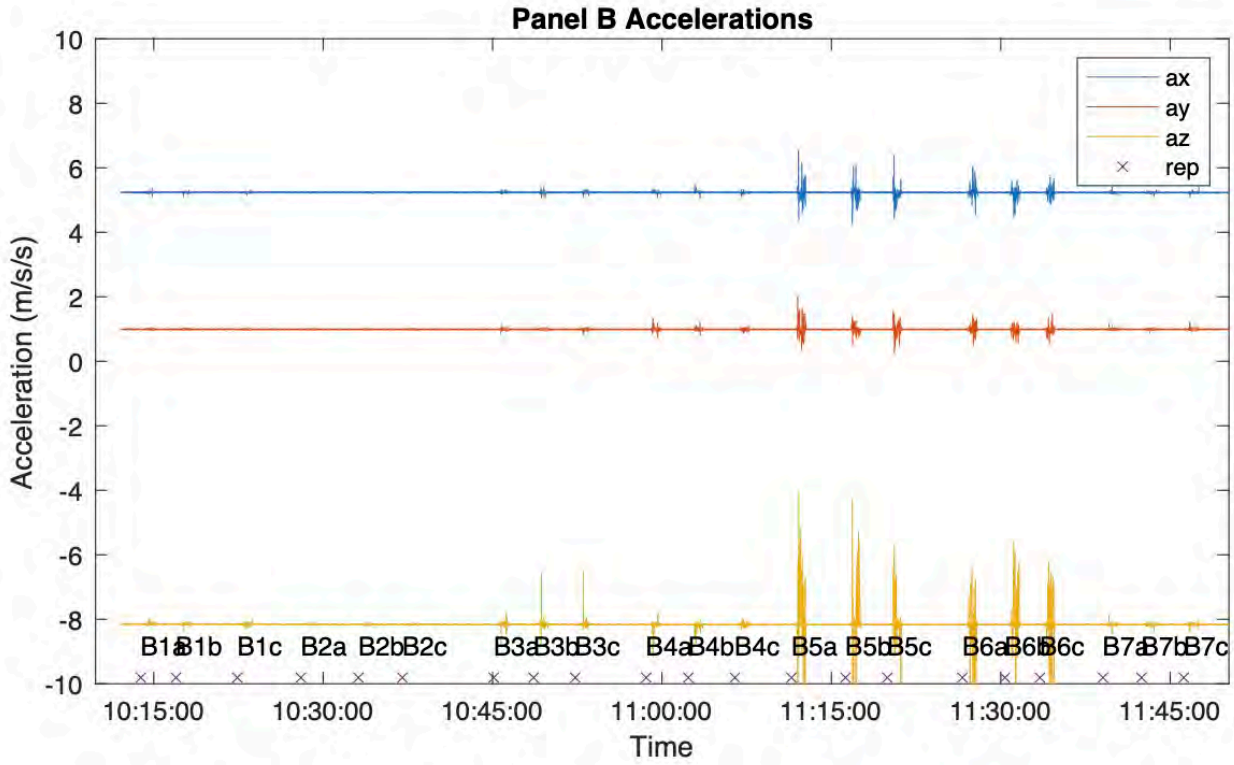


Figure 25. Acceleration measurements during all B series tests for the Defender™ model.

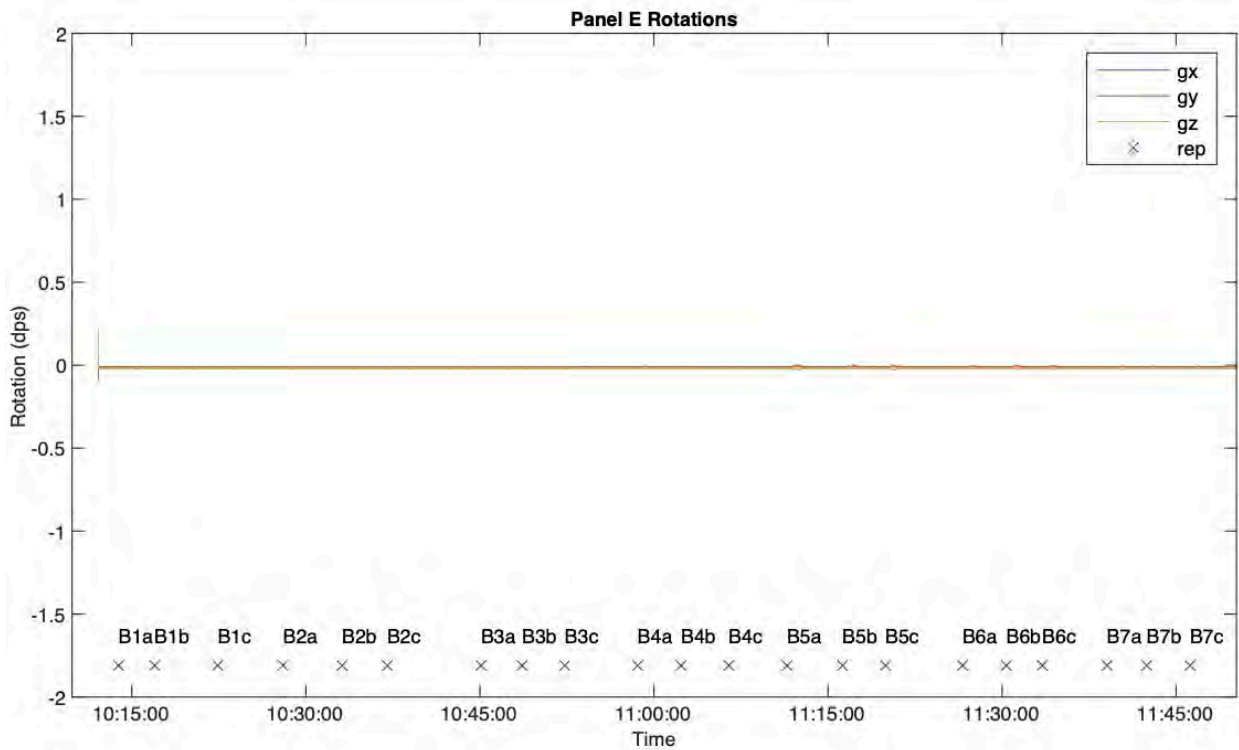
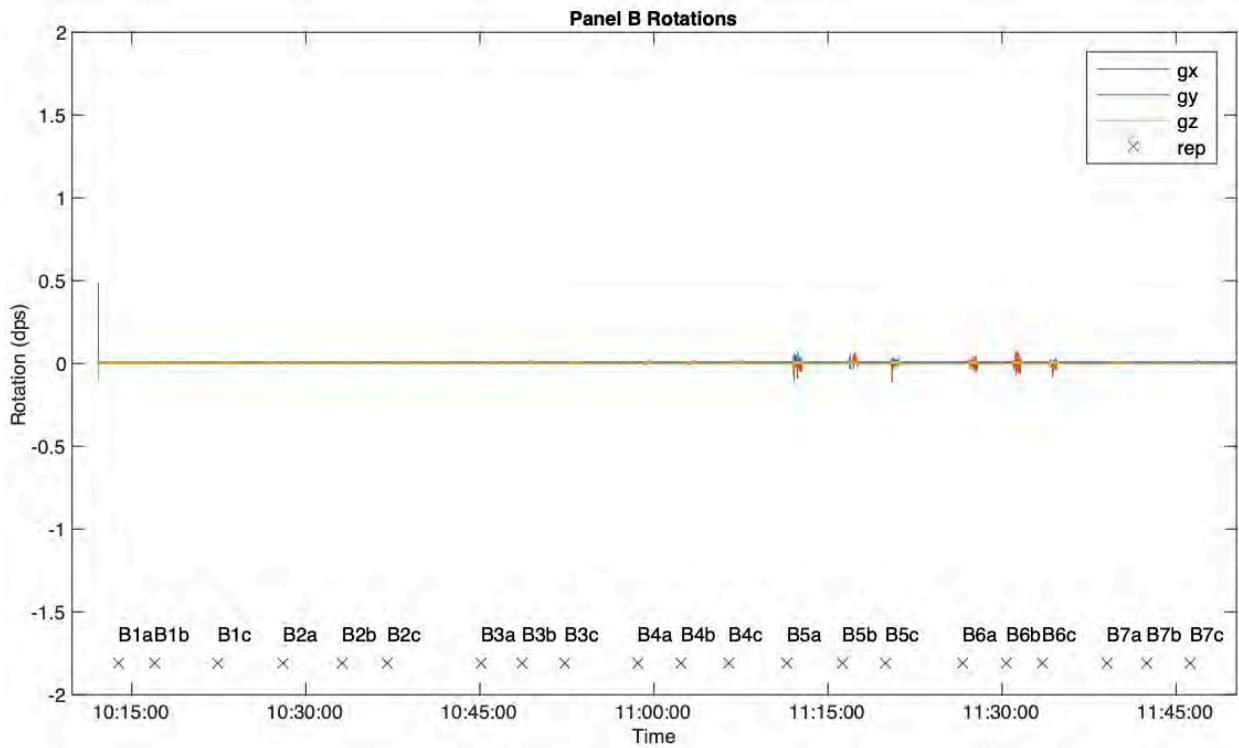


Figure 26. Rotational measurements during all B series tests for the Defender™ model.

## 21x60 (with cap) Model Results

Representative profiles of incident wave height as a function of distance along the flume are shown for the lowest water level (most emergence), the water level at the structure crest, and the highest level (most submergence) are provided in Figure 27, Figure 28, and Figure 29, respectively. All profiles of measured and incident wave height variation with flume length are shown in the appendices and are available in the Master Synthesis Spreadsheet file. These figures clearly show two behaviors: the reduction in wave height on the protected, or lee, side of the structure ( $x > 7000$  mm); and the increase in transmitted wave heights with increasing water levels. For reference, the model testing area generally corresponds to the area  $5000 \text{ mm} < x < 7000 \text{ mm}$ . As would be expected, wave attenuation (i.e., lower transmission) is strongest when water levels are low relative to the structure crest, and it is weakest when water levels are above the structure crest. This pattern is consistent with our understanding of wave transmission as a function of water level for many types of coastal engineering structures (e.g., breakwaters, reefs, sills, etc.).

Using the methodologies described previously, the transmission and reflection coefficients for each test case are summarized for the 21x60 model experiments in Table 13. Note that some values for transmission ( $K_t$ ) and/or dissipation ( $K_d$ ,  $K_{davg}$ ) appear in italics and gray text. These values should be considered irrelevant due to their magnitude or their sign as described previously for the 24x80 model results.

A correlation analysis was performed on most of the parameter values listed in Table 13 to determine the most salient relationships between wave transmission, wave reflection and other independent variables. The resulting correlation matrix is shown in Table 14. The independent variables for percent emergence, freeboard, and relative freeboard are essentially expressing the same thing, though the latter incorporates information about the wave height, which can be important for addressing transmission through wave overtopping. Though wave reflection and wave transmission appear to be better correlated to emergence and freeboard than to relative freeboard, we recommend focusing on the relative freeboard parameter since it does incorporate incident wave height. However, an argument could be made for considering only freeboard or percent emergence for the 21x60 (with cap) model in future analyses. Wave reflection appears to have some considerable dependence on wave steepness (-0.58), though opposite in sign. Wave transmission appears to be dominated by relative freeboard and has almost no dependence on wave steepness by comparison (-0.10).

The relationships between wave transmission, wave reflection, and relative freeboard for the 21x60 model testing data are shown in Figure 30. An alternative presentation in Figure 31 shows those results relative to percent emergence since they are better correlated to that variable specifically. Generally speaking, wave transmission decreases as relative freeboard increases (negatively correlated, -0.16), but unlike other models the 21x60 testing shows that wave transmission begins to increase again for large values of relative freeboard. Also unlike other models that had a weaker trend, wave reflection clearly increases with increasing values of relative freeboard (positively correlated, 0.92). These dependencies are further analyzed and described in the Discussion section.

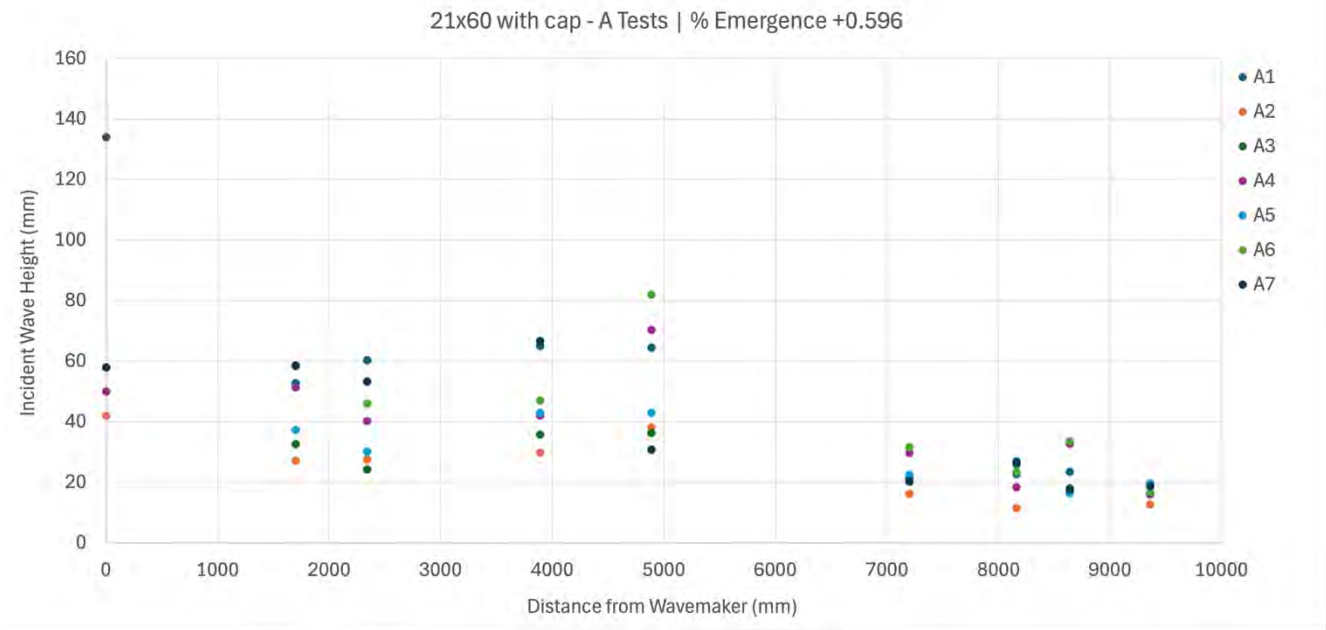


Figure 27. Incident wave heights along flume for 21x60 (with cap) A series tests (lowest water level).

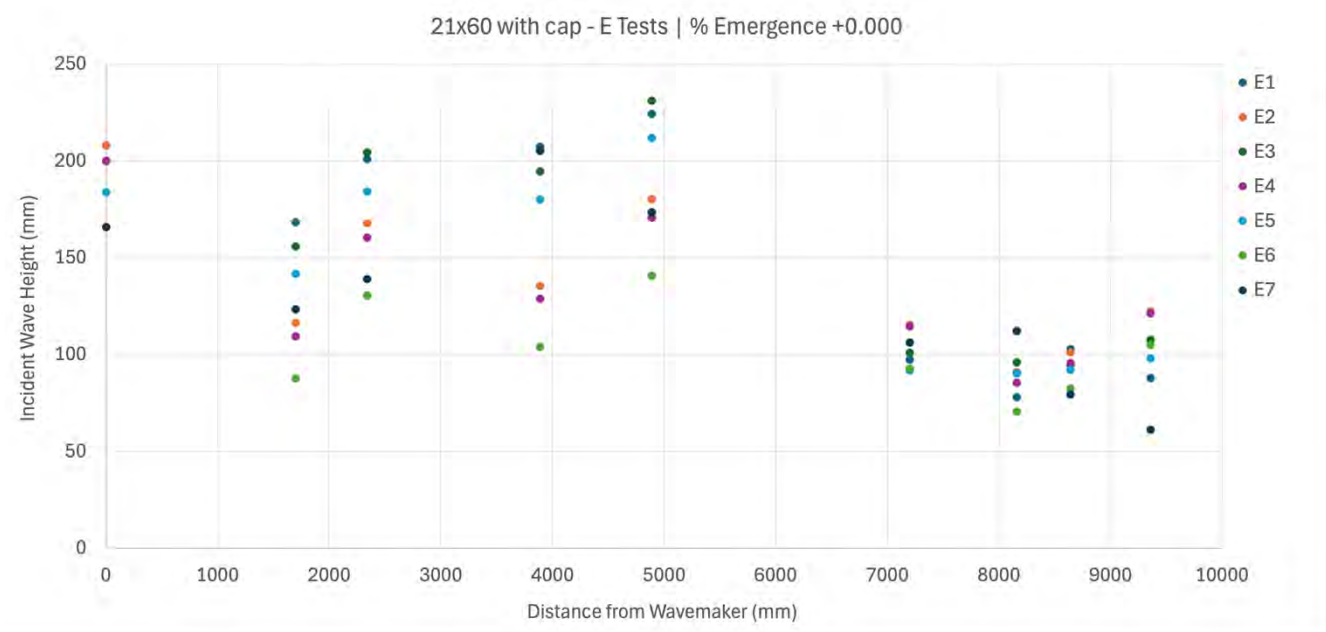


Figure 28. Incident wave heights along flume for 21x60 (with cap) E series tests (water level at crest).

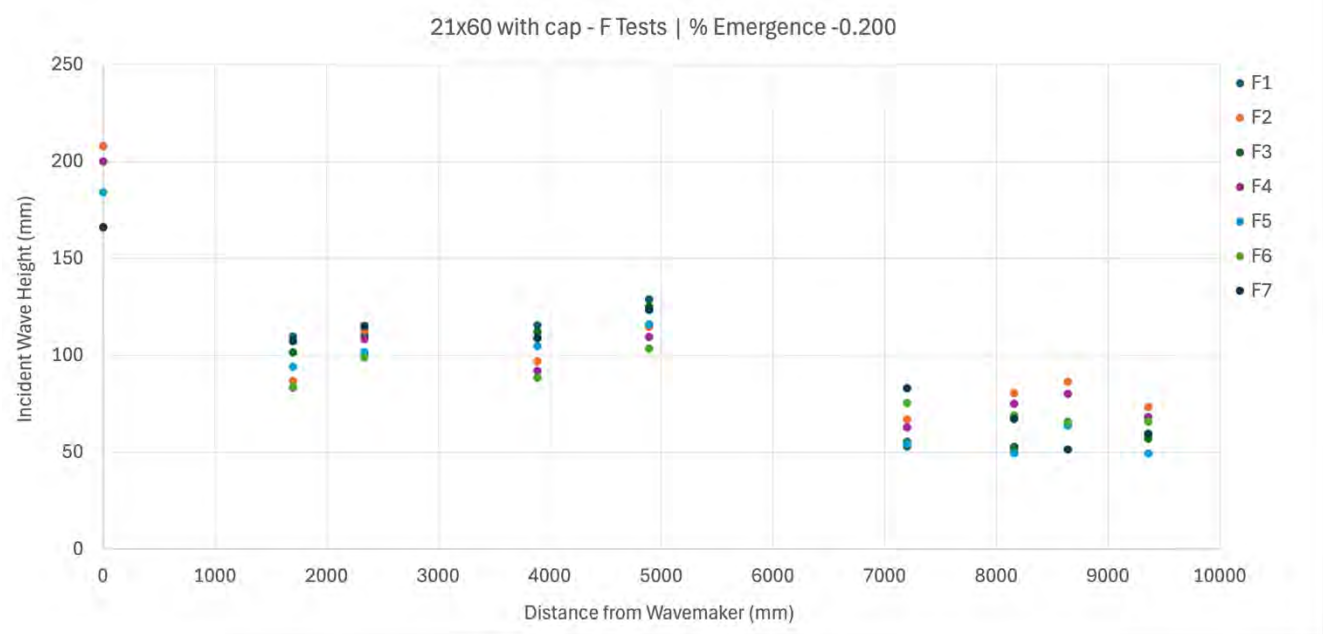


Figure 29. Incident wave heights along flume for 21x60 (with cap) F series tests (highest water level).

Table 13. Summary Wave Results for the 21x60 Model (with cap)

Case Name	Tank Depth (mm)	% Emerge	Freeboard (mm)	R <sub>c</sub> /H <sub>i</sub>	Ursell #	Wave Steepness	Bulk K <sub>t</sub>	K <sub>r</sub>	K <sub>d</sub>	K <sub>t</sub>	K <sub>davg</sub>	K <sub>tavg</sub>
A1	436	0.600	204	3.165	23	0.0354	0.38	0.52	0.15	0.33	0.14	0.34
A2	436	0.600	204	5.350	3	0.0185	0.43	0.45	0.13	0.42	0.15	0.41
A3	436	0.600	204	5.619	5	0.0177	0.52	0.44	0.00	0.56	-0.08	0.64
A4	436	0.600	204	2.902	8	0.0139	0.43	0.39	0.18	0.42	0.18	0.43
A5	436	0.600	204	4.749	6	0.0205	0.52	0.45	0.02	0.52	-0.03	0.58
A6	436	0.600	204	2.490	9	0.0162	0.39	0.39	0.23	0.39	0.19	0.43
A7	436	0.600	204	6.621	18	0.0114	0.66	0.50	-0.16	0.66	0.02	0.48
B1	504	0.400	136	2.126	4	0.0312	0.41	0.43	0.17	0.40	0.21	0.35
B2	504	0.400	136	4.930	18	0.0139	1.18	0.55	-0.59	1.04	-0.06	0.51
B3	504	0.400	136	1.778	5	0.0409	0.44	0.38	0.17	0.45	0.29	0.34
B4	504	0.400	136	1.152	7	0.0330	0.30	0.42	0.26	0.31	0.23	0.34
B5	504	0.400	136	0.784	15	0.0350	0.27	0.44	0.28	0.28	0.17	0.39
B6	504	0.400	136	0.771	23	0.0284	0.58	0.35	0.15	0.50	0.26	0.40
B7	504	0.400	136	1.321	39	0.0303	0.41	0.49	0.12	0.40	0.18	0.33
D1	572	0.200	68	0.586	6	0.0640	0.46	0.33	0.16	0.51	0.19	0.48
D2	572	0.200	68	0.484	15	0.0404	0.43	0.38	0.16	0.47	0.14	0.49
D3	572	0.200	68	0.268	10	0.0567	0.25	0.35	0.38	0.27	0.37	0.29
D4	572	0.200	68	0.431	17	0.0448	0.45	0.38	0.14	0.49	0.14	0.48
D5	572	0.200	68	0.252	11	0.0617	0.24	0.34	0.40	0.26	0.37	0.29
D6	572	0.200	68	0.379	18	0.0487	0.45	0.37	0.14	0.49	0.13	0.50
D7	572	0.200	68	0.442	30	0.0284	0.48	0.42	0.13	0.46	0.15	0.43
E1	640	0.000	0	0.000	9	0.0606	0.44	0.25	0.31	0.43	0.34	0.41
E2	640	0.000	0	0.000	15	0.0479	0.56	0.26	0.10	0.64	0.09	0.65
E3	640	0.000	0	0.000	9	0.0583	0.40	0.25	0.31	0.44	0.28	0.46
E4	640	0.000	0	0.000	14	0.0460	0.59	0.27	0.06	0.67	0.07	0.67
E5	640	0.000	0	0.000	8	0.0536	0.39	0.26	0.31	0.43	0.28	0.46
E6	640	0.000	0	0.000	12	0.0382	0.59	0.27	0.07	0.66	0.06	0.67
E7	640	0.000	0	0.000	24	0.0269	0.67	0.27	0.11	0.61	0.15	0.58
F1	708	-0.200	-68	-0.528	8	0.0577	0.43	0.17	0.41	0.41	0.40	0.43
F2	708	-0.200	-68	-0.594	12	0.0455	0.56	0.17	0.25	0.58	0.13	0.70
F3	708	-0.200	-68	-0.544	7	0.0554	0.46	0.17	0.38	0.44	0.37	0.46
F4	708	-0.200	-68	-0.621	12	0.0438	0.56	0.17	0.26	0.57	0.15	0.68
F5	708	-0.200	-68	-0.586	7	0.0510	0.49	0.17	0.36	0.47	0.36	0.47
F6	708	-0.200	-68	-0.657	10	0.0363	0.71	0.16	0.11	0.73	0.09	0.75
F7	708	-0.200	-68	-0.551	20	0.0256	0.78	0.16	0.17	0.67	0.19	0.65

Table 14. Summary Wave Results Correlation Matrix for the 21x60 Model (with cap)

Correlation Matrix	% Emerge	Freeboard (mm)	$R_c/H_i$	Ursell #	Wave Steepness	$K_r$	$K_d$	$K_t$	$K_{davg}$	$K_{tavg}$
% Emergence	1.00									
Freeboard (mm)	1.00	1.00								
$R_c/H_i$	0.84	0.84	1.00							
Ursell #	0.03	0.03	-0.10	1.00						
Wave Steepness	-0.64	-0.64	-0.73	-0.21	1.00					
$K_r$	0.92	0.92	0.78	0.23	-0.58	1.00				
$K_d$	-0.39	-0.39	-0.48	-0.26	0.62	-0.40	1.00			
$K_t$	-0.22	-0.22	0.15	0.14	-0.32	-0.11	-0.57	1.00		
$K_{davg}$	-0.21	-0.21	-0.32	-0.34	0.54	-0.27	0.87	-0.61	1.00	
$K_{tavg}$	-0.47	-0.47	-0.16	-0.04	-0.10	-0.49	-0.46	0.72	-0.57	1.00

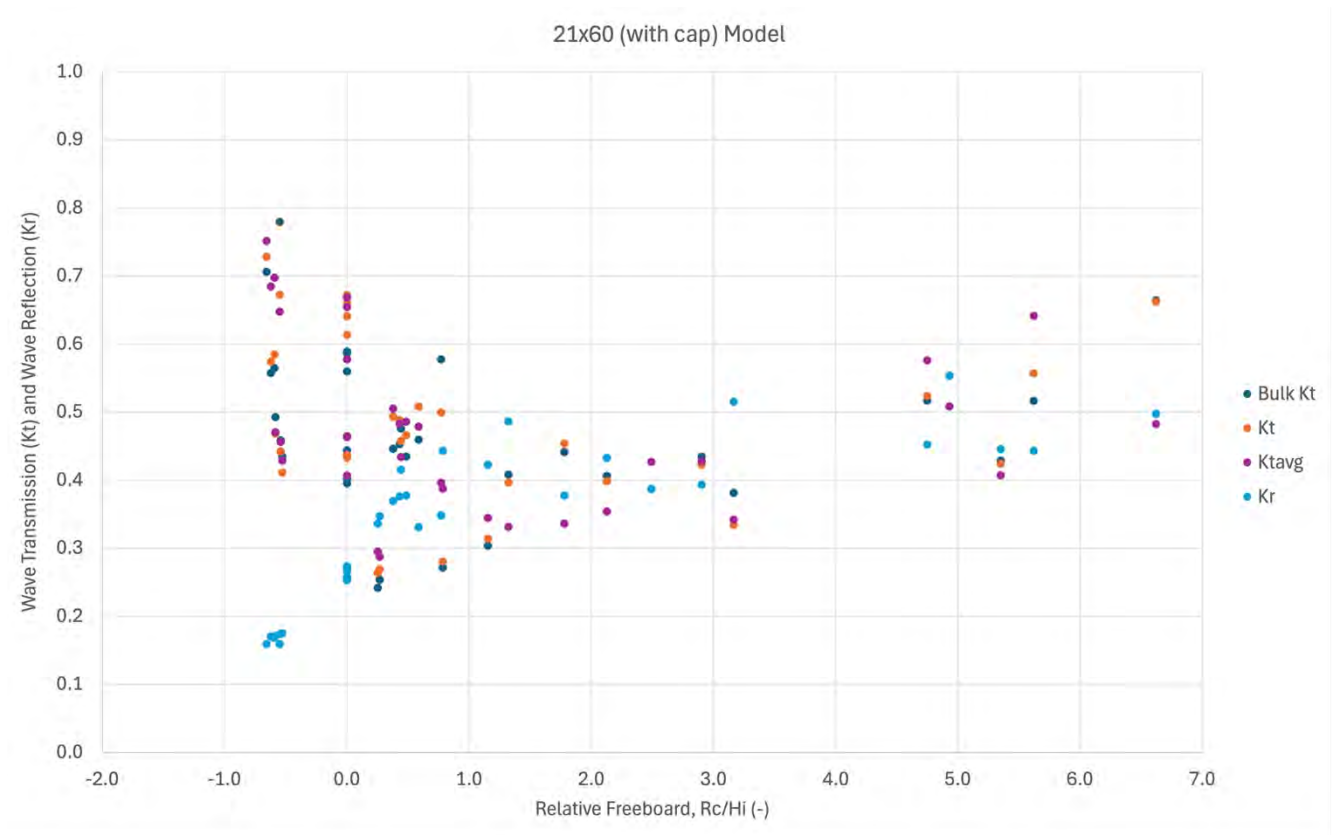


Figure 30. Wave transmission and wave reflection coefficient values as a function of relative freeboard for the 21x60 (with cap) model.

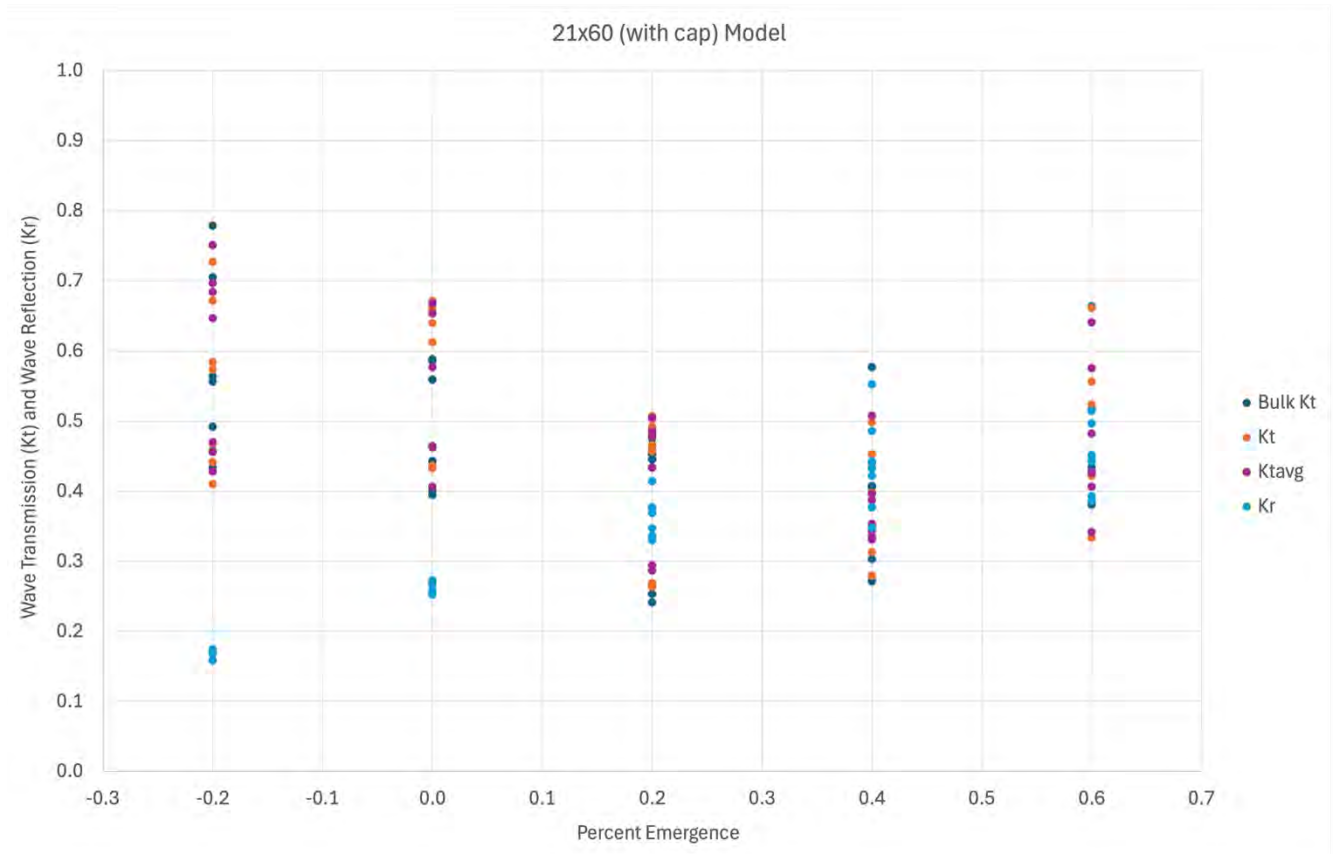


Figure 31. Wave transmission and wave reflection coefficient values as a function of percent emergence for the 21x60 (with cap) model.

Representative velocity time histories for the 21x60 model test case B5 are provided in Figure 32. The “u” and “v” velocity components show a clear correspondence with the monochromatic wave forcing while the “w” velocity component remains small with little consistent phasing to the other components. Note the small magnitude of all velocity components, generally speaking.

The testing configurations were mostly unable to motivate significant movement of the 21x60 panels. Some minor movement was noted visually during experiments and appear in the accelerometer and gyroscope measurements shown in Figure 33 and Figure 34, respectively. For the 21x60 model testing, some motion was detected for all water level cases, but was more pronounced for water levels near the crest (like water level case D). As shown in these representative results from water level case D (just below the structure crest), all panels experienced some movement, but those rotations were typically very small at < 0.1 degree per second. Panel E experienced the most substantial movements with rotation values nearing 0.5 degrees per second, but these motions are still relatively minor. The presence of rotation in both the x- and y-directions suggests another wobbling or rocking issue associated with protruding aggregates.

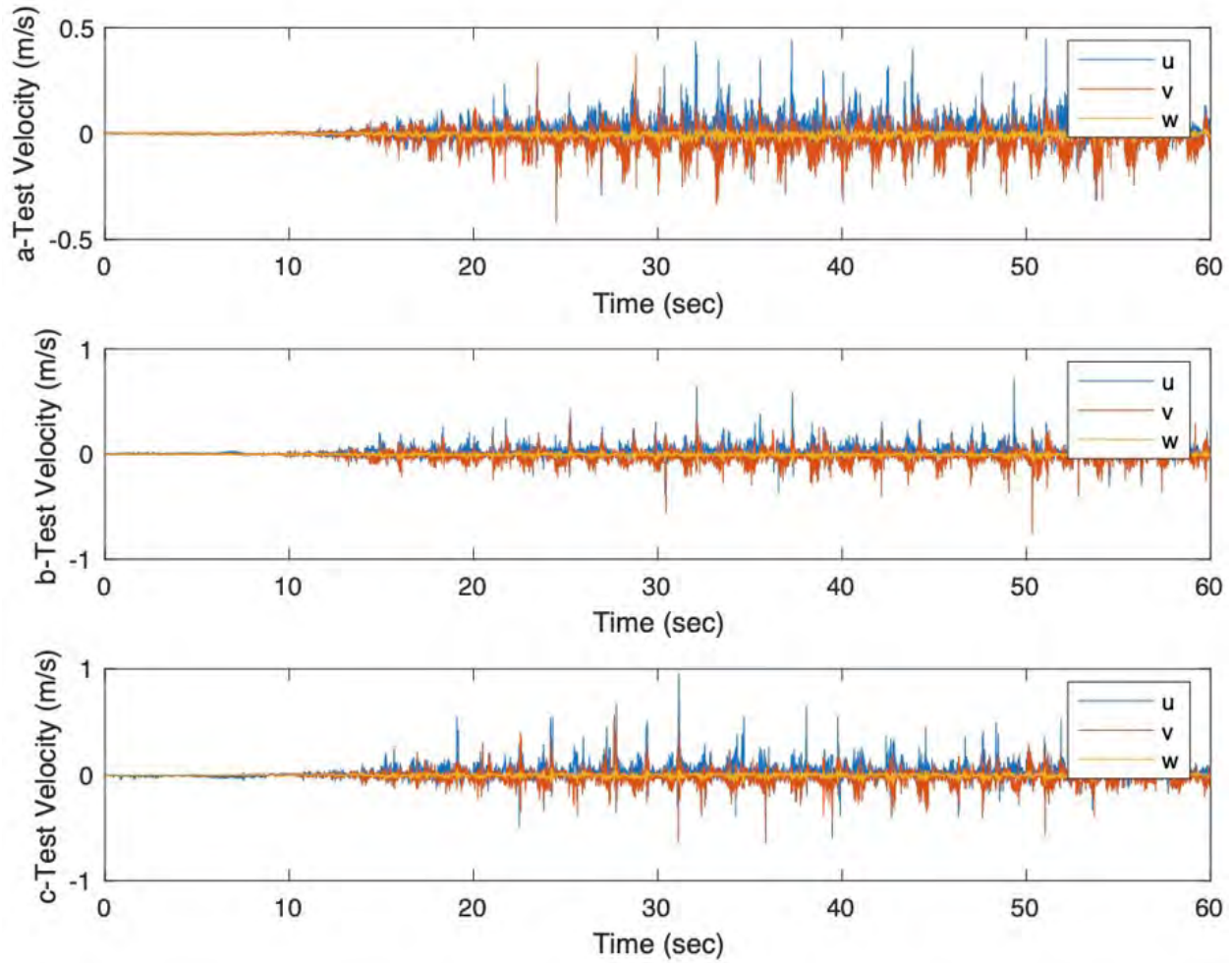


Figure 32. Sample velocity measurements from each replicate of test B5 for the 21x60 (with cap) model.

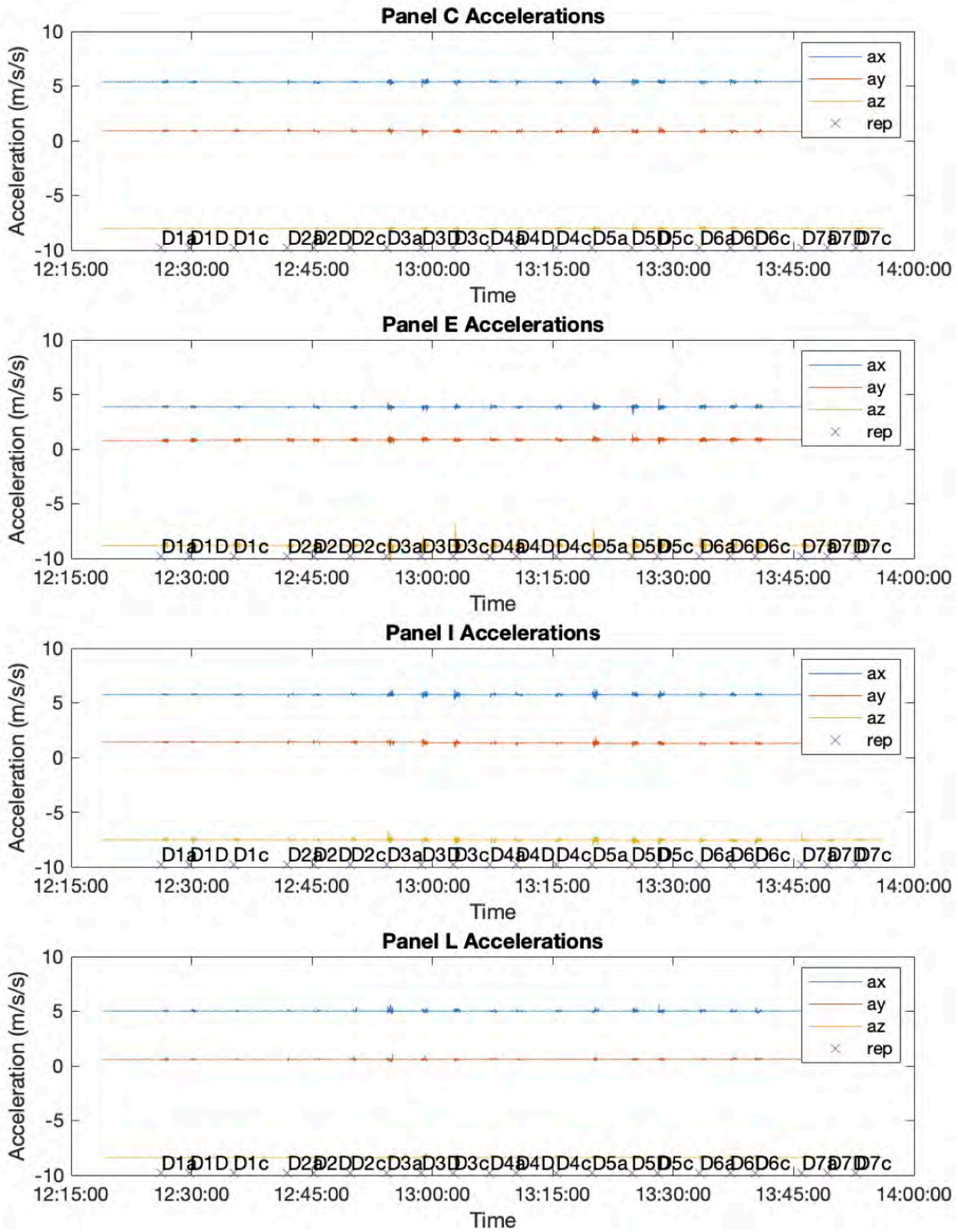


Figure 33. Acceleration measurements during all D series tests for the 21x60 (with cap) model.

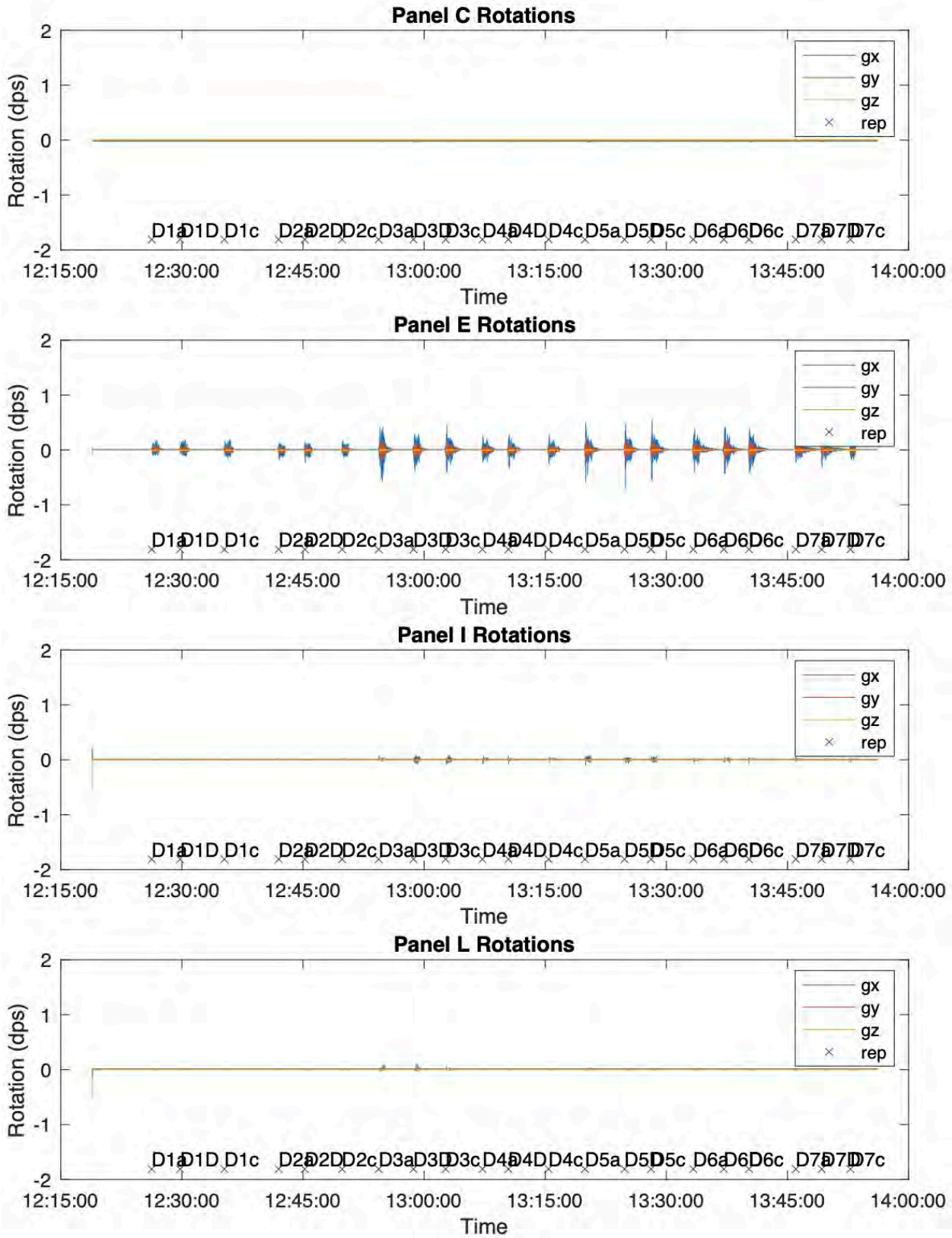


Figure 34. Rotational measurements during all D series tests for the 21x60 (with cap) model.

## Discussion

Given that most of the QuickReef® models show a strong relationship between wave transmission and relative freeboard, empirical models were derived through regression analysis. With the exception of the 21x60 model, values of wave transmission fit a simple exponential relationship for relative freeboard. A least squares regression technique was used to derive expressions that best fit the data. The resulting regression equations for the 24x80, Defender™, and 21x60 (with cap) models are given in Equations 9-11, respectively. Graphical representations of these predictive equations are shown relative to the average of all wave transmission values computed (bulk, incident, average incident) in Figure 35, Figure 36, and Figure 37 for the 24x80, Defender™, and 21x60 (with cap) structures, respectively.

$$K_t = 0.4 \exp\left(-0.5 \frac{R_c}{H_i}\right) \quad (9)$$

$$K_t = 0.48 \exp\left(-0.23 \frac{R_c}{H_i}\right) \quad (10)$$

$$K_t = 0.5 \exp\left(-0.19 \frac{R_c}{H_i}\right) \quad (11)$$

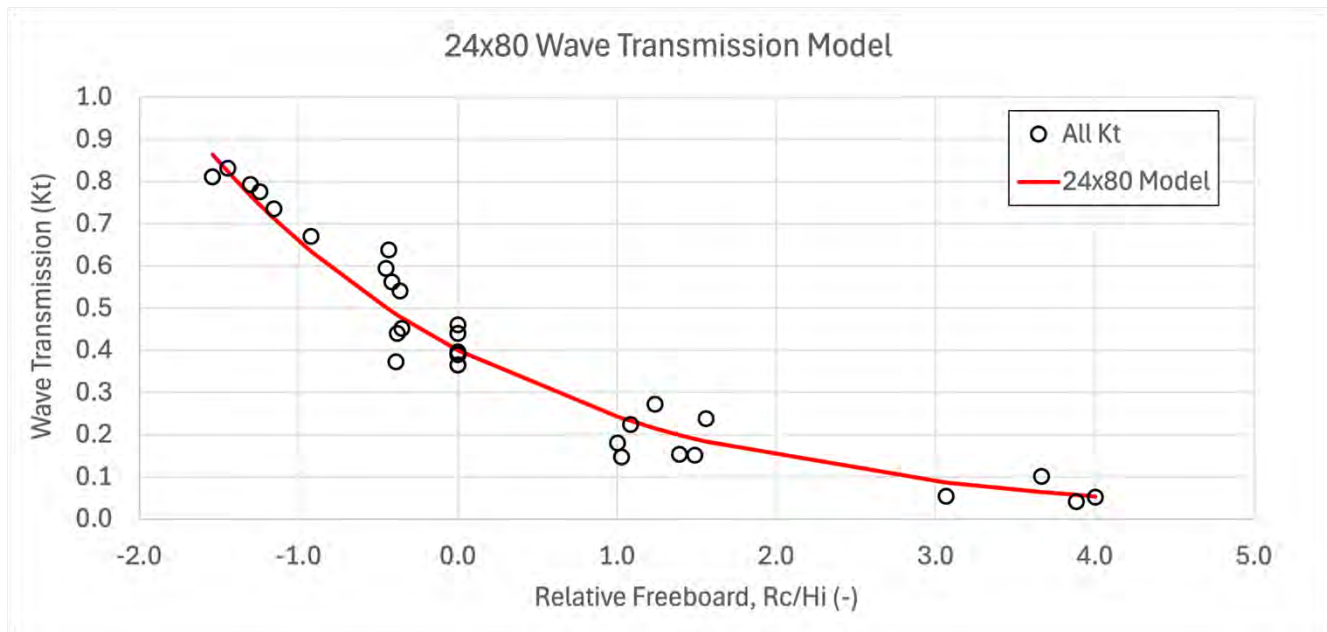


Figure 35. Predictive model of wave transmission for the 24x80 model (Equation 9).

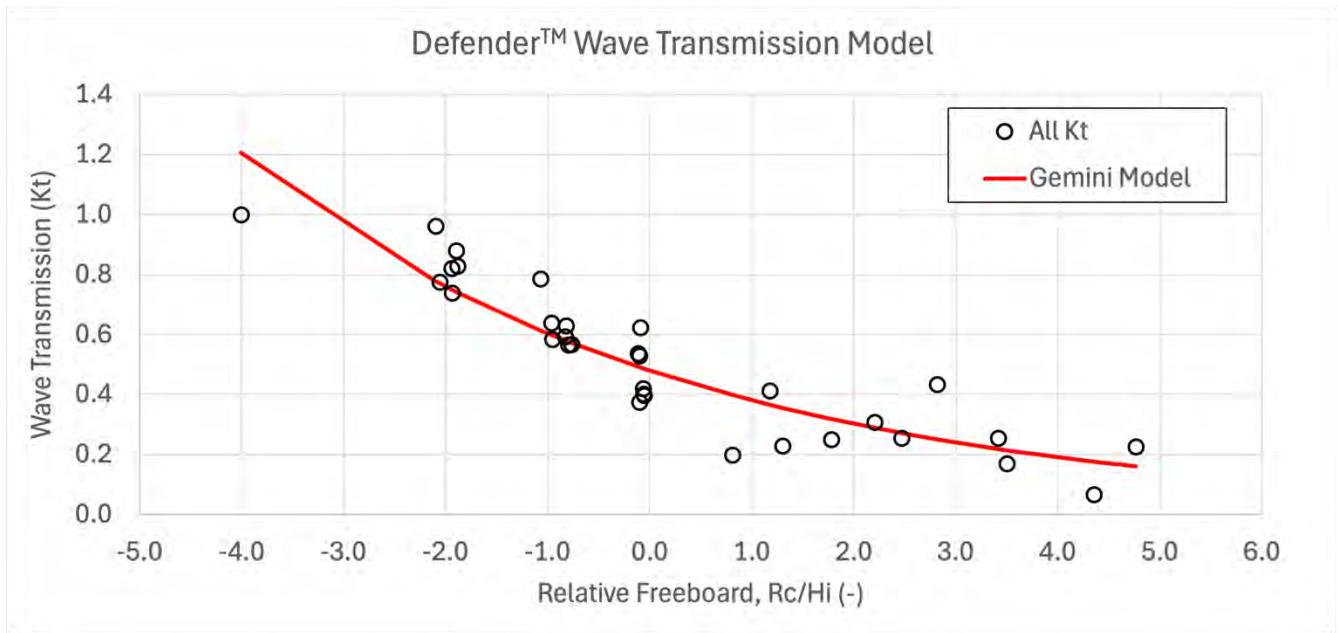


Figure 36. Predictive model of wave transmission for the Defender™ model (Equation 10).

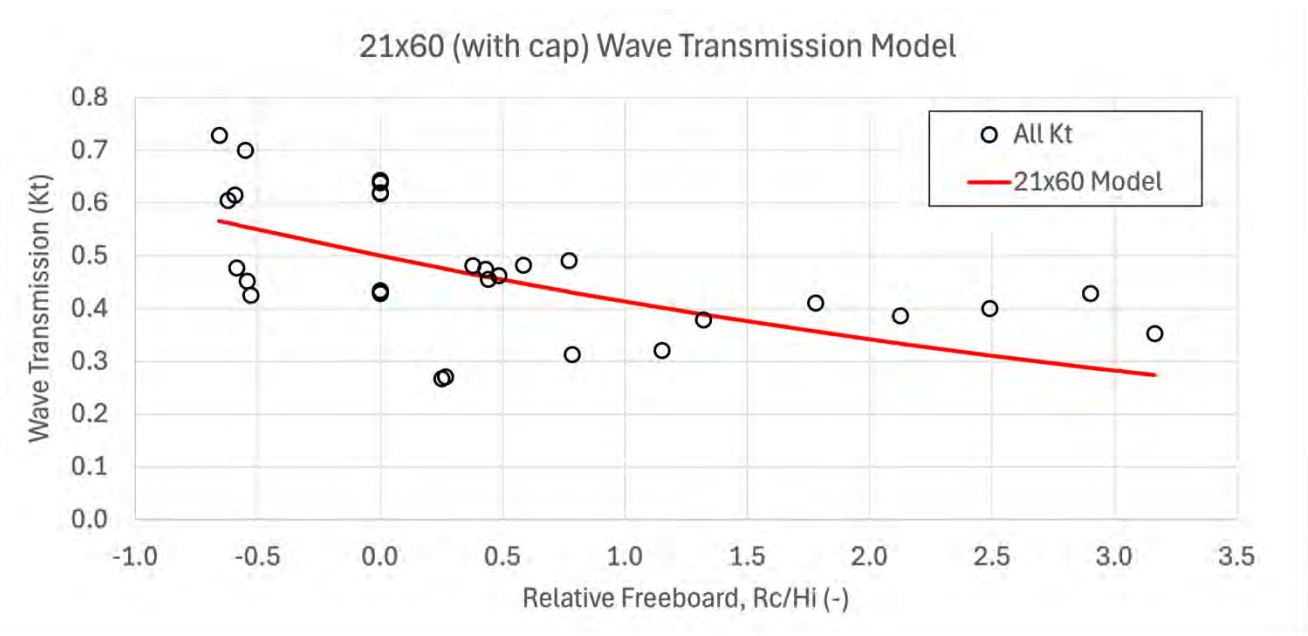


Figure 37. Predictive model of wave transmission for the 21x60 (with cap) model (Equation 11).

The results of an error analysis for each predictive equation are summarized in Table 15. Three metrics are used to assess the goodness of fit for each model type: root mean square error (RMSE), absolute error, and mean bias. The equations for those metrics are given in Equations 12-14, respectively, where  $N$  is the number of observations,  $K_{tmod}$  is the modeled or predicted value from the equation, and  $K_{tall}$  is the observed value of wave transmission. The magnitudes of each error estimate can be taken as a percentage since the practical range for wave transmission coefficients is 0 to 1.0. In other words, Equation 9 yields a 5 percent root mean square error, a 16 percent absolute error, and tends to overestimate wave transmission by about 5 percent. Note that while the error estimates for the 21x60 model do not appear substantially worse than those for the 24x80 or Defender™ model types, the visual fit to the data in Figure 37 looks relatively poor. Though the error metrics for the 21x60 (with cap) model type are not poor overall, the exponential regression model given in Equation 11 should not be considered robust.

Table 15. Wave Transmission Model Error Analysis

Model	RMSE	Absolute Error	Mean Bias
24x80	0.05	0.16	0.05
Defender™	0.09	0.23	0.09
21x60 (with cap)	0.10	0.20	0.02

$$RMSE = \sqrt{\frac{\sum(K_{tmod} - K_{tall})^2}{N}} \quad (12)$$

$$Absolute\ Error = \frac{\sum_{i=1}^N abs\left(\frac{K_{tmod} - K_{tall}}{K_{tall}}\right)}{N} \quad (13)$$

$$Mean\ Bias = \frac{\sum_{i=1}^N \left(\frac{K_{tmod} - K_{tall}}{K_{tall}}\right)}{N} \quad (14)$$

There was no attempt to fit simple predictive equations for wave reflection. This is because wave reflection depends on at least two variables for the structures tested: freeboard and wave steepness. Instead of attempting the regression analysis for this variable, some general relationships are drawn from a presentation of wave reflection values plotted as a function of both dependent variables. Wave reflection values were separated into unique series for each water level case and then plotted as a function of wave steepness as shown in Figure 38, Figure 39, and Figure 40.

Three general trends or characteristics of wave reflection are evident in these figures. First, and perhaps most obviously, wave reflection coefficients are largest when water levels are lowest. This makes sense because there is little opportunity for waves to transmit past the structure when water levels are below the crest. Since the QuickReef® products are generally not porous below their crest, most of the wave reflections should occur during these lower water levels. However, unlike seawalls that have reflection coefficients approaching 1.0, the QuickReef® products never had a reflection coefficient exceeding 0.7. This is likely due to the geometry of

their structures, which encourage wave dissipation in between the gapped panels and central stem wall or spine. For comparison, a typical sloping permeable rubble mound structure might have reflection coefficients ranging from 0.4 to 0.6.

Second, when water levels are below the structure crest, reflection coefficients increase with increasing wave steepness. Generally speaking, the relationship between wave reflection and wave steepness appears to be mostly linear (as an approximation) for all of the QuickReef® products tested.

Third, as water levels increase relative to the structure crest, reflection coefficients decrease overall, but also decrease with increasing wave steepness. In other words, when the QuickReef® structures are submerged, longer period waves tend to have higher reflection coefficients as compared to shorter waves.

These three observations regarding wave reflection are consistent across all of the model types tested in this study.

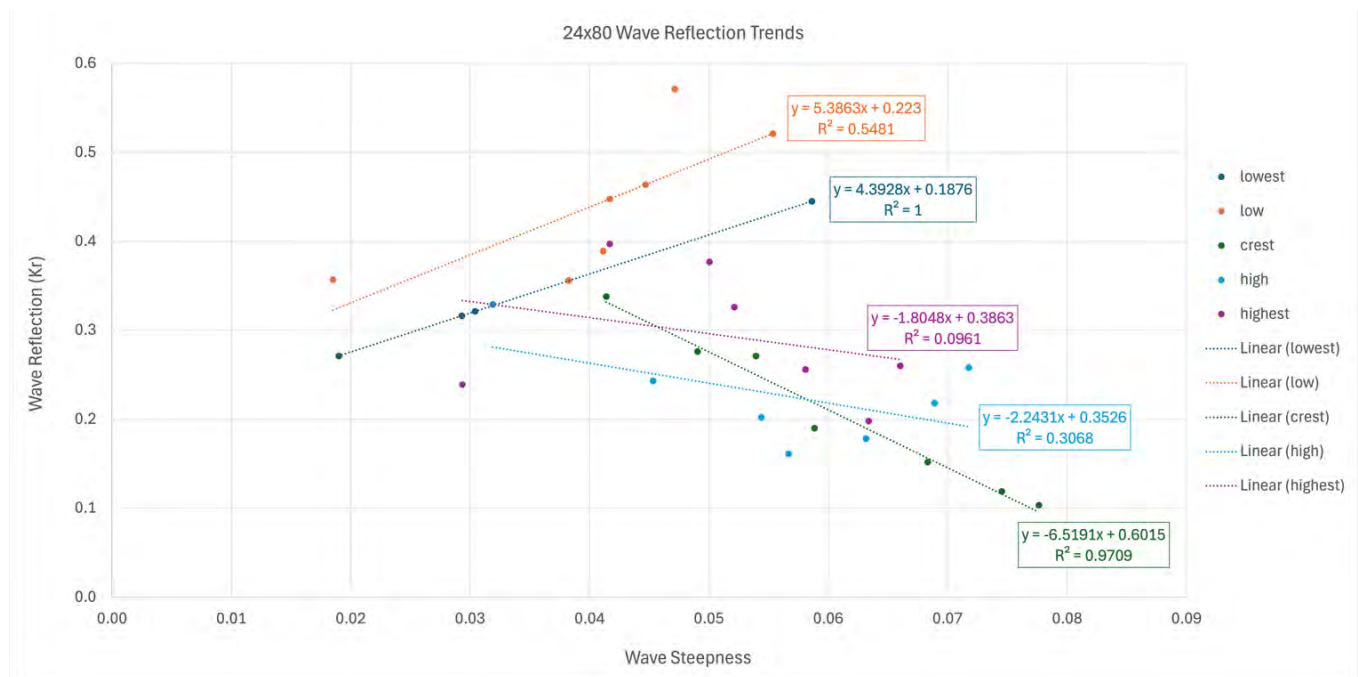


Figure 38. Trends in wave reflection as functions of wave steepness and relative freeboard for the 24x80 model.

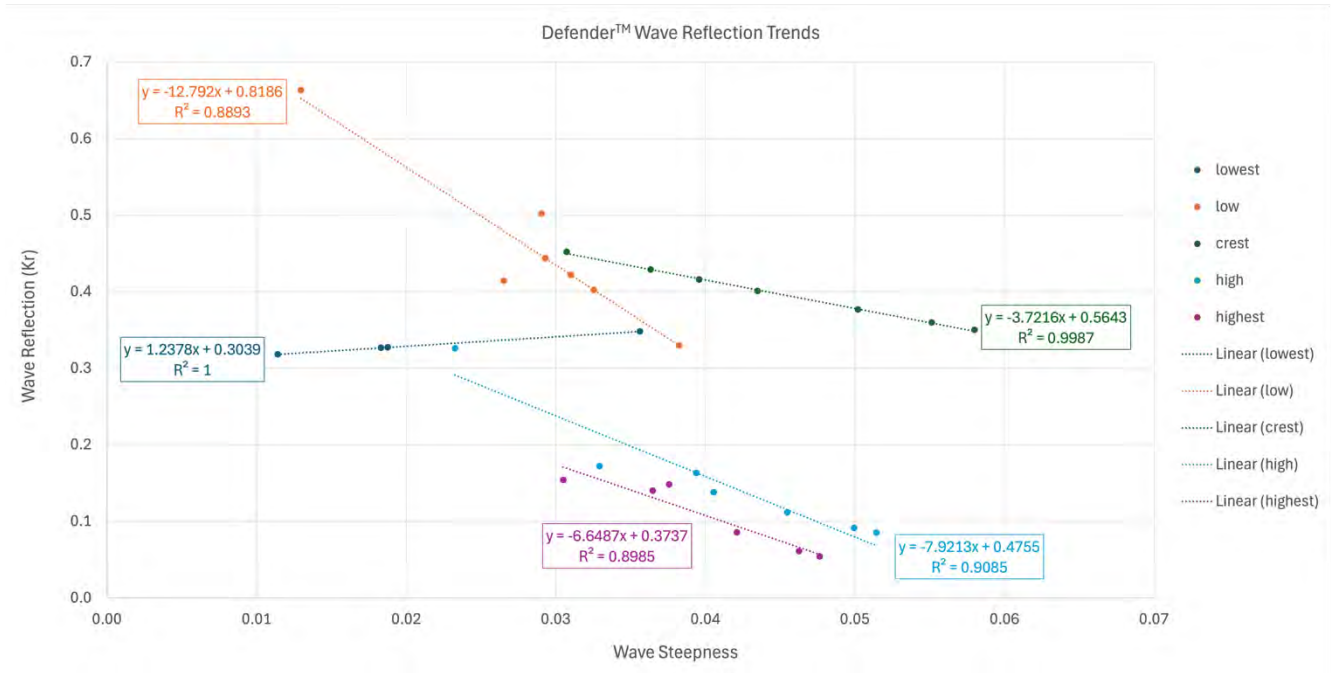


Figure 39. Trends in wave reflection as functions of wave steepness and relative freeboard for the Defender™ model.

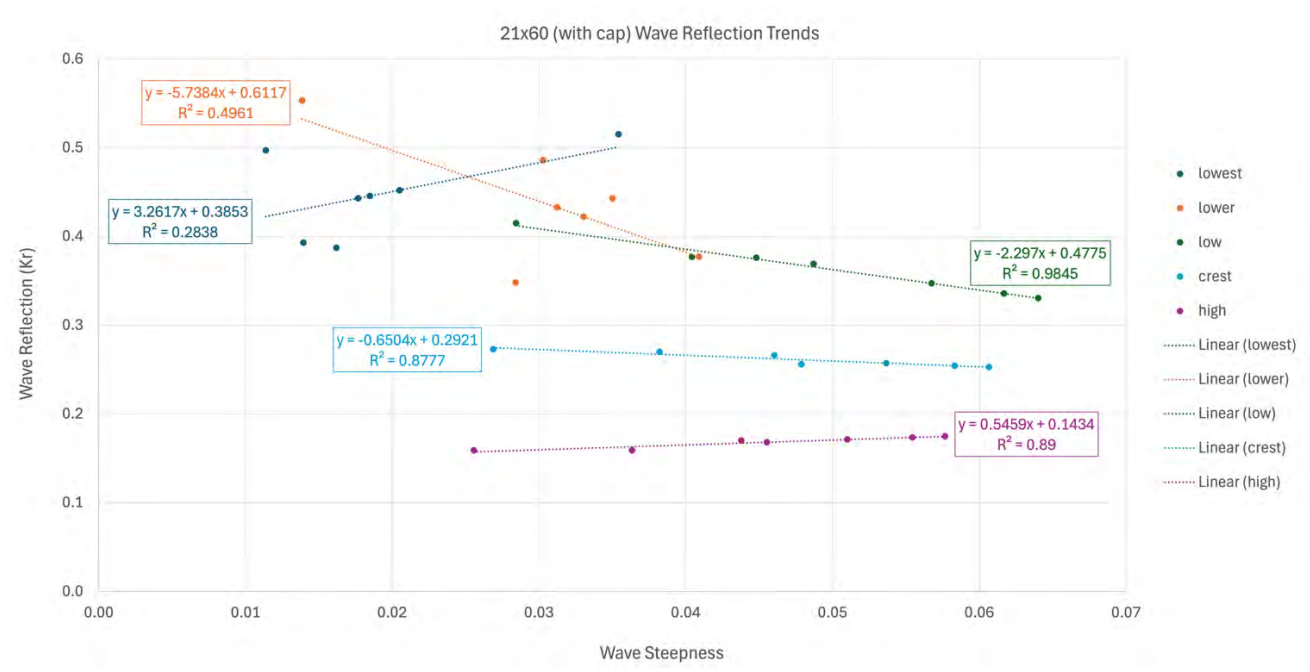


Figure 40. Trends in wave reflection as functions of wave steepness and relative freeboard for the 21x60 (with cap) model.

## References

Isaacson, M. 1991. "Measurement of Regular Wave Reflection." *J. Waterway, Port, Coastal, Ocean Eng.*, 117 (6): 553–569. [https://doi.org/10.1061/\(ASCE\)0733-950X\(1991\)117:6\(553\)](https://doi.org/10.1061/(ASCE)0733-950X(1991)117:6(553)).

Mansard, E. P. D., and E. R. Funke. 1980. "The Measurement of Incident and Reflected Spectra Using a Least Squares Method." *Proceedings of the International Conference on Coastal Engineering*, 154–172.

Zelt, J. A., and J. E. Skjelbreia. 1993. "Estimating Incident and Reflected Wave Fields Using an Arbitrary Number of Wave Gauges." *Coastal Engineering 1992*, 777–789. Venice, Italy: American Society of Civil Engineers.

# Appendix

## 24x80 Model – Wave Height Profiles

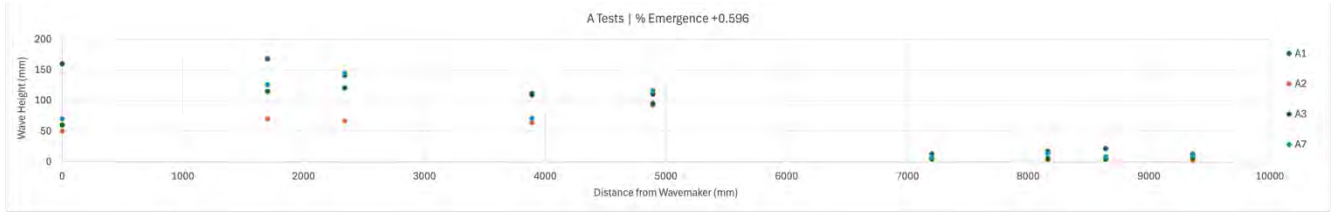


Figure 41. Measured wave height variation along the flume for A tests of the 24x80 model.

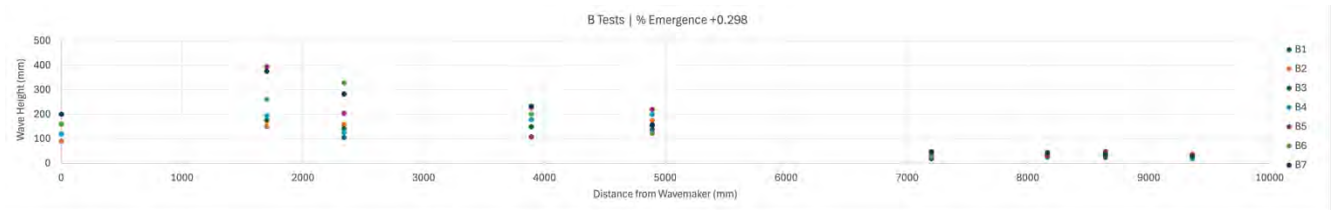


Figure 42. Measured wave height variation along the flume for B tests of the 24x80 model.

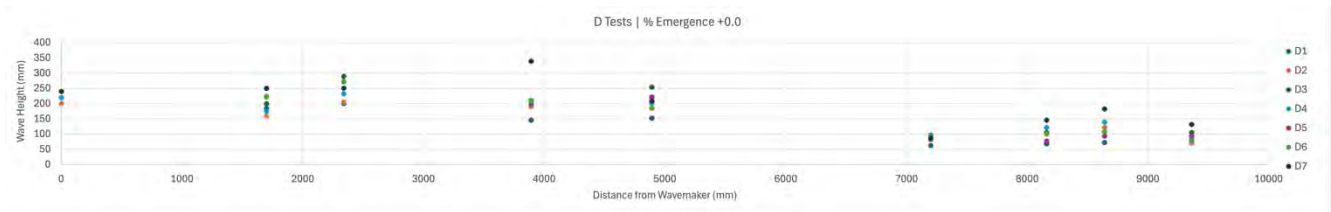


Figure 43. Measured wave height variation along the flume for D tests of the 24x80 model.

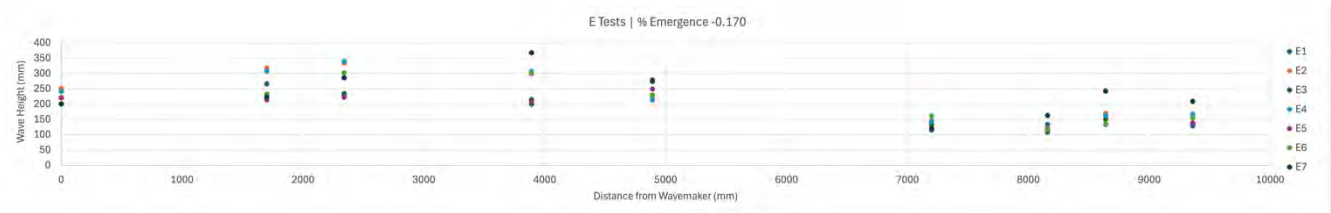


Figure 44. Measured wave height variation along the flume for E tests of the 24x80 model.

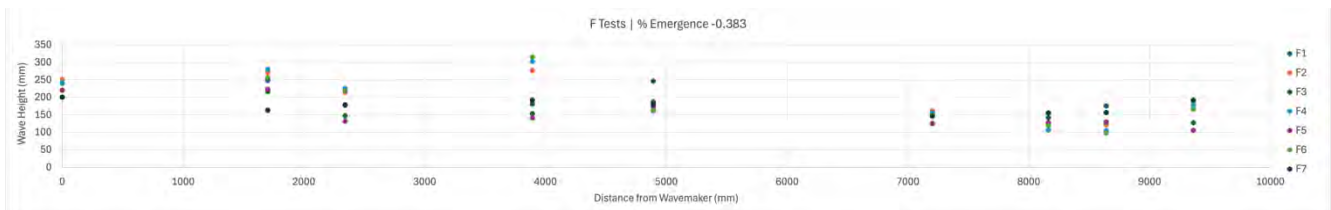


Figure 45. Measured wave height variation along the flume for F tests of the 24x80 model.

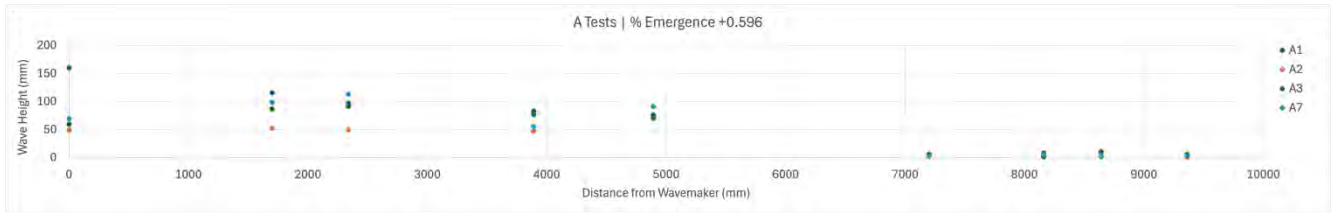


Figure 46. Incident wave height variation along the flume for A tests of the 24x80 model.

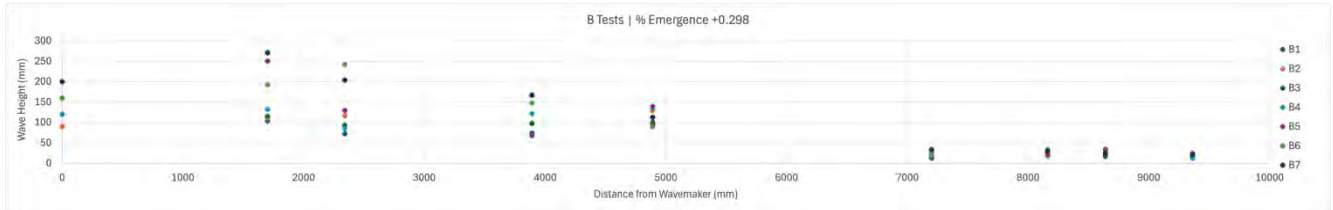


Figure 47. Incident wave height variation along the flume for B tests of the 24x80 model.

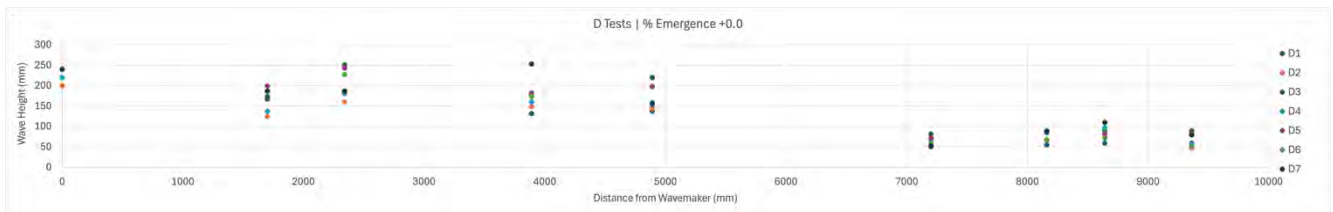


Figure 48. Incident wave height variation along the flume for D tests of the 24x80 model.

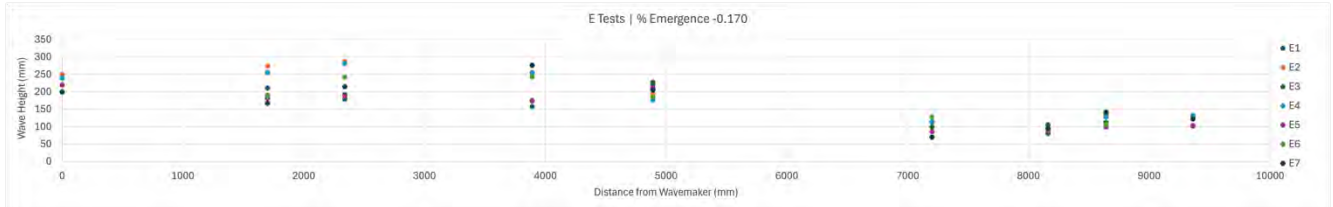


Figure 49. Incident wave height variation along the flume for E tests of the 24x80 model.

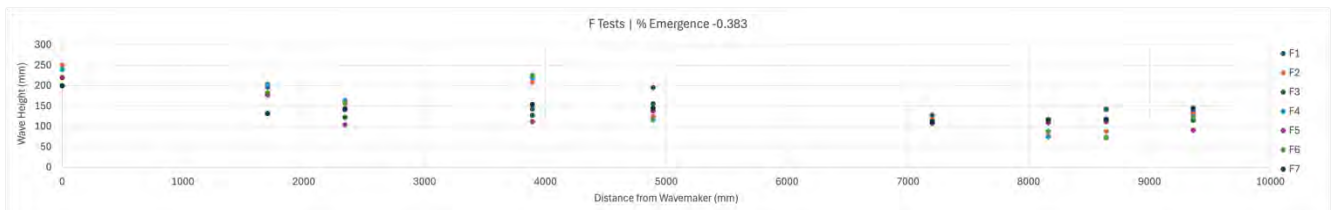


Figure 50. Incident wave height variation along the flume for F tests of the 24x80 model.

## Defender™ Model – Wave Height Profiles



Figure 51. Measured wave height variation along the flume for A tests of the Defender™ model.

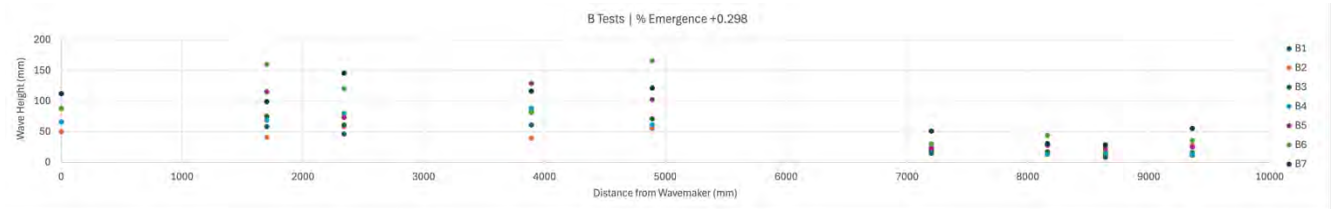


Figure 52. Measured wave height variation along the flume for B tests of the Defender™ model.



Figure 53. Measured wave height variation along the flume for D tests of the Defender™ model.

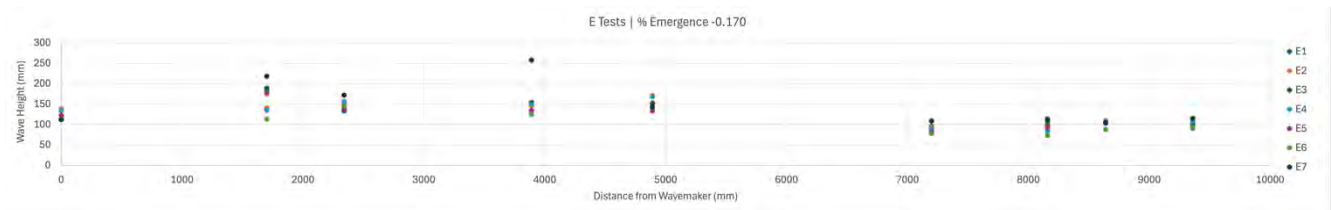


Figure 54. Measured wave height variation along the flume for E tests of the Defender™ model.

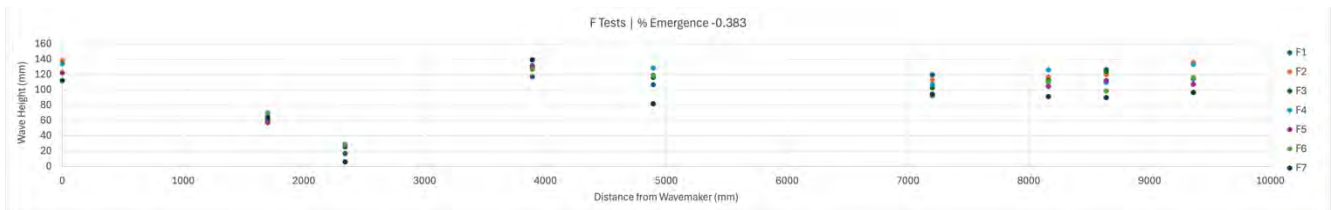


Figure 55. Measured wave height variation along the flume for F tests of the Defender™ model.

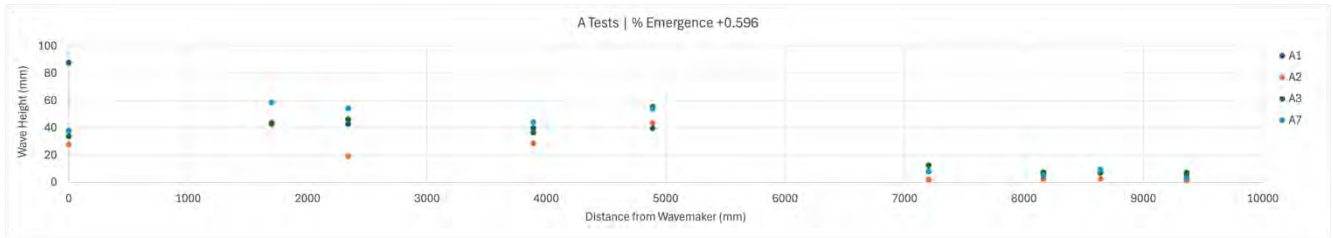


Figure 56. Incident wave height variation along the flume for A tests of the Defender™ model.

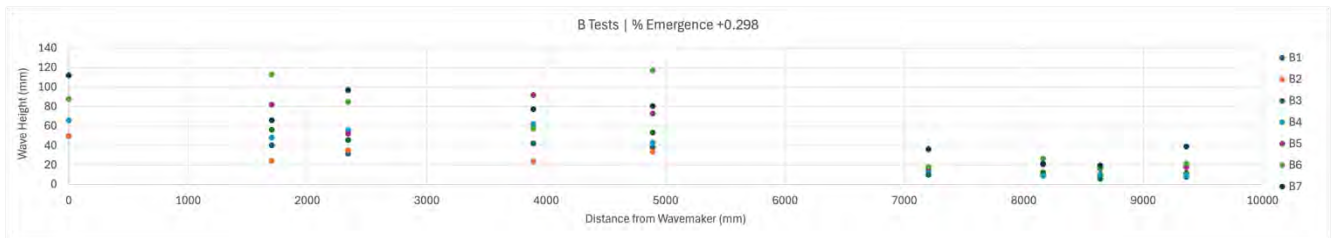


Figure 57. Incident wave height variation along the flume for B tests of the Defender™ model.

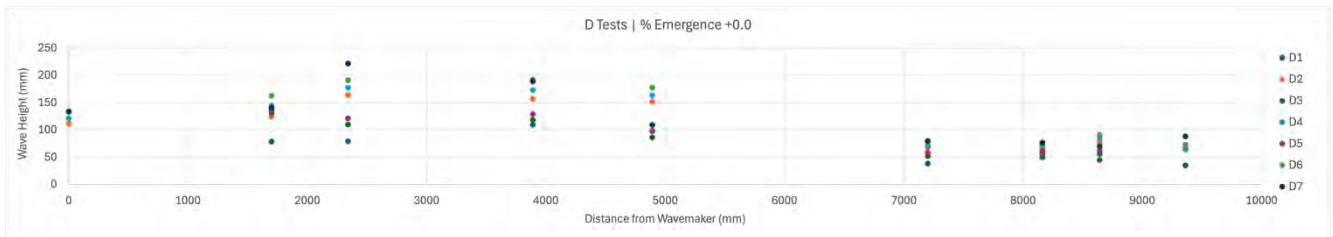


Figure 58. Incident wave height variation along the flume for D tests of the Defender™ model.

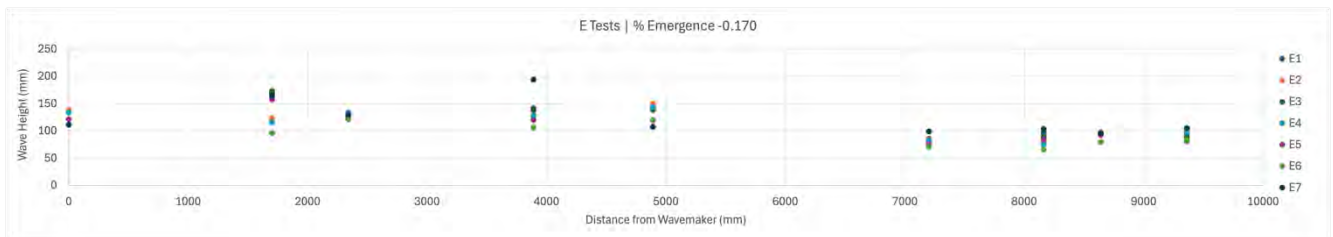


Figure 59. Incident wave height variation along the flume for E tests of the Defender™ model.

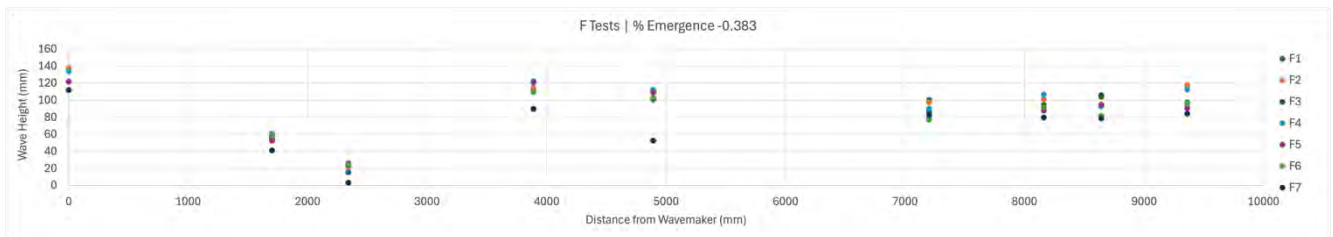


Figure 60. Incident wave height variation along the flume for F tests of the Defender™ model.

## 21x60 (with cap) Model – Wave Height Profiles

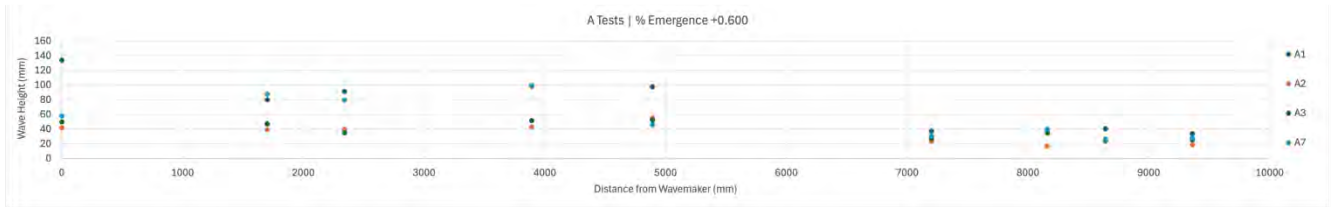


Figure 61. Measured wave height variation along the flume for A tests of the 21x60 (with cap) model.

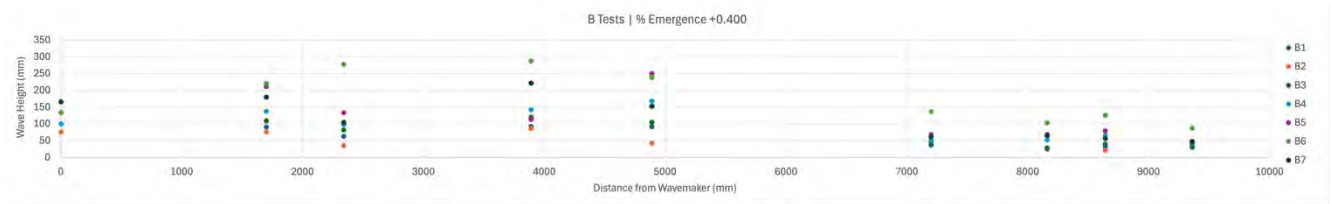


Figure 62. Measured wave height variation along the flume for B tests of the 21x60 (with cap) model.

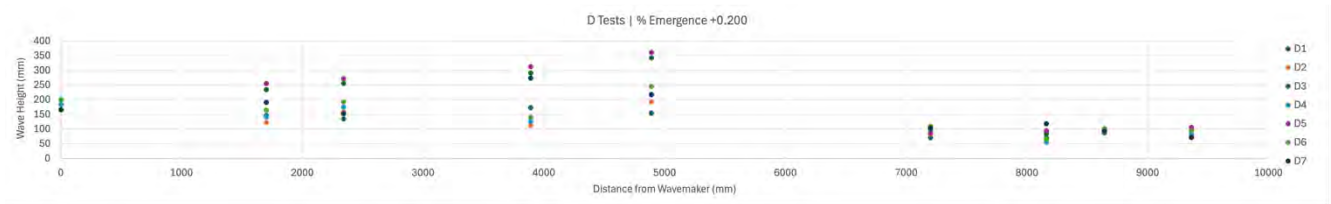


Figure 63. Measured wave height variation along the flume for D tests of the 21x60 (with cap) model.

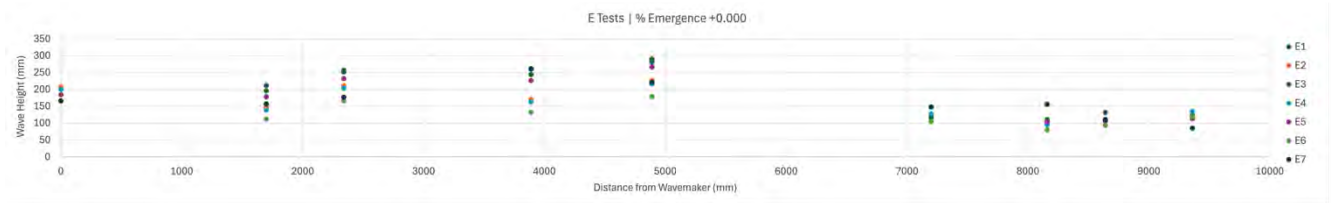


Figure 64. Measured wave height variation along the flume for E tests of the 21x60 (with cap) model.

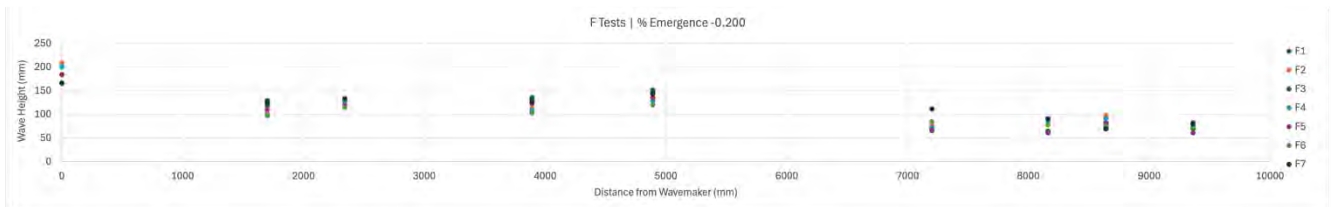


Figure 65. Measured wave height variation along the flume for F tests of the 21x60 (with cap) model.

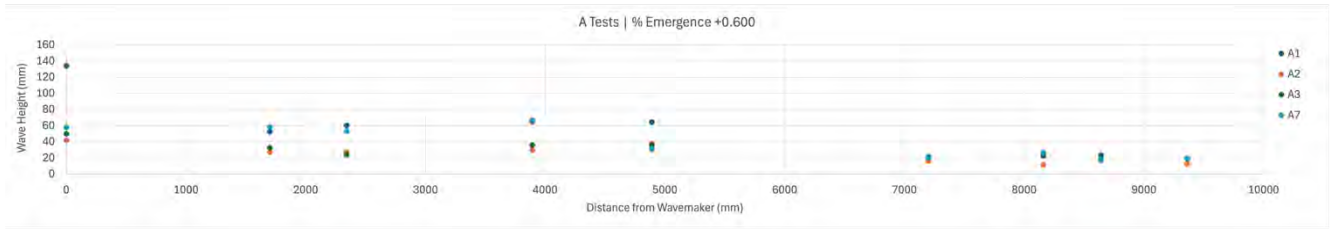


Figure 66. Incident wave height variation along the flume for A tests of the 21x60 (with cap) model.

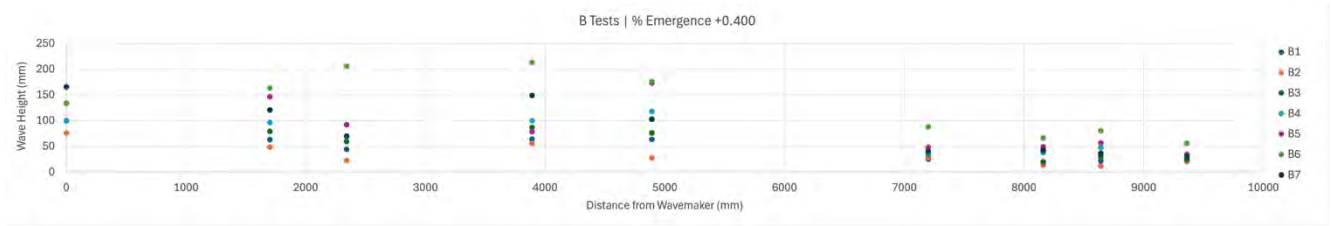


Figure 67. Incident wave height variation along the flume for B tests of the 21x60 (with cap) model.

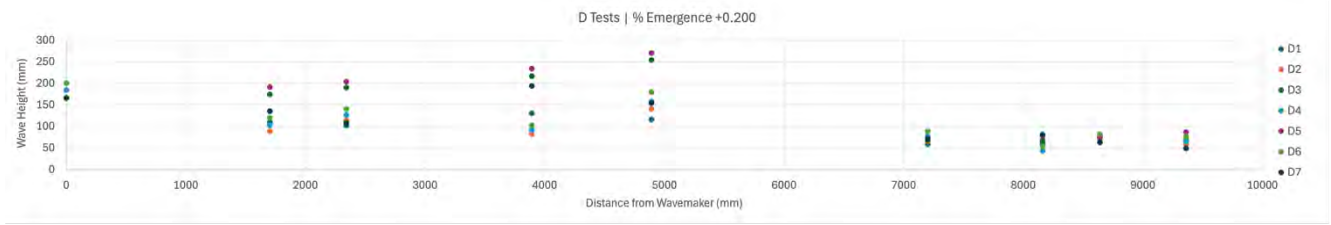


Figure 68. Incident wave height variation along the flume for D tests of the 21x60 (with cap) model.

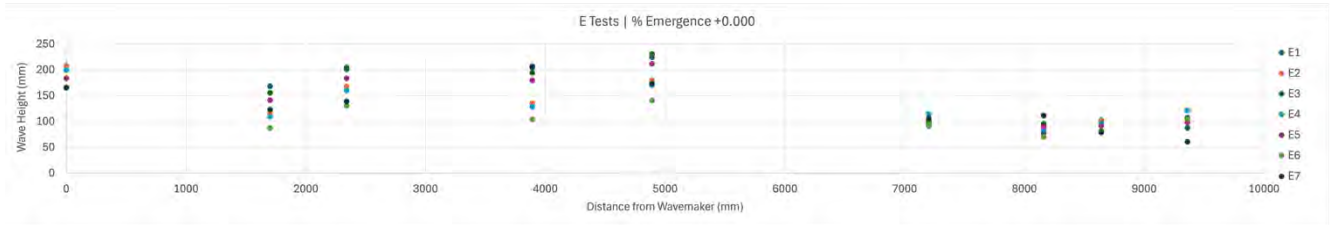


Figure 69. Incident wave height variation along the flume for E tests of the 21x60 (with cap) model.

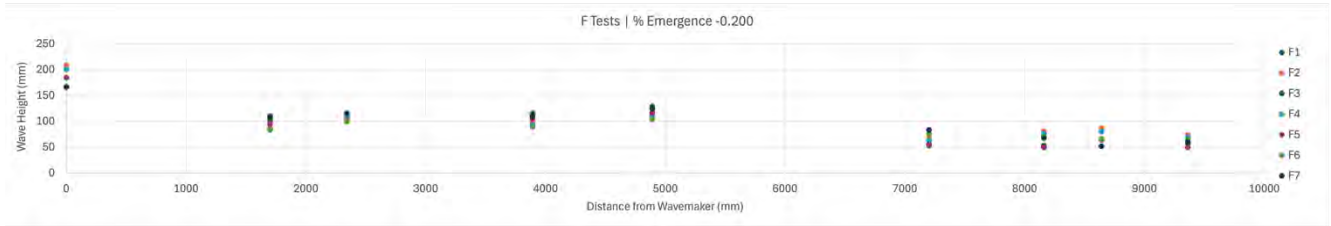


Figure 70. Incident wave height variation along the flume for F tests of the 21x60 (with cap) model.